NEUTRON MONITOR BOOTCAMP 2021

CHIANG MAI UNIVERSITY

ASTRONOMY LODGE AT KM31ST, DOI INTHANON

AND PRINCESS SIRINDHORN NEUTRON MONITOR, CHIANG MAI

Presented by

Waraporn Nuntiyakul, Ph.D.

Department of Physics and Materials Science, Faculty of Science, Chiang Mai Univ.

Asst. Prof. Dr. Waraporn Nuntiyakul
Position: Professor of Physics
Institution: Chiang Mai University
E-mail: waraporn.n@cmu.ac.th

Dr. Achara Seripienlert
Position: Researcher
E-mail: achara.seri@gmail.com

B.Sc.

Sidarat Khamphakdee

Research Topic: Analysis of the Changvan Neutron Monitor Operation in Latitude Surveys during 2019-2020
Institution: Chiang Mai University

Kittinan Jomprasert

Research Topic: To determine a correlation function between counting rates of two Antarctic neutron monitor stations (Jang Bogo – McMurdo) and time lag
Institution: Chiang Mai University

M.Sc.

Yanee Tangjai

Research Topic: Analysis of Ice Cherenkov Detector Operation during a Latitude Survey
Institution: Chiang Mai University

Panutda Yakum

Research Topic: Analyzing Neutron Time-Delay Histograms from Changvan Latitude Surveys
Institution: Chiang Mai University

Audcharaporn Pagwhan

Research Topic: Monte-Carlo simulation of the response of bare neutron counters at the South Pole to vertical secondary particles from cosmic rays
Institution: Chiang Mai University

Jetsada Maburee

Research Topic: LHAASO, Moon shadow analysis cosmic rays.
Institution: Chiang Mai University

Ph.D.

Kledsai Pupakun

Research Topic: Solar magnetic polarity effect on neutron monitor count rates from latitude surveys versus Antarctic stations and data analysis from Muon telescope
Institution: Chiang Mai University

Montree Phetra

Research Topic: Studying of water maser in the star-forming region: W49 N using KaVA observatory
Institution: Chiang Mai University

Ekawit Kittiya

Research Topic: VB6 & Coding C++ on FPGA of new Readout electronics board, correlation function with the full 10-s McMurdo & Jang Bogo datasets
Institution: Chiang Mai University

OUTLINE

- Introduction
  - Cosmic Rays
  - Standard-Neutron Monitor
  - Semi-leaded Neutron Detector
- Cosmic Ray Spectra
- Latitude Surveys
  - 1994-2007 (13 survey years)
  - 1995
  - 2009
  - 2018-Present
- Output

Introduction: Cosmic rays

- Energetic particles or γ-rays from space
- Discovered by Hess in 1912 (Nobel Prize in 1936)
- Ordinary matter accelerated to high energies
  - p, ^{4}He, ^{12}C, ^{16}O, heavy nuclei and γ, e^{+}, e^{-}, μ, ν, ...
- Key sources of cosmic rays for Earth's radiation environment:
  - From solar storms (solar energetic particles)
  - From supernova explosions inside the Milky-Way Galaxy (Galactic cosmic rays)
  - From intense events/objects GRB, AGN outside the Galaxy (Extra Galactic cosmic rays)
- Key cause of biological mutation

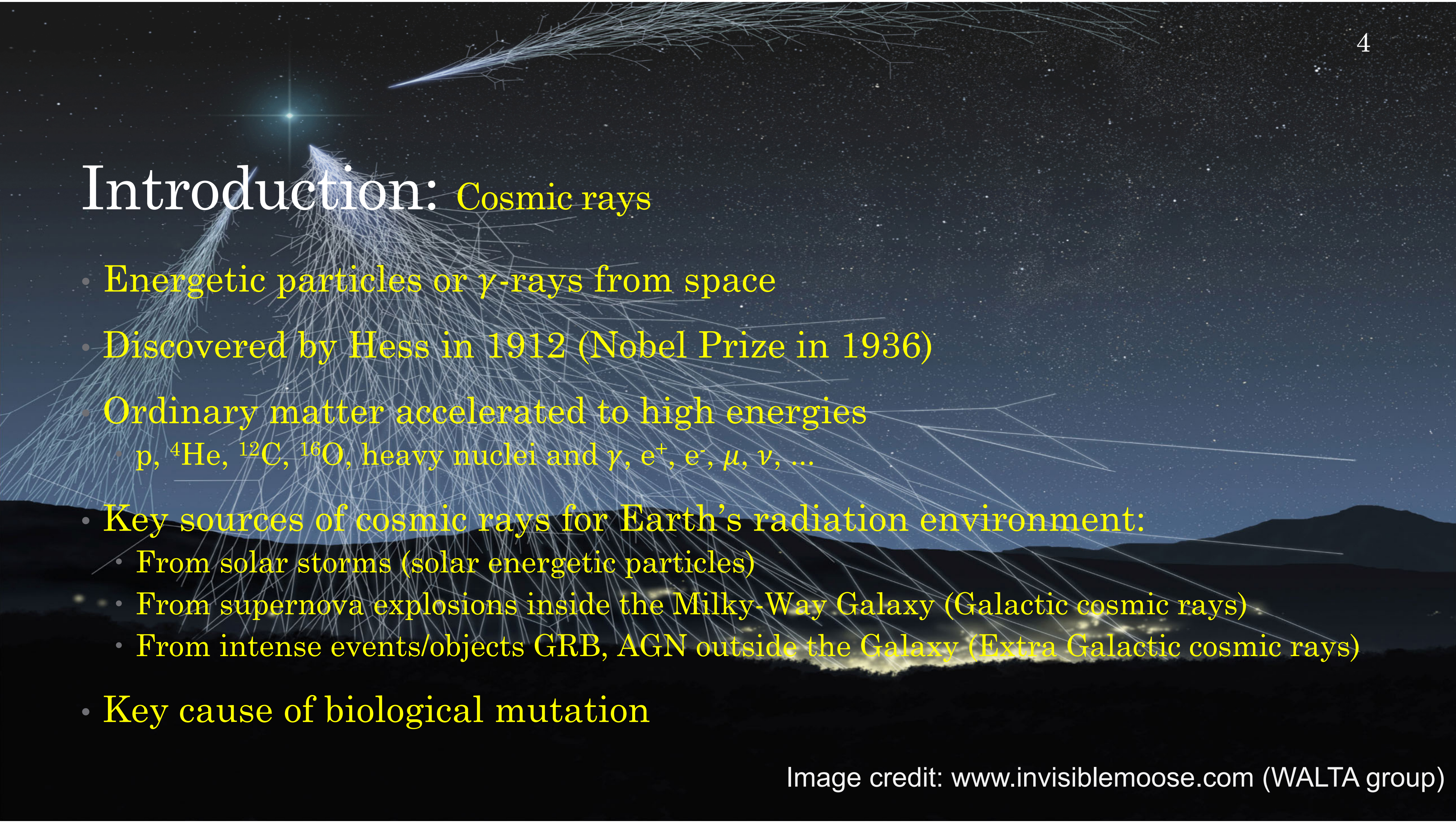

Image credit: www.invisiblemoose.com (WALTA group)

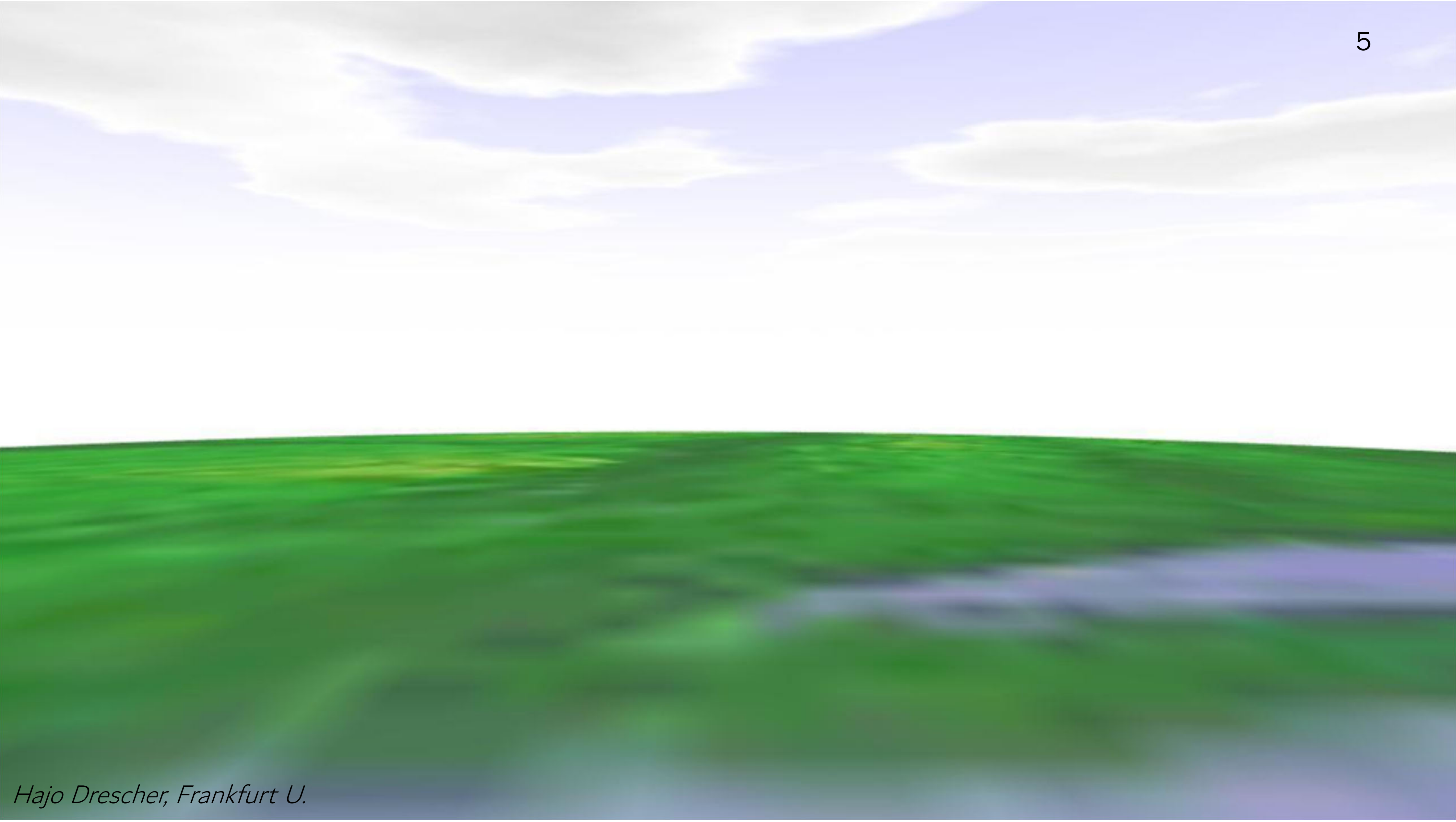
Hajo Drescher, Frankfurt U.

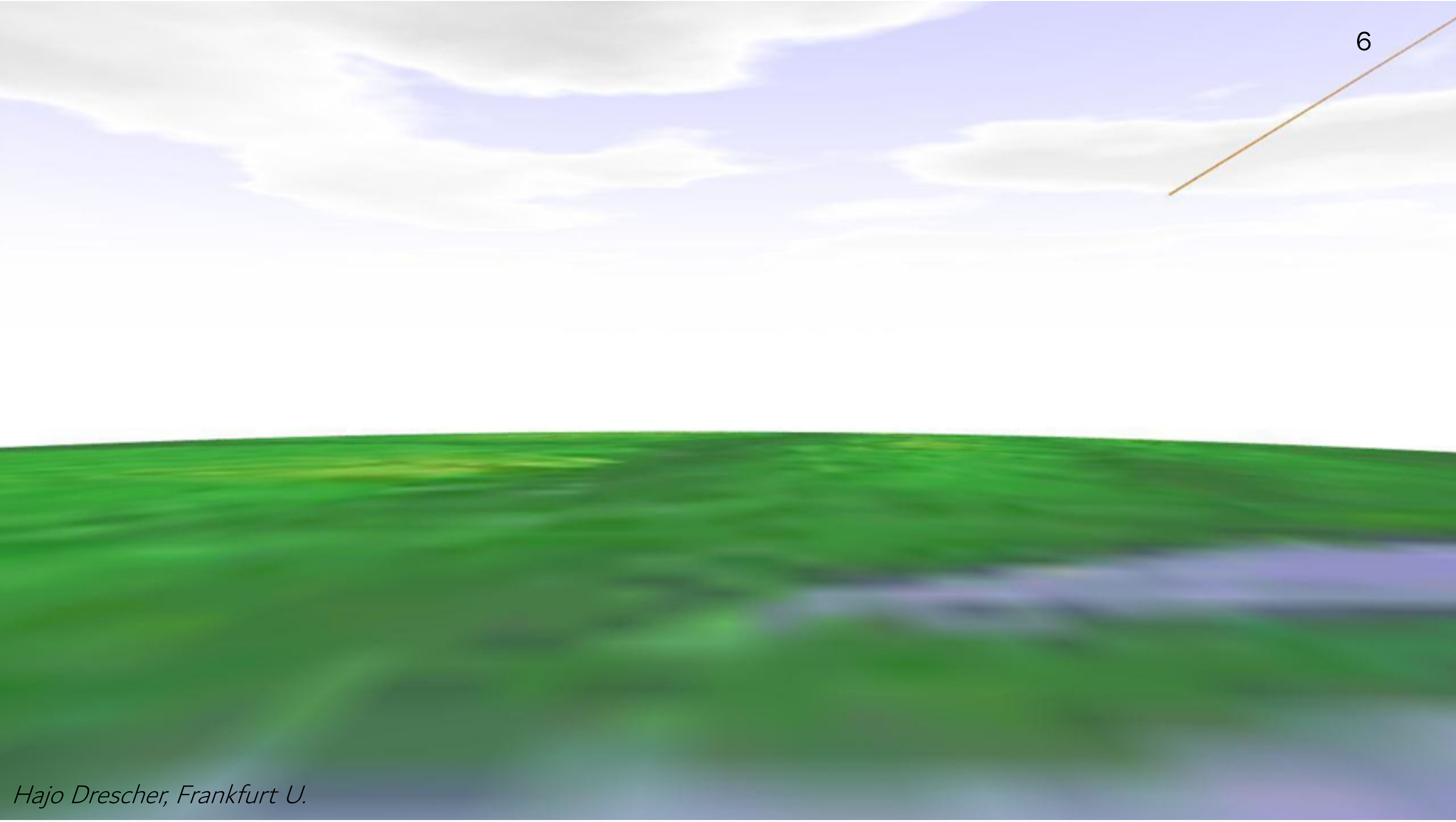
Hajo Drescher, Frankfurt U.

Hajo Drescher, Frankfurt U.

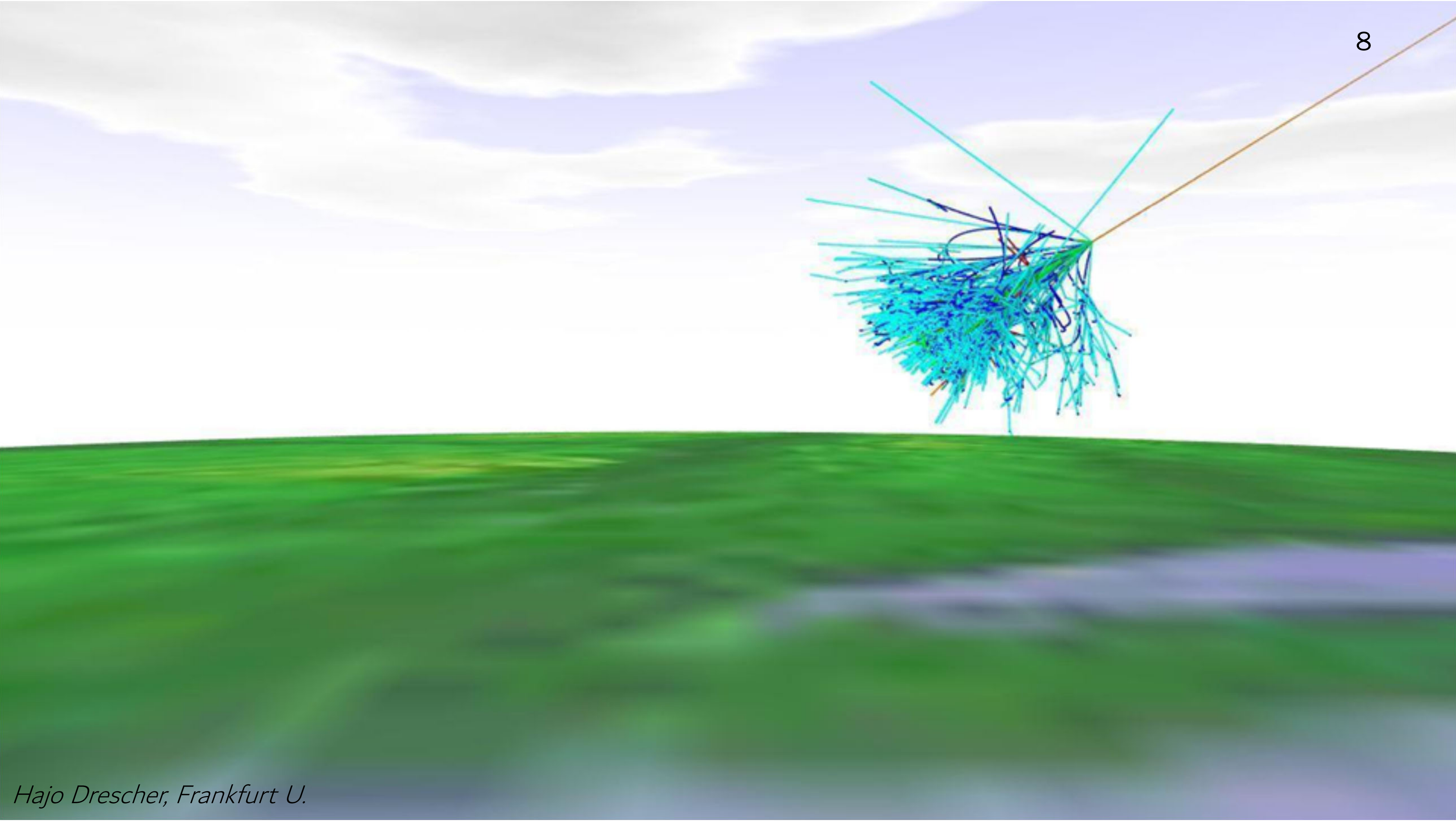
Hajo Drescher, Frankfurt U.

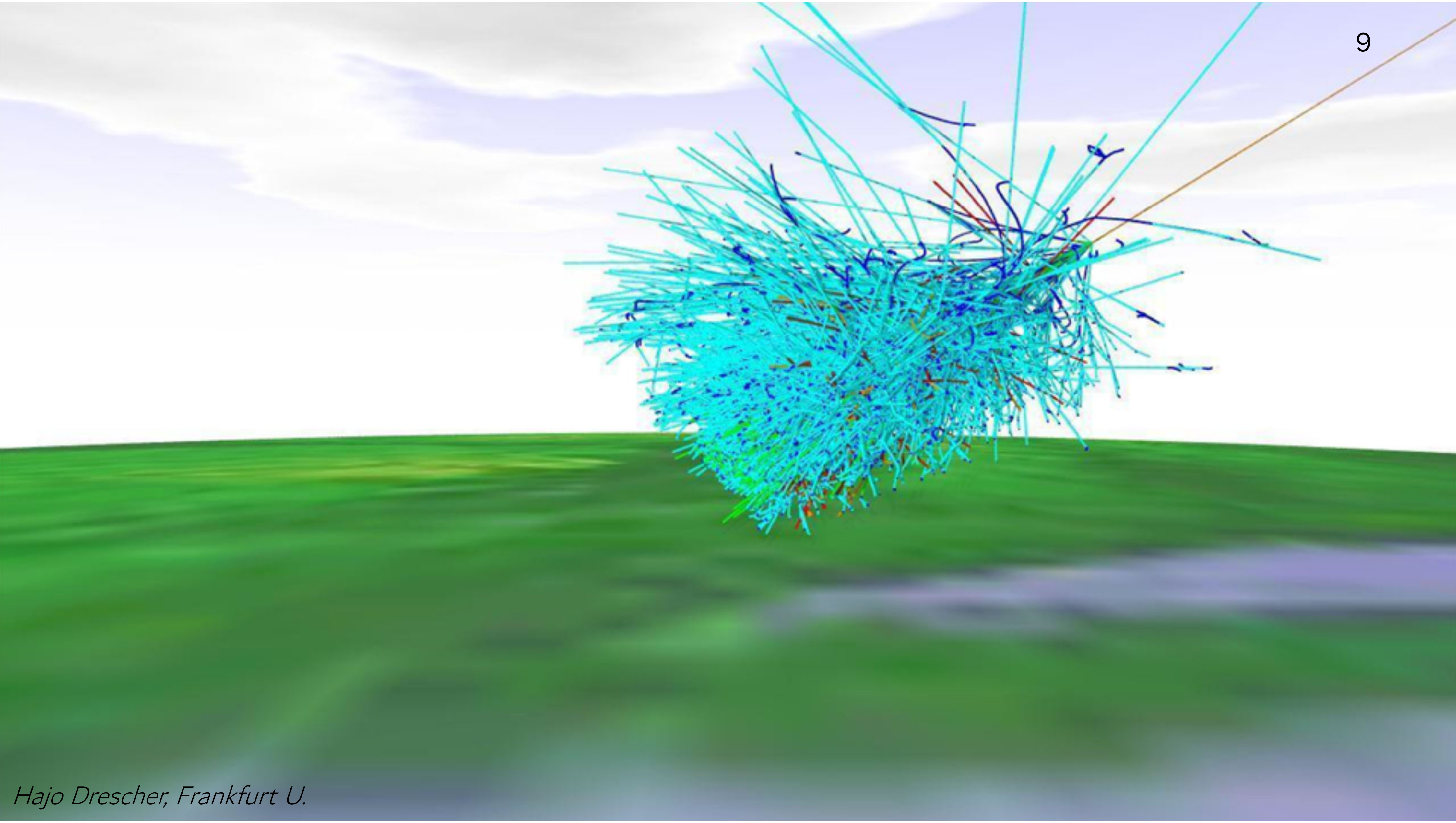

Hajo Drescher, Frankfurt U.

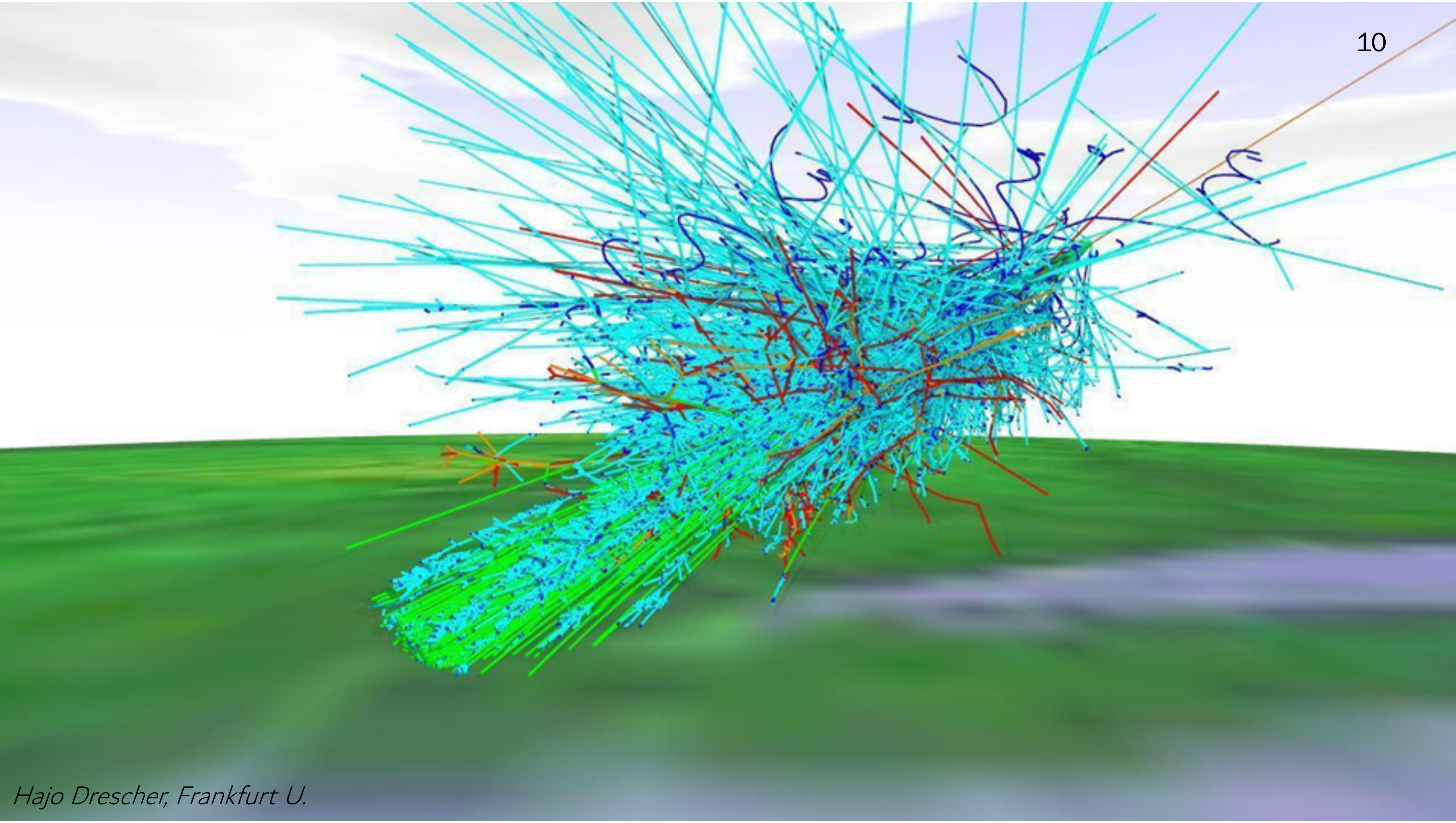

Hajo Drescher, Frankfurt U.

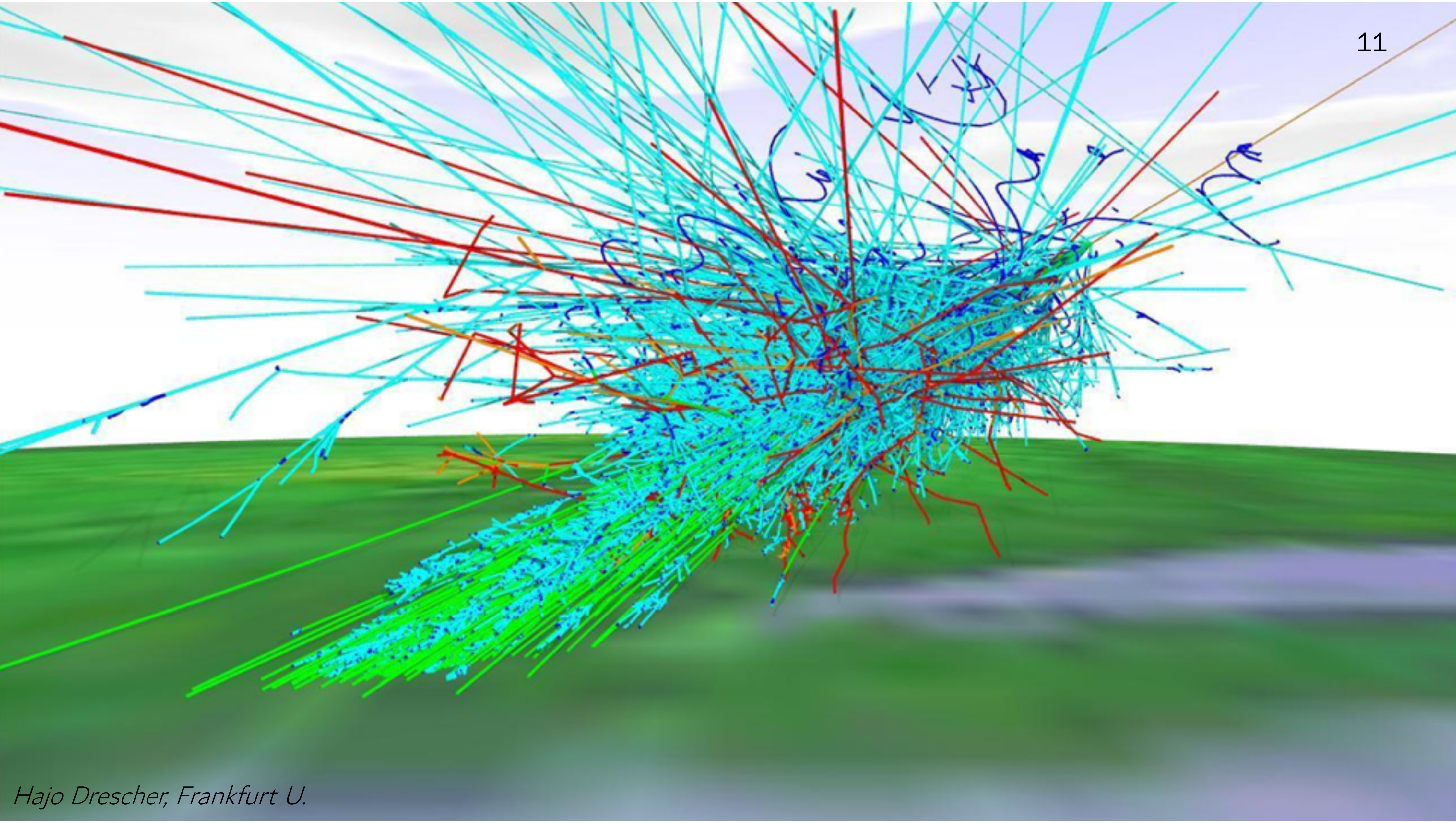

Hajo Drescher, Frankfurt U.

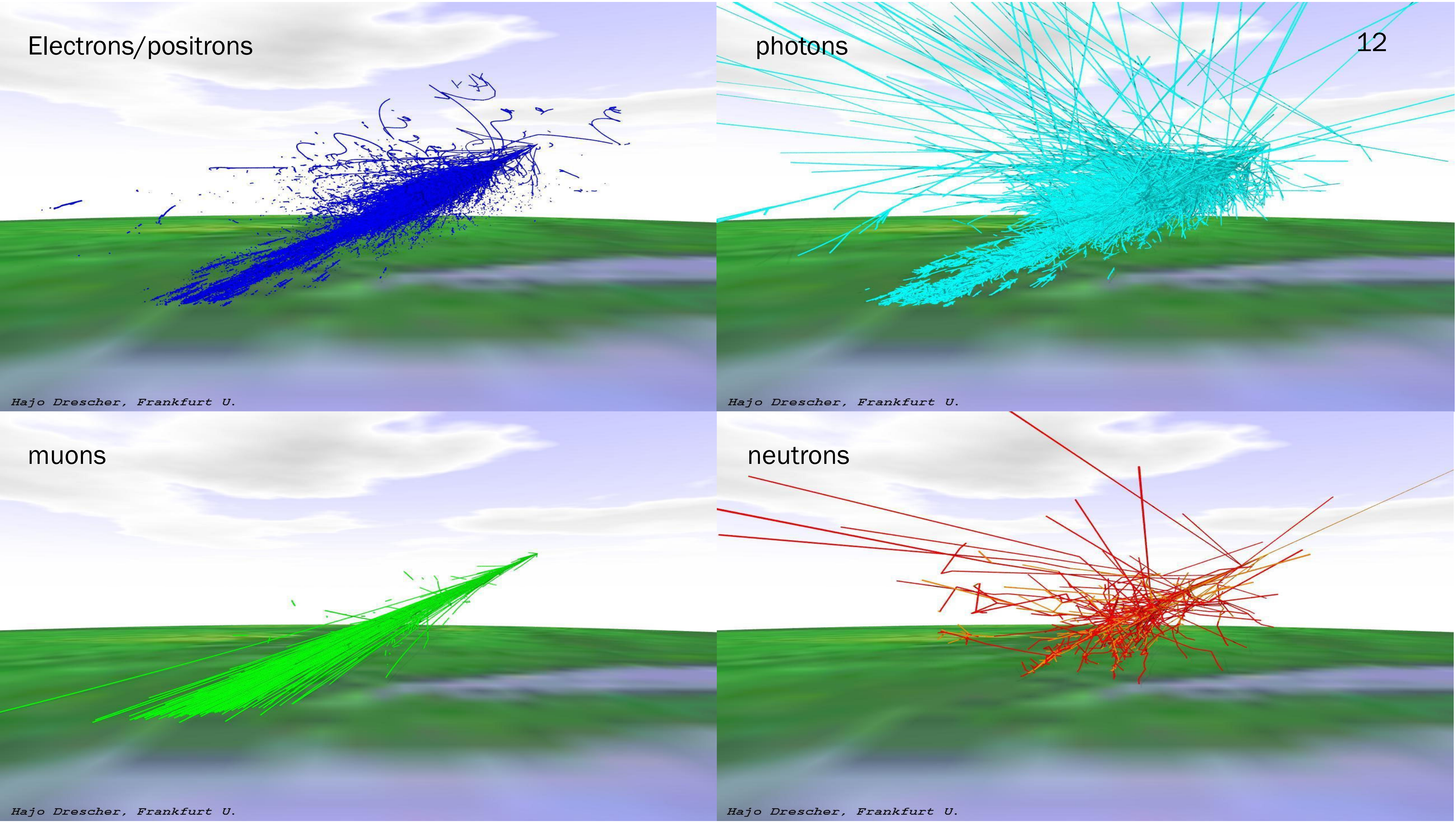
Electrons/positrons
Hajo Drescher, Frankfurt U.
photons
Hajo Drescher, Frankfurt U.
muons
Hajo Drescher, Frankfurt U.
neutrons
Hajo Drescher, Frankfurt U.

INTRODUCTION: STANDARD NEUTRON MONITOR (NM64)

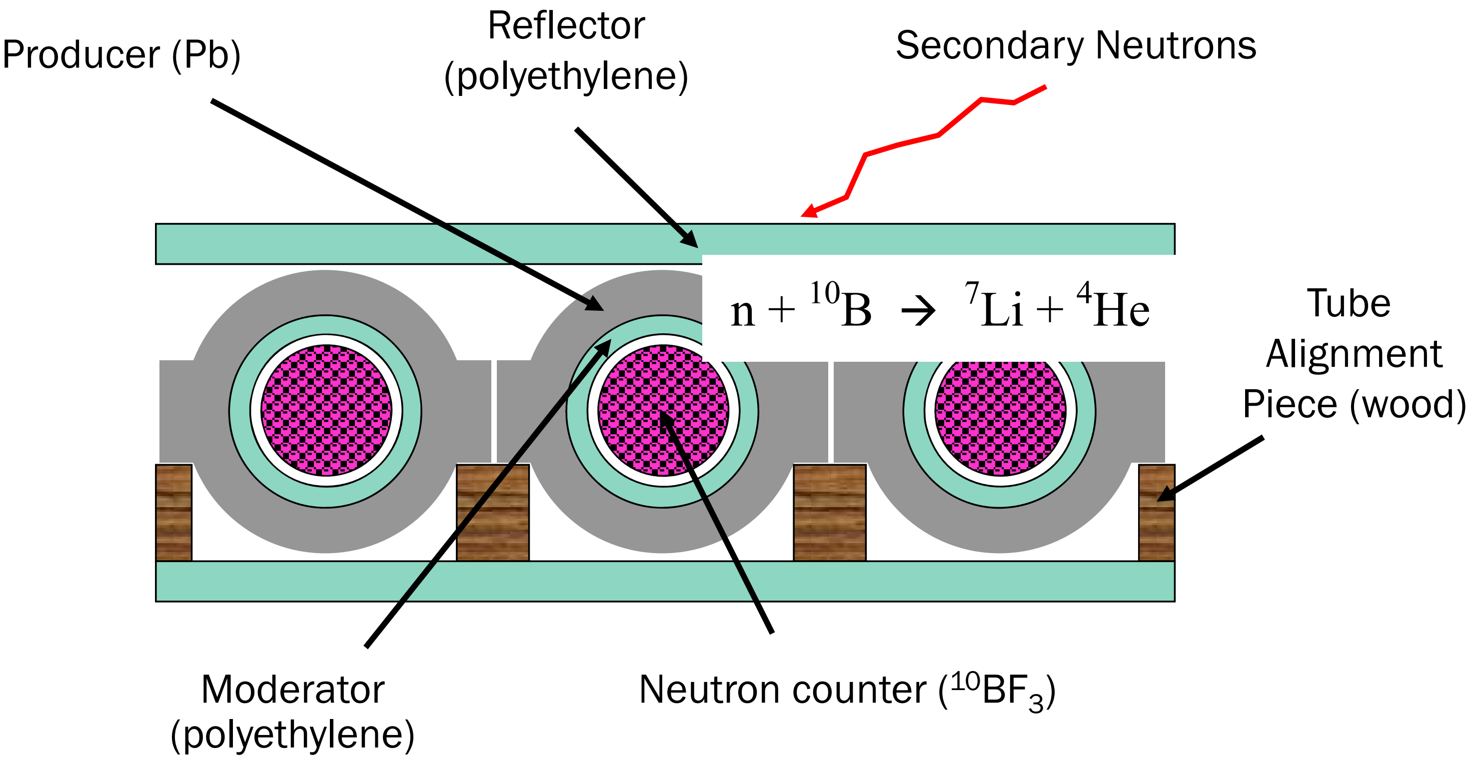

FIGURE 1 3NM64

INTRODUCTION: SEMI LEADED COUNTER

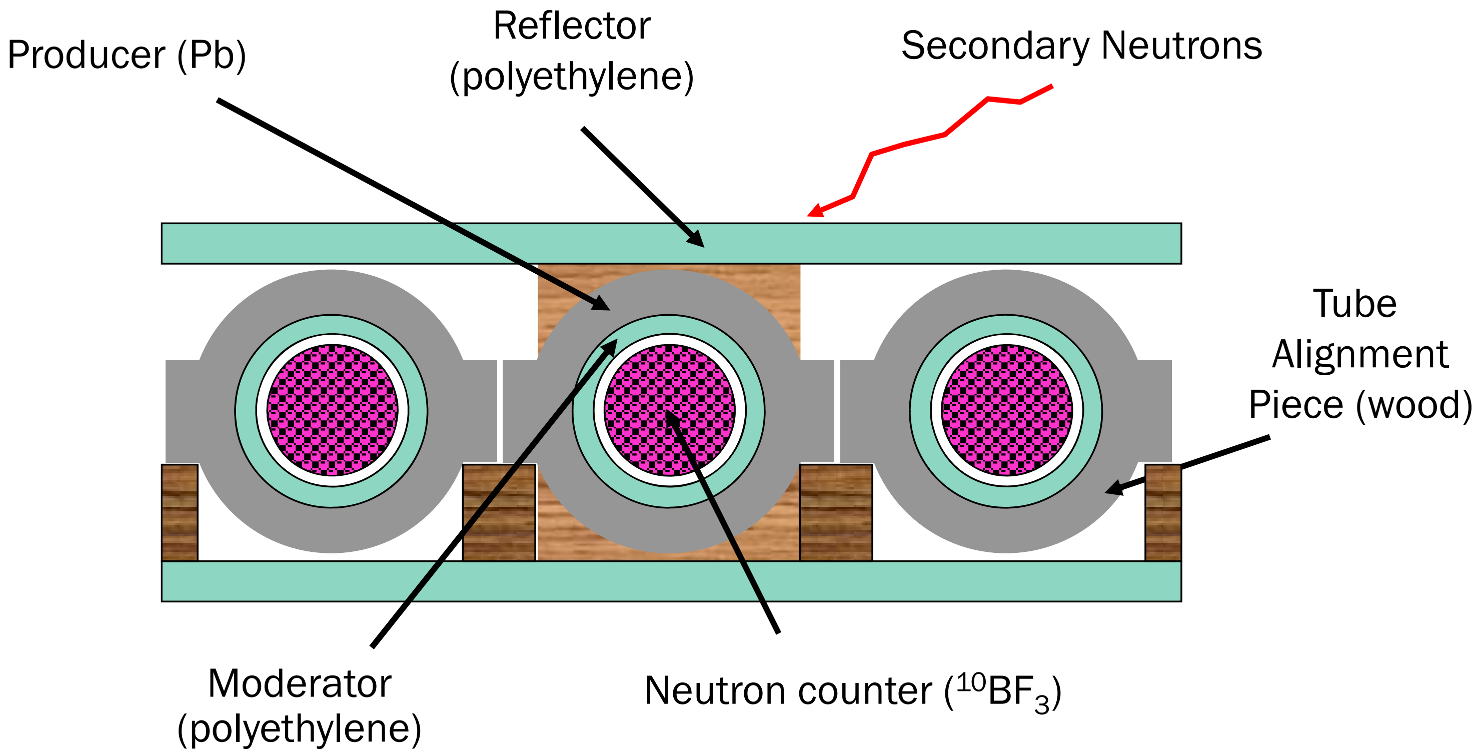

FIGURE 2 Semi leaded neutron detector

INTRODUCTION: BARE COUNTER

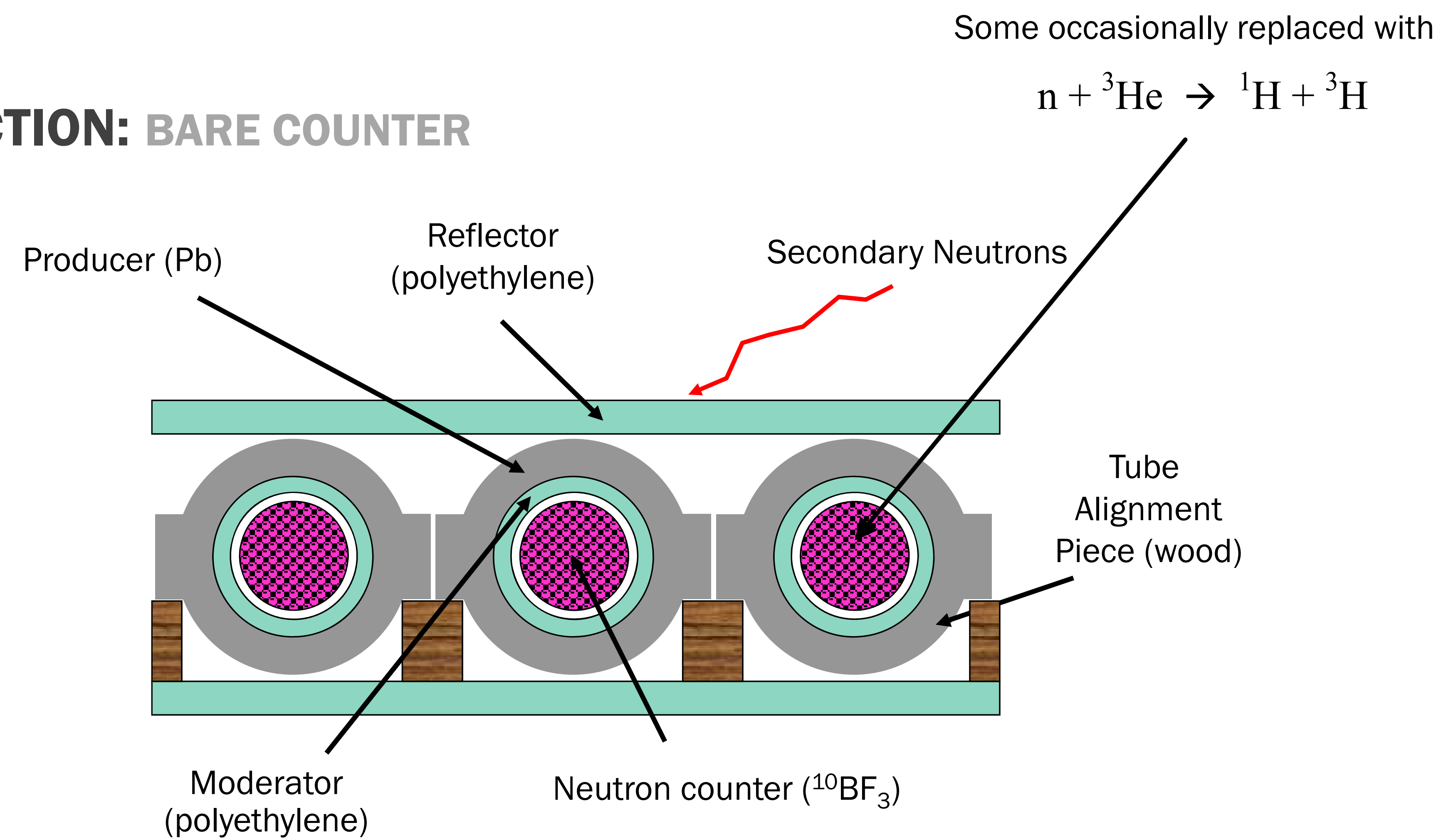

FIGURE 3 Semi leaded neutron detector

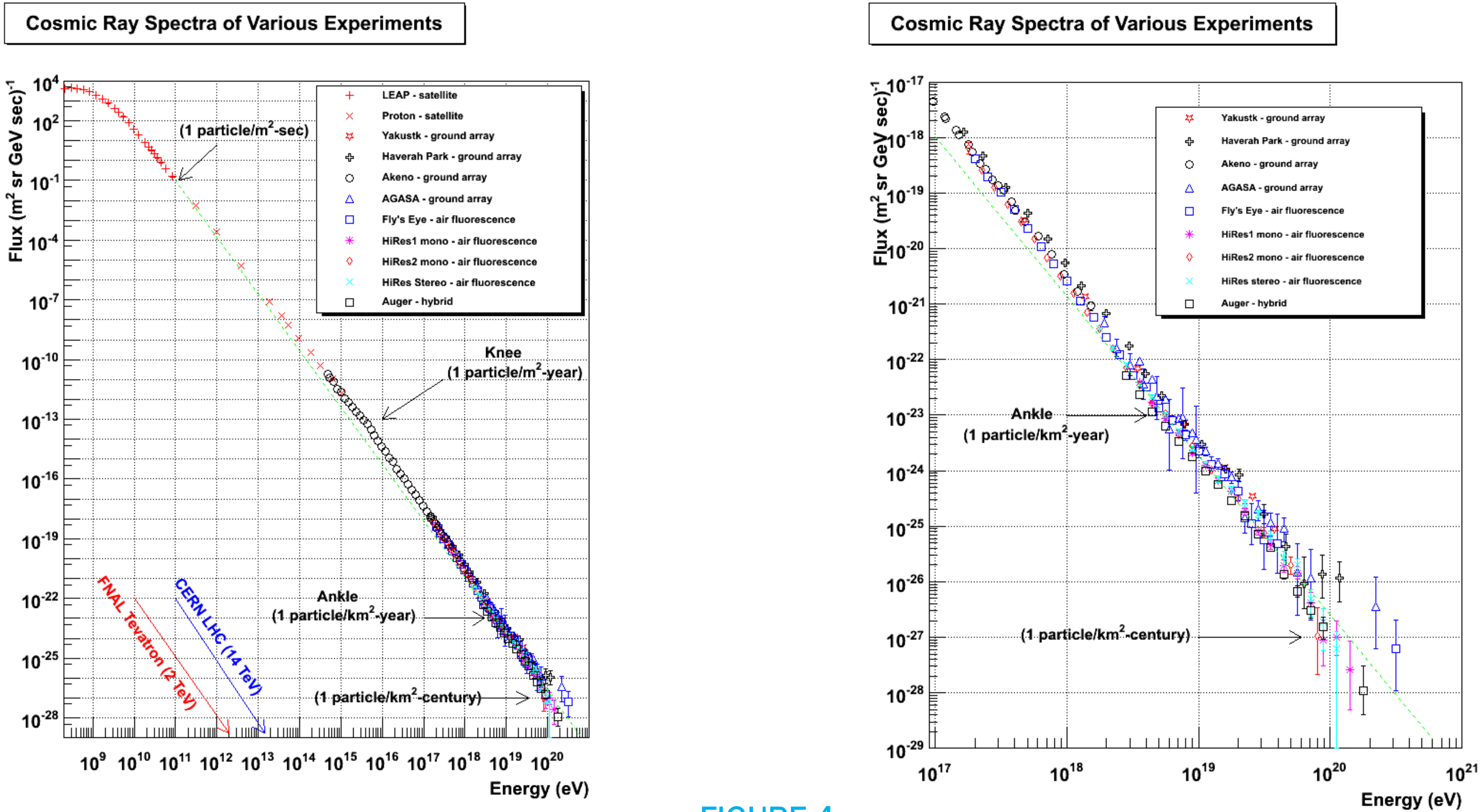

FIGURE 4

https://www.physics.utah.edu/~whanlon/spectrum.html

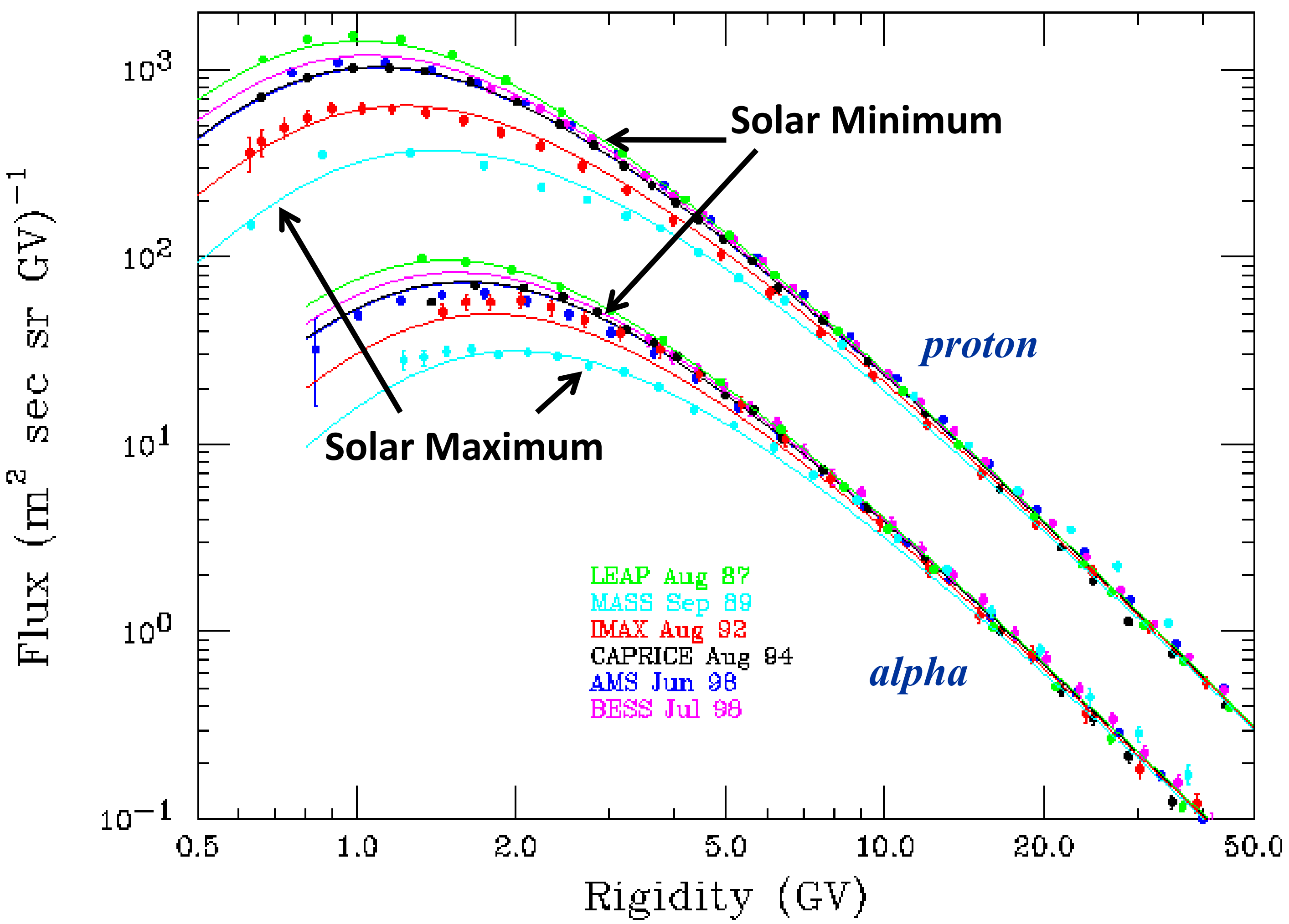
Solar Minimum
Solar Maximum
proton
alpha
LEAP Aug 87
MASS Sep 89
IMAX Aug 92
CAPRICE Aug 94
AMS Jun 98
BESS Jul 98
Flux (m2 sec sr GV)-1
Rigidity (GV)
0.5
1.0
2.0
5.0
10.0
20.0
50.0

FIGURE 5

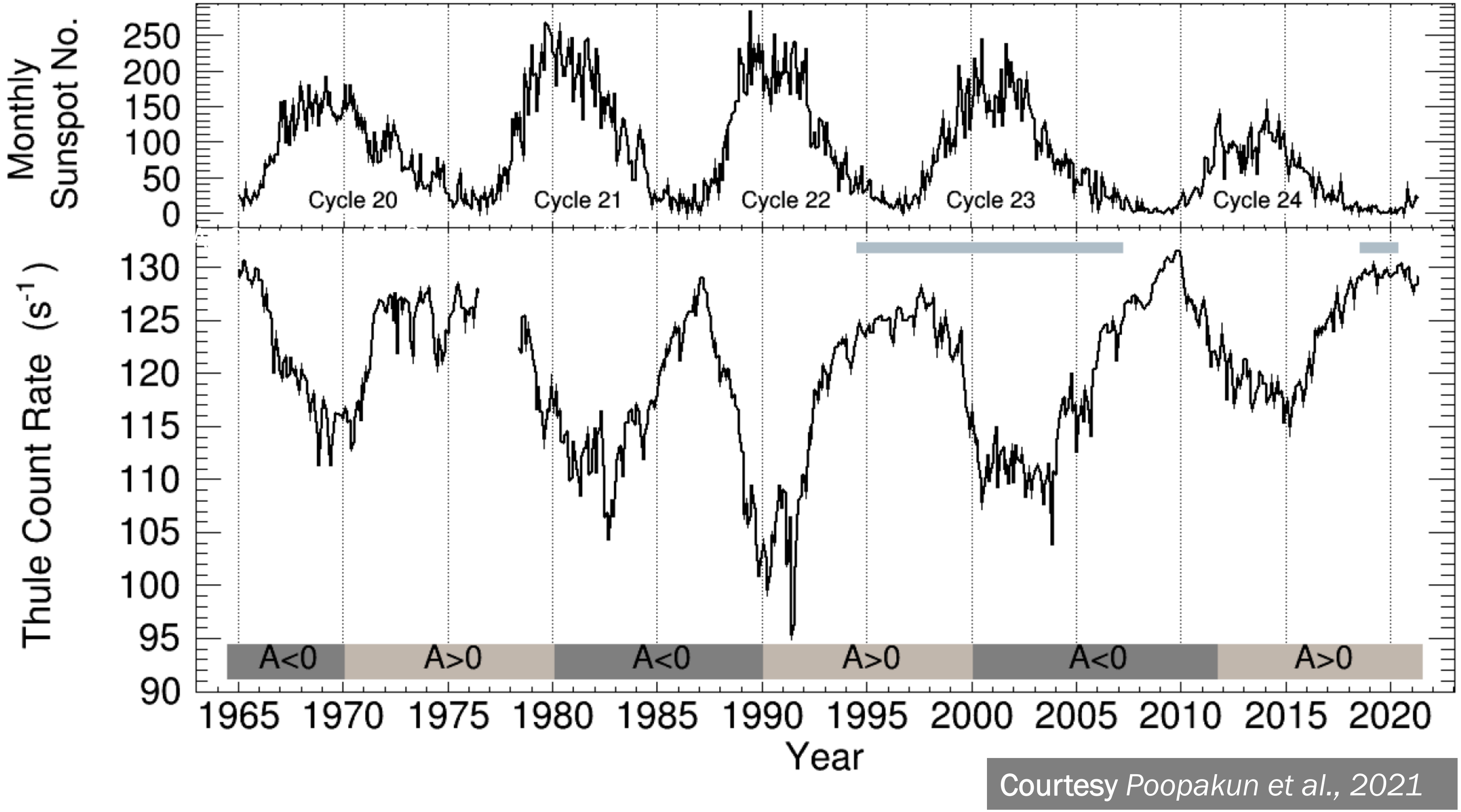

Figure 6 Solar modulation

FIXED NM STATIONS

PAM

25Dec 09:00 – 10:30 Hrs

MISS. KLEDSAI POOPAKUN

Comparative Analysis of Data from Neutron and Muon Detectors at Antarctica

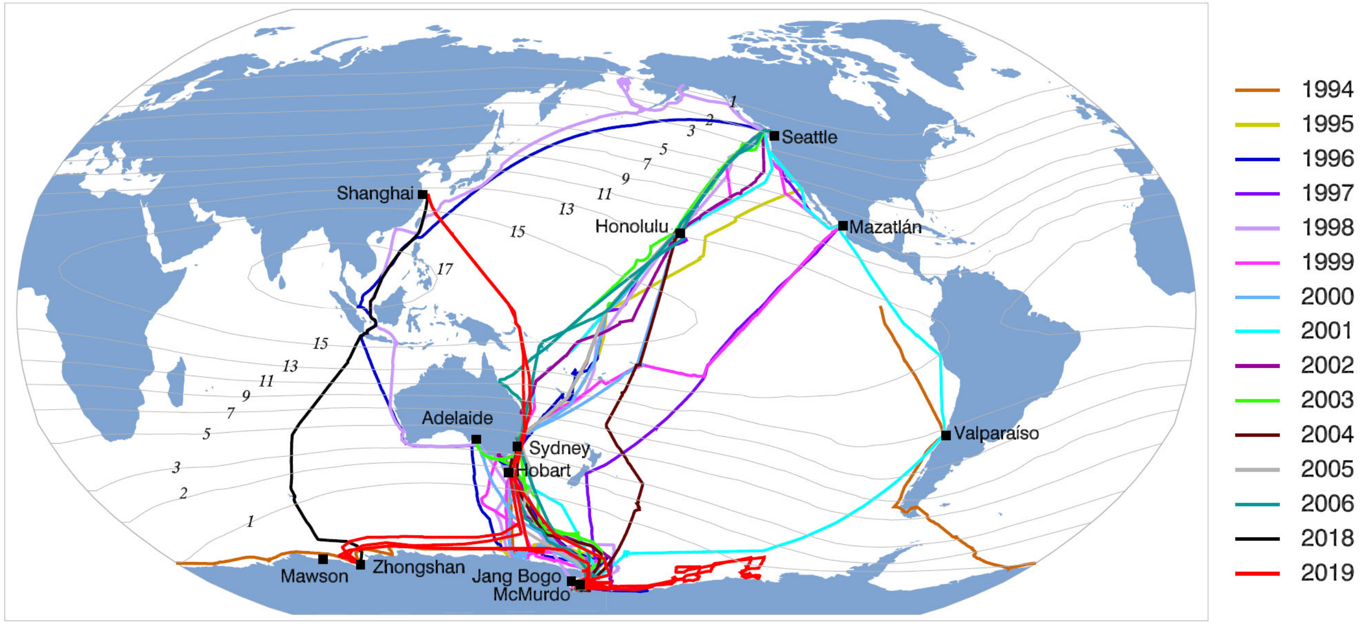

FIGURE 7 The track of the ship-borne neutron monitor latitude surveys for 1994-2007, and 2019-2020, superimposed on contours of the vertical cutoff rigidity (GV).

Courtesy *Poopakun et al., 2021*

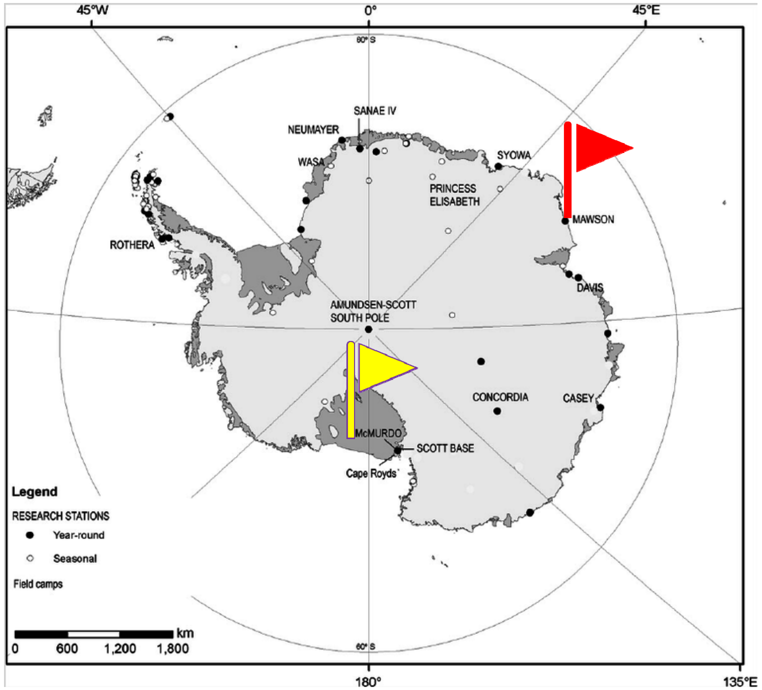

Kledsai also works on the data analysis of the Muon Telescope at Mawson, Antarctica

Taken photo by Pradiphat Muangha

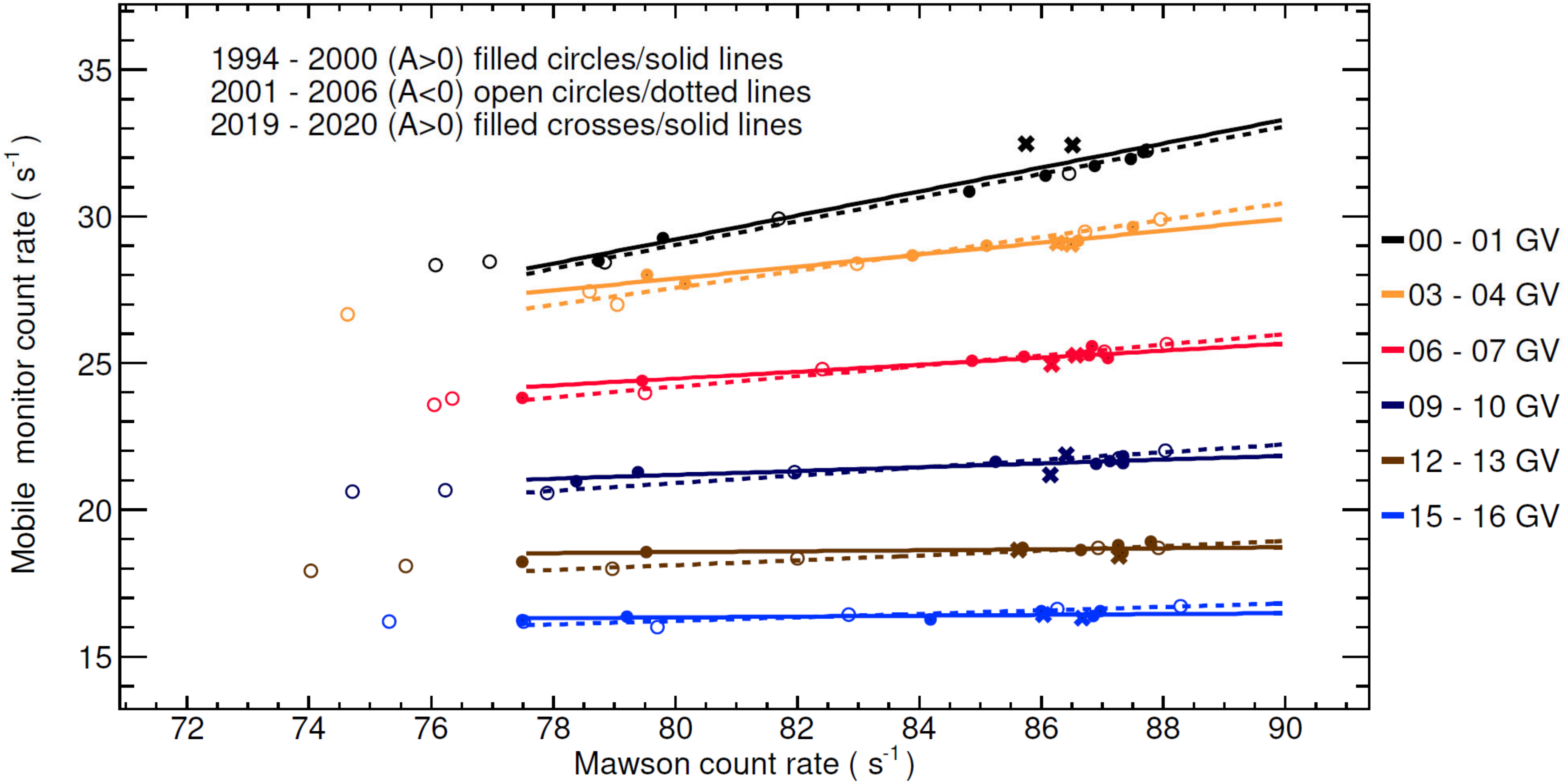

Figure 8 Regression of the mobile neutron monitor count rate in different apparent cutoff rigidity bins against the count rate of Mawson neutron monitor superimposing the data for different solar magnetic polarities.

Courtesy Poopakun et al., 2021

PLANS TO REPORT IN THE BOOTCAMP 2021 ARE:

- Update results about Mawson vs. mobile neutron monitor analysis
- In addition to the correlation work, Kledsai also has progress reports on the analysis of Muon detector!

Jumbo

25 Dec 11:00 – 12:30 Hrs

MR. EKAWIT KITTIYA

Cosmic Ray Flux Correlation between McMurdo and Jang Bogo Stations

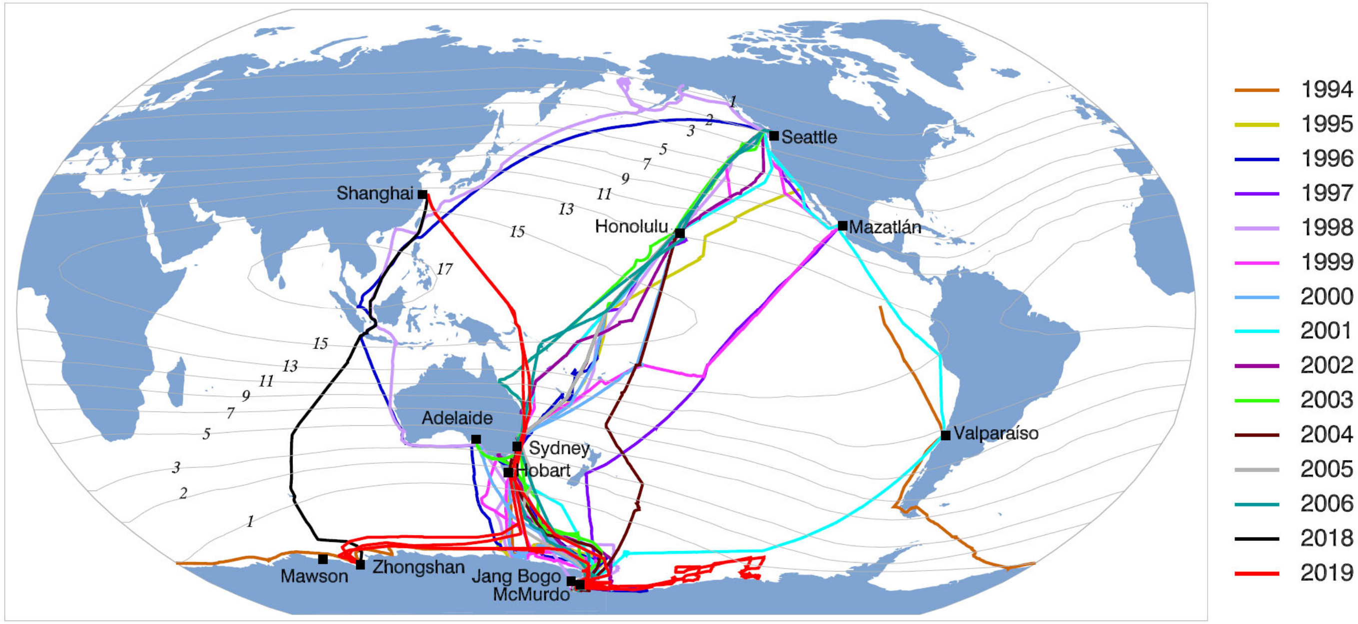

FIGURE 9 The track of the ship-borne neutron monitor latitude surveys for 1994-2007, and 2019-2020, superimposed on contours of the vertical cutoff rigidity (GV).

Courtesy Poopakun et al., 2021

McMurdo and Jang Bogo Stations

Figure 10 Bird-eye view of McMurdo Station (courtesy: nmdb database)

Figure 11 Bird-eye view of Jang Bogo Station (courtesy: KOPRI)

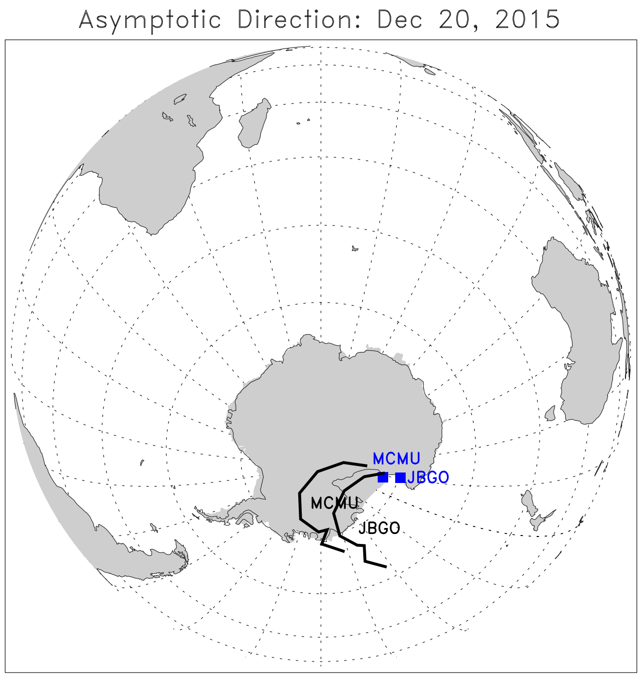

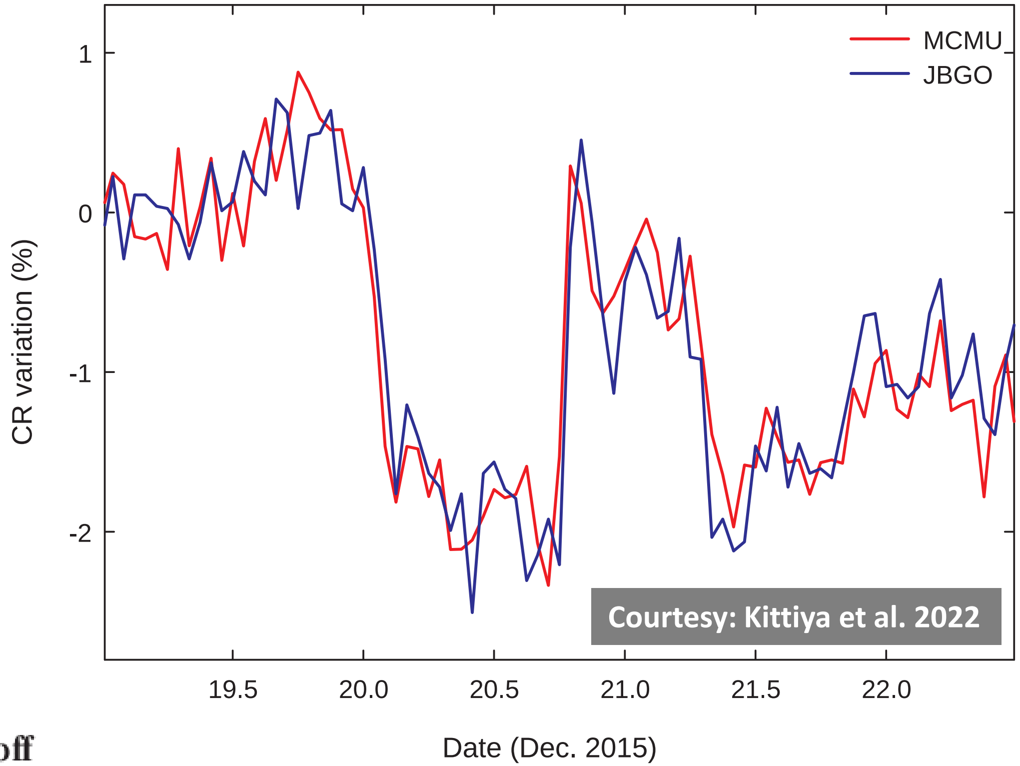

Station	Location		Altitude	Cutoff Rigidity
	Geographic	Geomagnetic		
Jang Bogo	74° 37.4´S 164° 13.7´E	77° 3´S 85° 18´W	29 m	< 0.2 GV
McMurdo	77° 51´S 166° 40´E	78° 58.8´S 72° 22.8´E	48 m	< 0.2 GV

- Distance apart ~ 300 km
- Similar Geomagnetic latitude, but different Geomagnetic longitude

FIGURE 12 LEFT: Asymptotic directions on December 20, 2015 at 18:00 UT.
RIGHT: Small scale features as seen by Jang Bogo and McMurdo neutron monitors.

METHODOLOGY

- Initial Processing
  - Datasets are 10-second data from December 16, 2015, to October 20, 2016
  - We made histograms to remove clear outliers beyond SD $\pm 4.5\sigma$ from 24-hr moving average
  - Filled data gaps with the mean of the rest data
  - Calculate Local Time for each station's location from LT = UT + LON/15°. We applied both UT & LT in our analysis
- Barometric Pressure Correction

Station	Barometric Pressure Coef. (%/mmHg)	Reference Pressure (mmHg)
Jang Bogo	1.00090	733.6
McMurdo	0.99994	730.0

- Calculate relative values from $r = \frac{(c - \bar{c})}{\sigma}$
- Determine auto- & cross-correlation value (cf) from $cf[\tau] = \sum_{m=0}^{N-1} r_1[m] \cdot r_2[\tau + m]$
- Optimize reasonable linear regression fit to find time lag (τ)

Autocorrelation

MCMU-MCMU

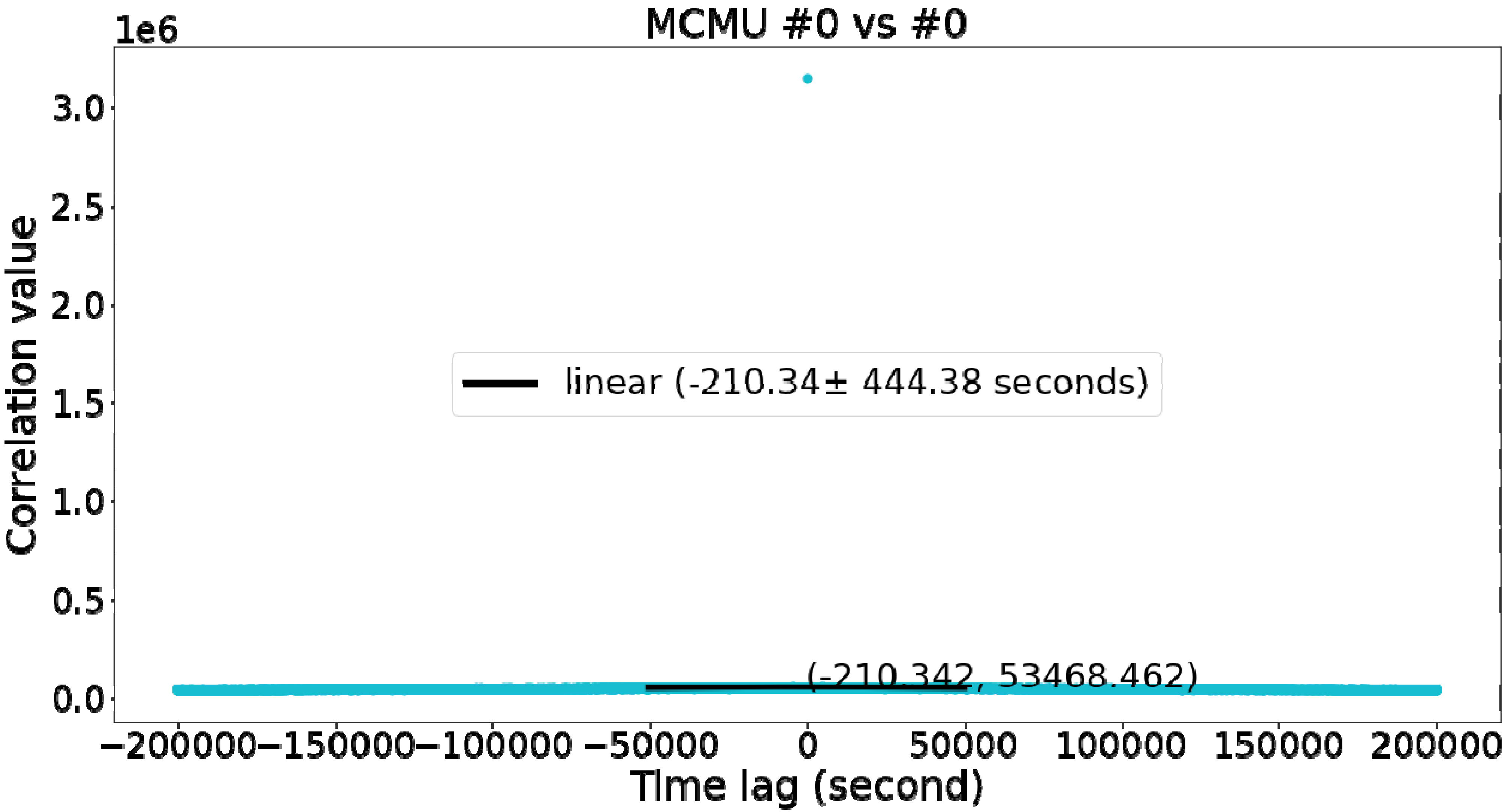
MCMU #0 vs #0
1e6
3.0
2.5
2.0
1.5
1.0
0.5
0.0
Correlation value
linear (-210.34± 444.38 seconds)
(-210.342, 53468.462)
−200000
−150000
−100000
−50000
0
50000
100000
150000
200000
Time lag (second)

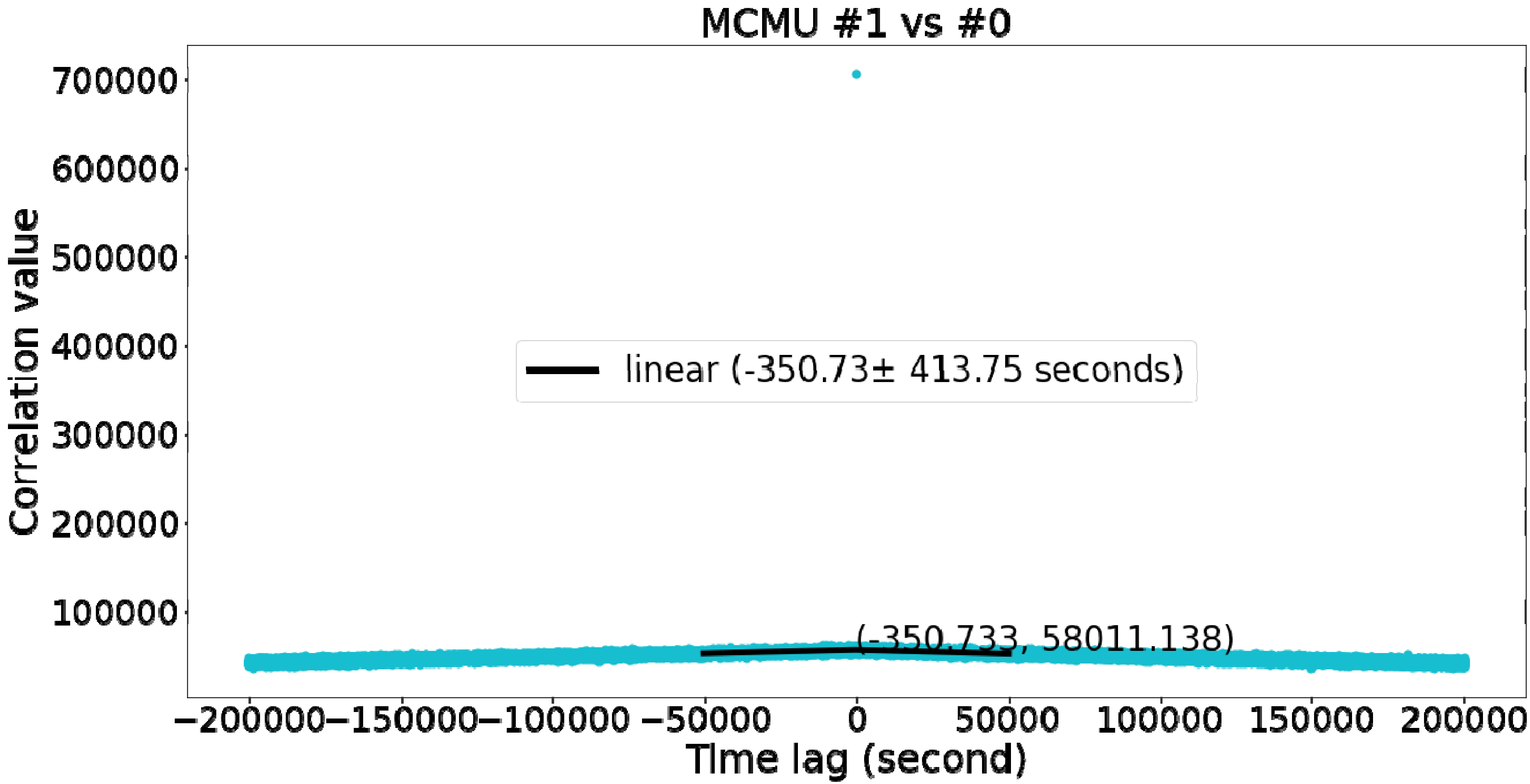
MCMU #1 vs #0
Correlation value
700000
600000
500000
400000
300000
200000
100000
linear (-350.73± 413.75 seconds)
(-350.733, 58011.138)
−200000
−150000
−100000
−50000
0
50000
100000
150000
200000
Time lag (second)

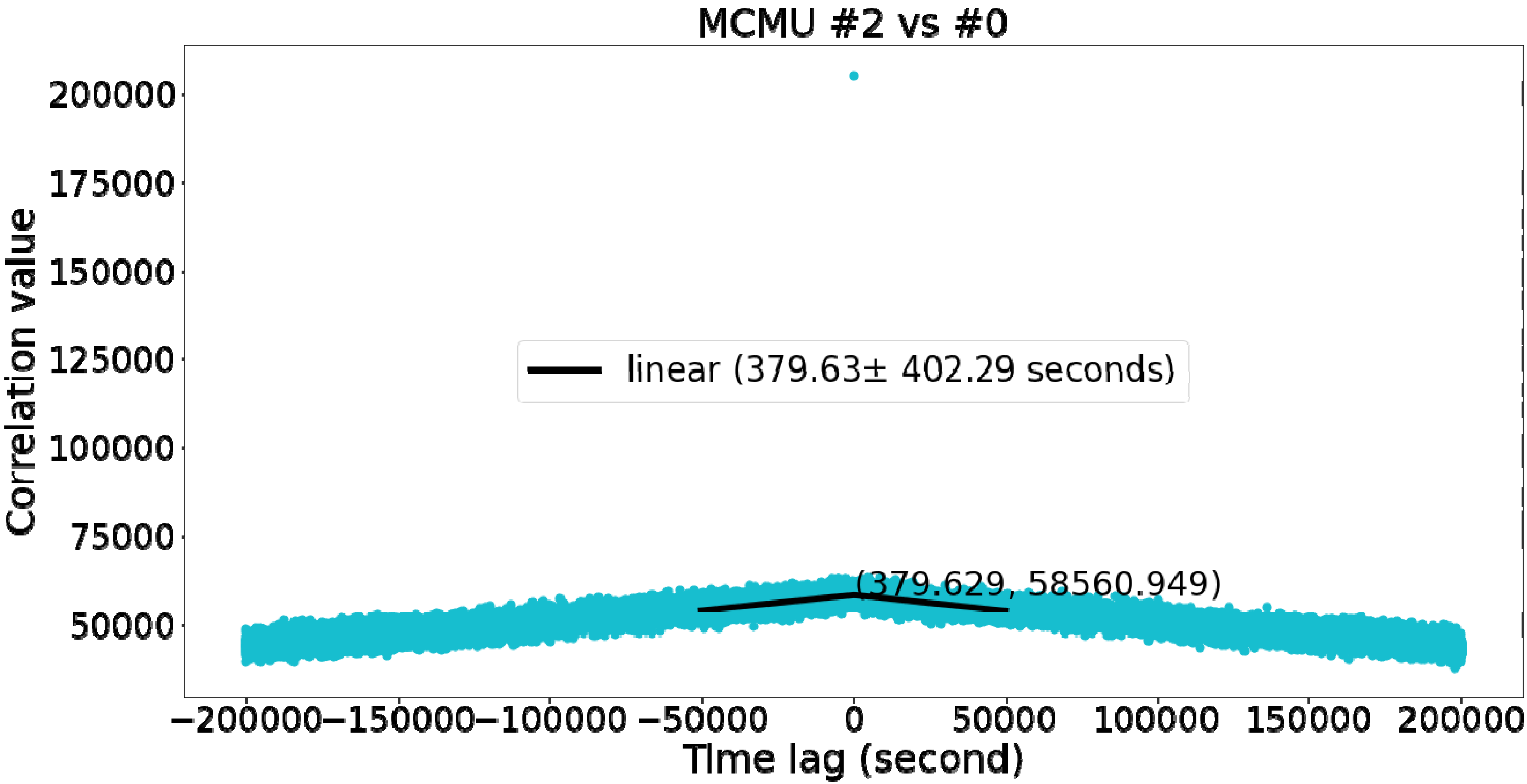
MCMU #2 vs #0
linear (379.63± 402.29 seconds)
(379.629, 58560.949)
Correlation value
Time lag (second)
200000
175000
150000
125000
100000
75000
50000
−200000
−150000
−100000
−50000
0
50000
100000
150000
200000

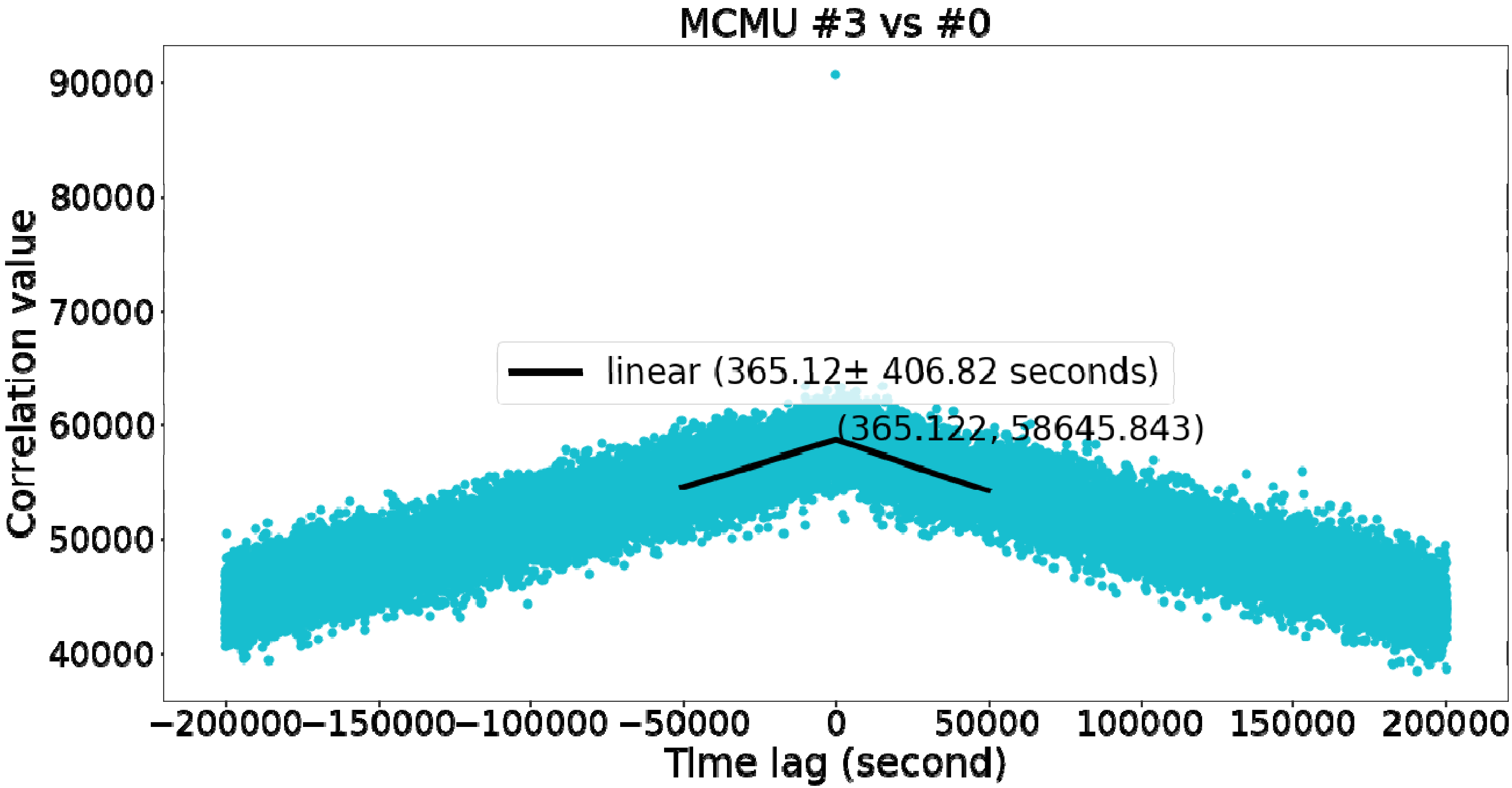
MCMU #3 vs #0
90000
80000
70000
60000
50000
40000
Correlation value
linear (365.12± 406.82 seconds)
(365.122, 58645.843)
−200000
−150000
−100000
−50000
0
50000
100000
150000
200000
Time lag (second)

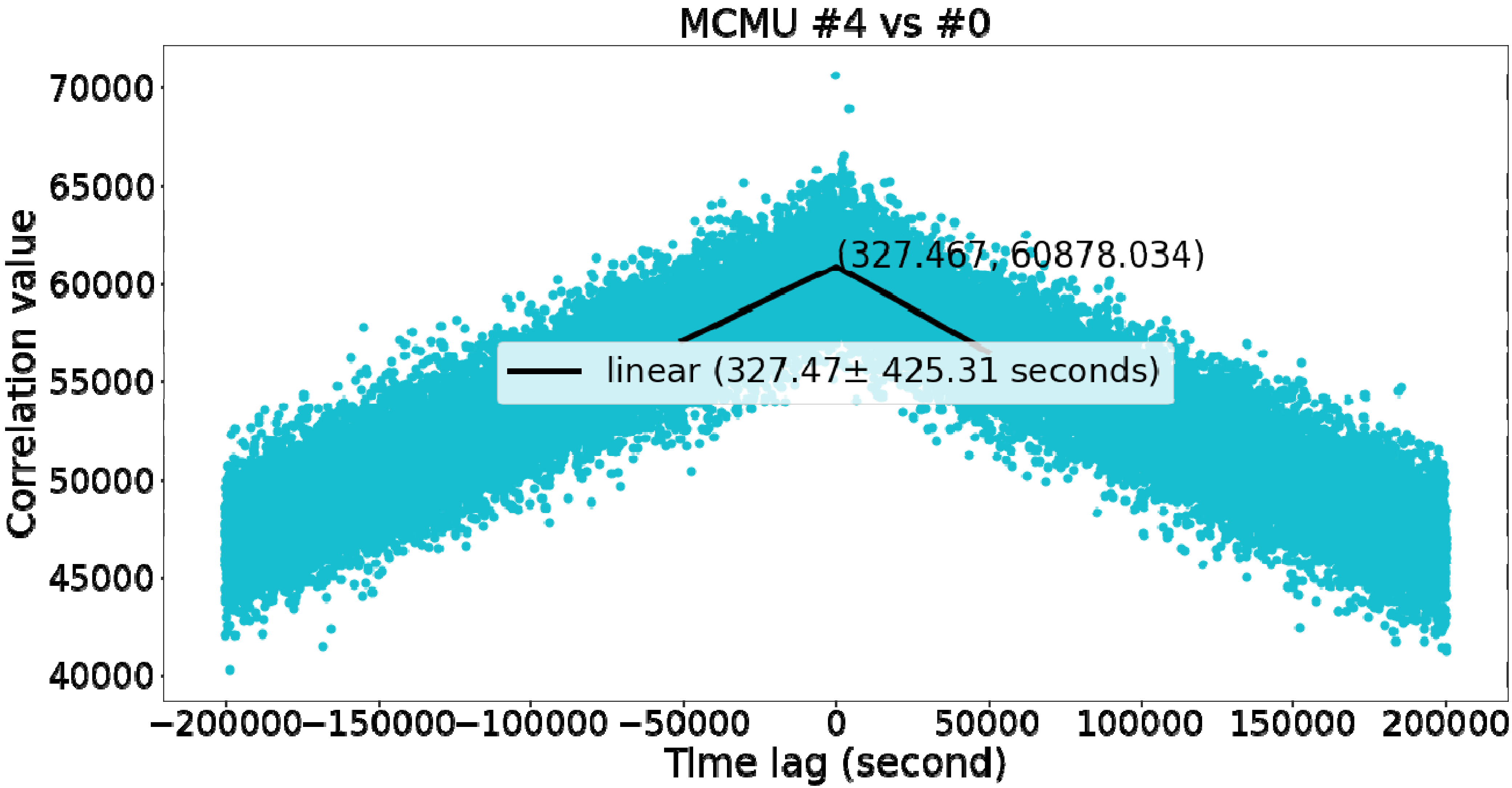
MCMU #4 vs #0
Correlation value
70000
65000
60000
55000
50000
45000
40000
(327.467, 60878.034)
linear (327.47± 425.31 seconds)
−200000
−150000
−100000
−50000
0
50000
100000
150000
200000
TIme lag (second)

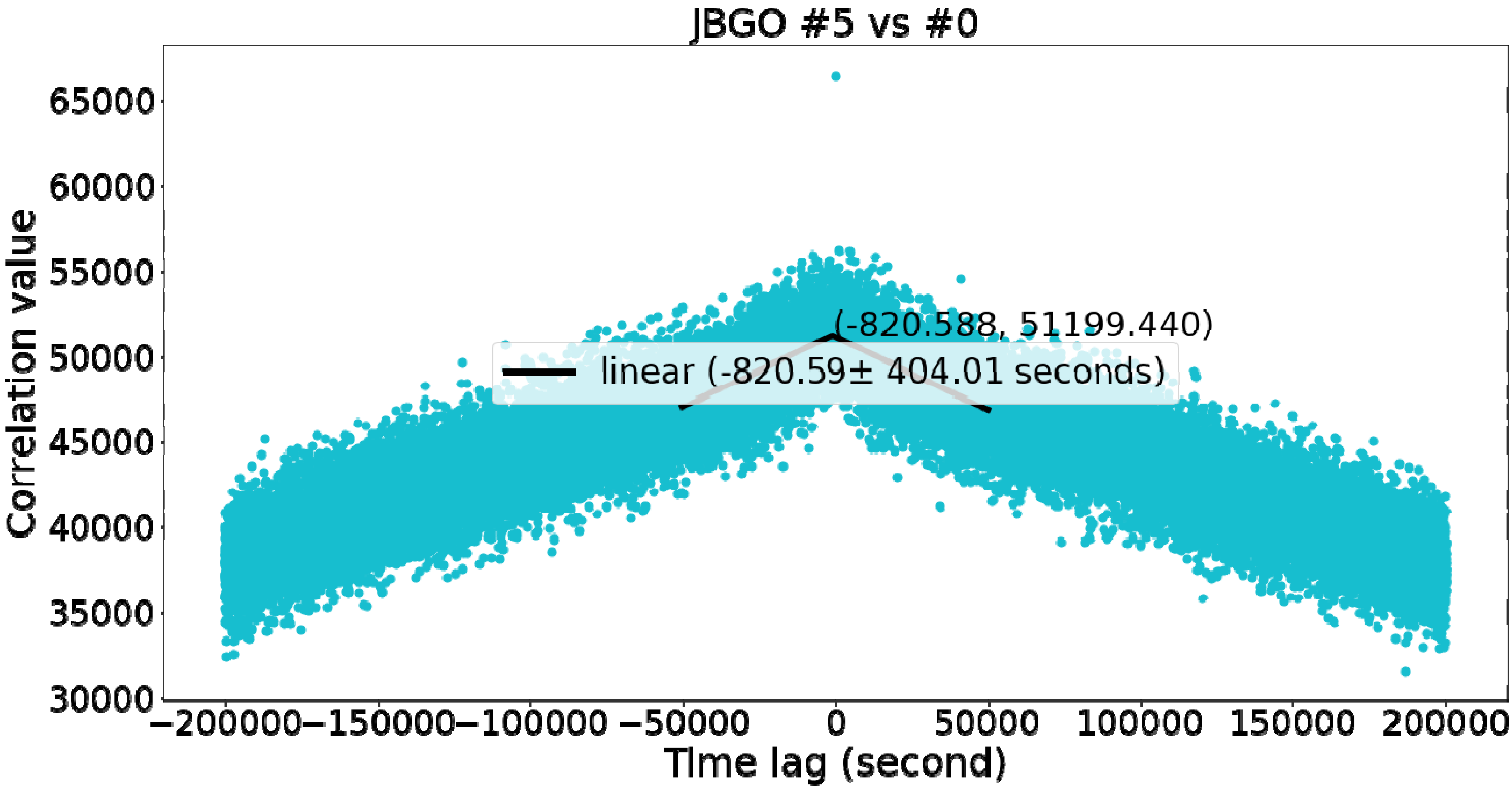
JBGO #5 vs #0
(-820.588, 51199.440)
linear (-820.59± 404.01 seconds)
Correlation value
65000
60000
55000
50000
45000
40000
35000
30000
−200000
−150000
−100000
−50000
0
50000
100000
150000
200000
TIme lag (second)

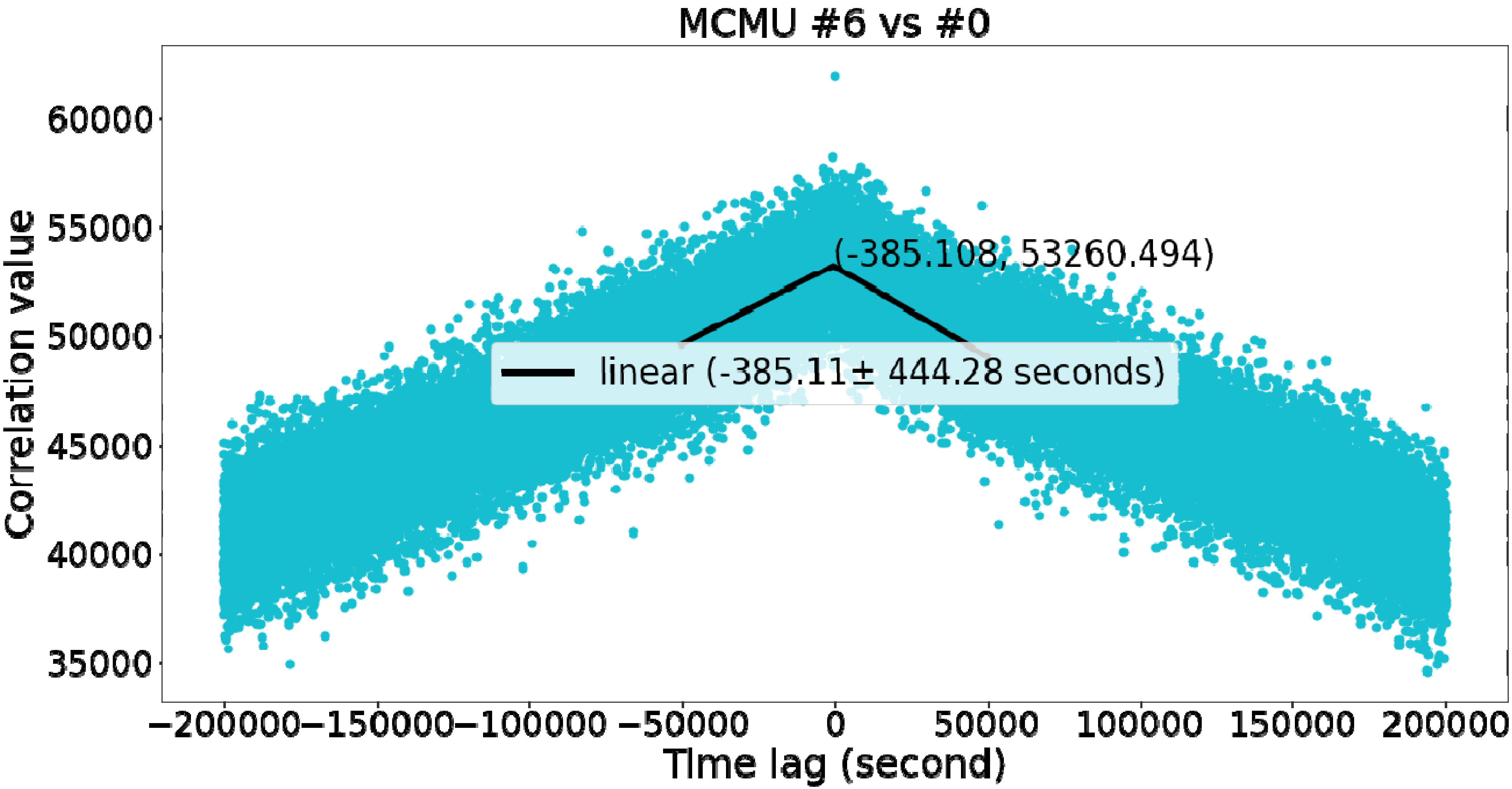
MCMU #6 vs #0
(-385.108, 53260.494)
linear (-385.11± 444.28 seconds)
Correlation value
60000
55000
50000
45000
40000
35000
−200000
−150000
−100000
−50000
0
50000
100000
150000
200000
TIme lag (second)

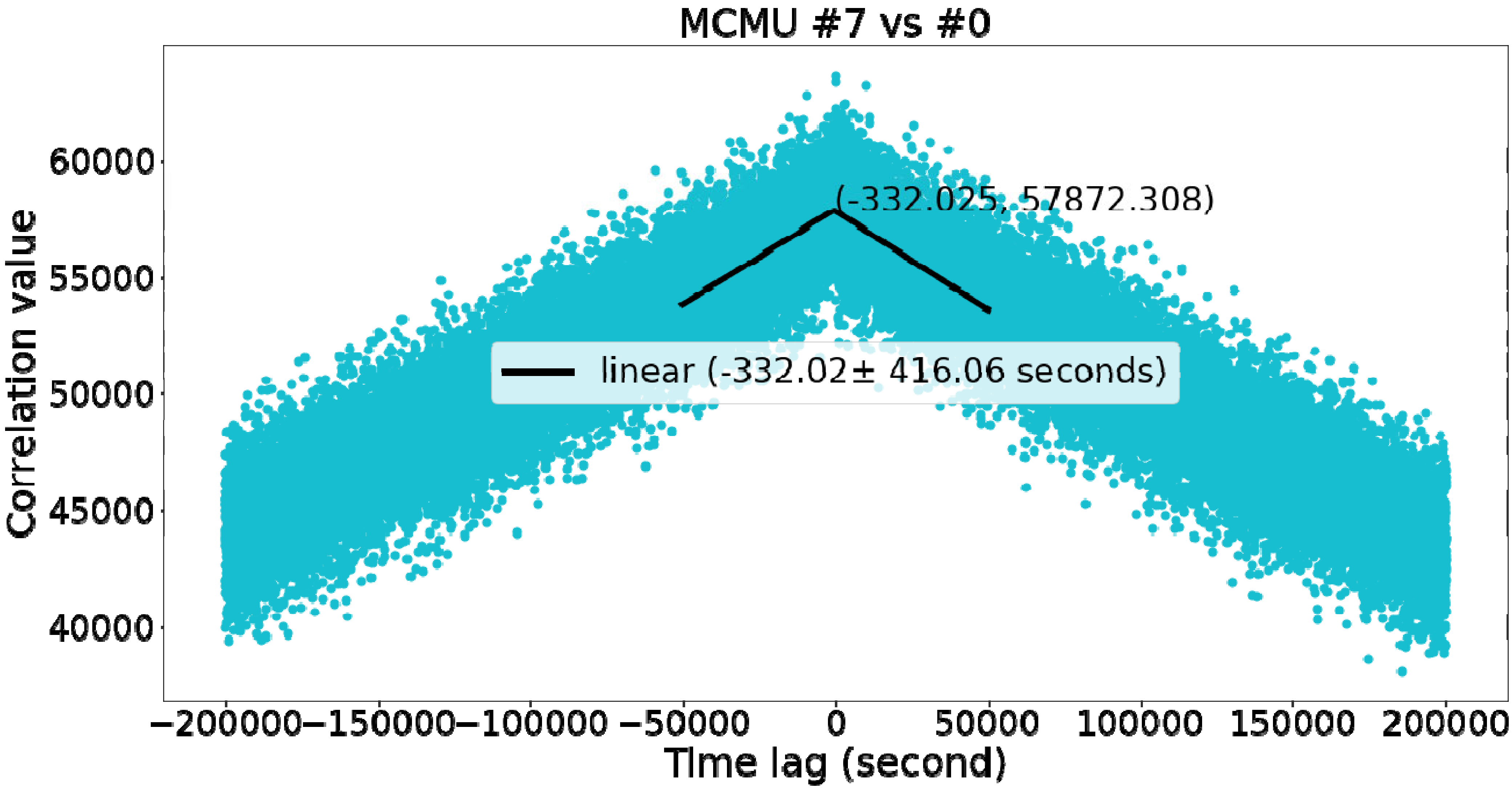
MCMU #7 vs #0
Correlation value
60000
55000
50000
45000
40000
(-332.025, 57872.308)
linear (-332.02± 416.06 seconds)
−200000
−150000
−100000
−50000
0
50000
100000
150000
200000
TIme lag (second)

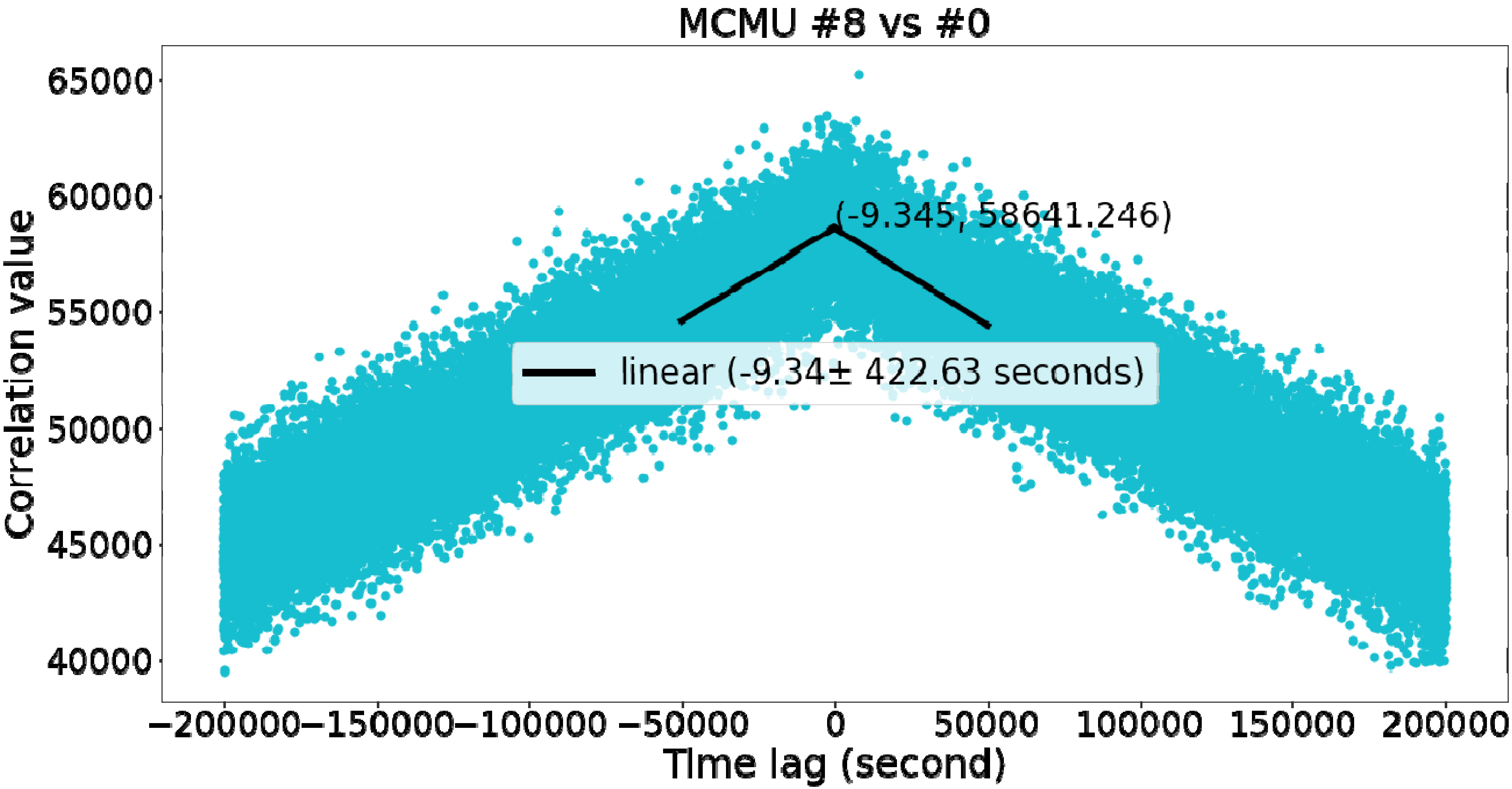
MCMU #8 vs #0
Correlation value
65000
60000
55000
50000
45000
40000
−200000
−150000
−100000
−50000
0
50000
100000
150000
200000
Time lag (second)
(-9.345, 58641.246)
linear (-9.34± 422.63 seconds)

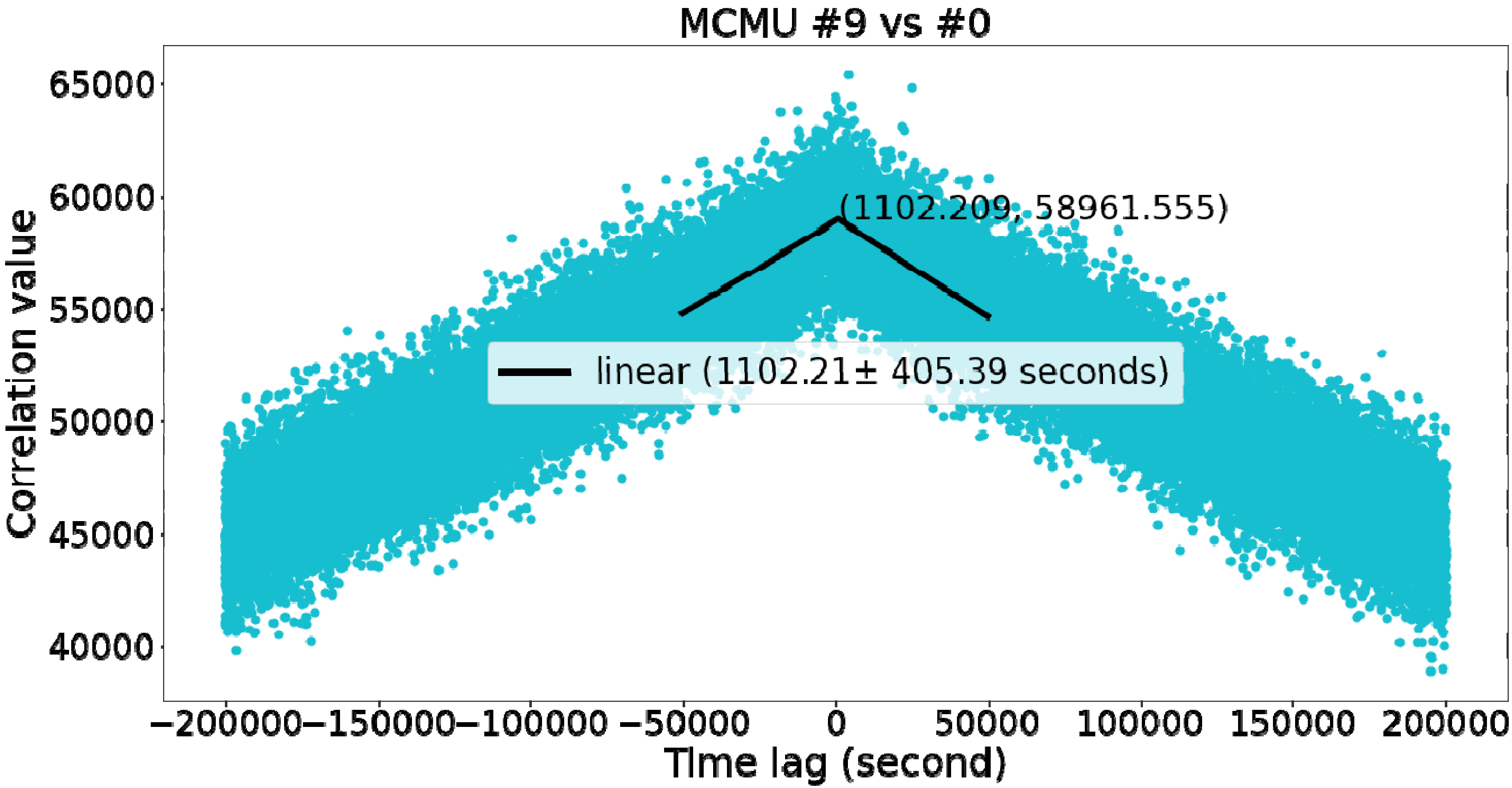
MCMU #9 vs #0
Correlation value
65000
60000
55000
50000
45000
40000
(1102.209, 58961.555)
linear (1102.21± 405.39 seconds)
−200000
−150000
−100000
−50000
0
50000
100000
150000
200000
TIme lag (second)

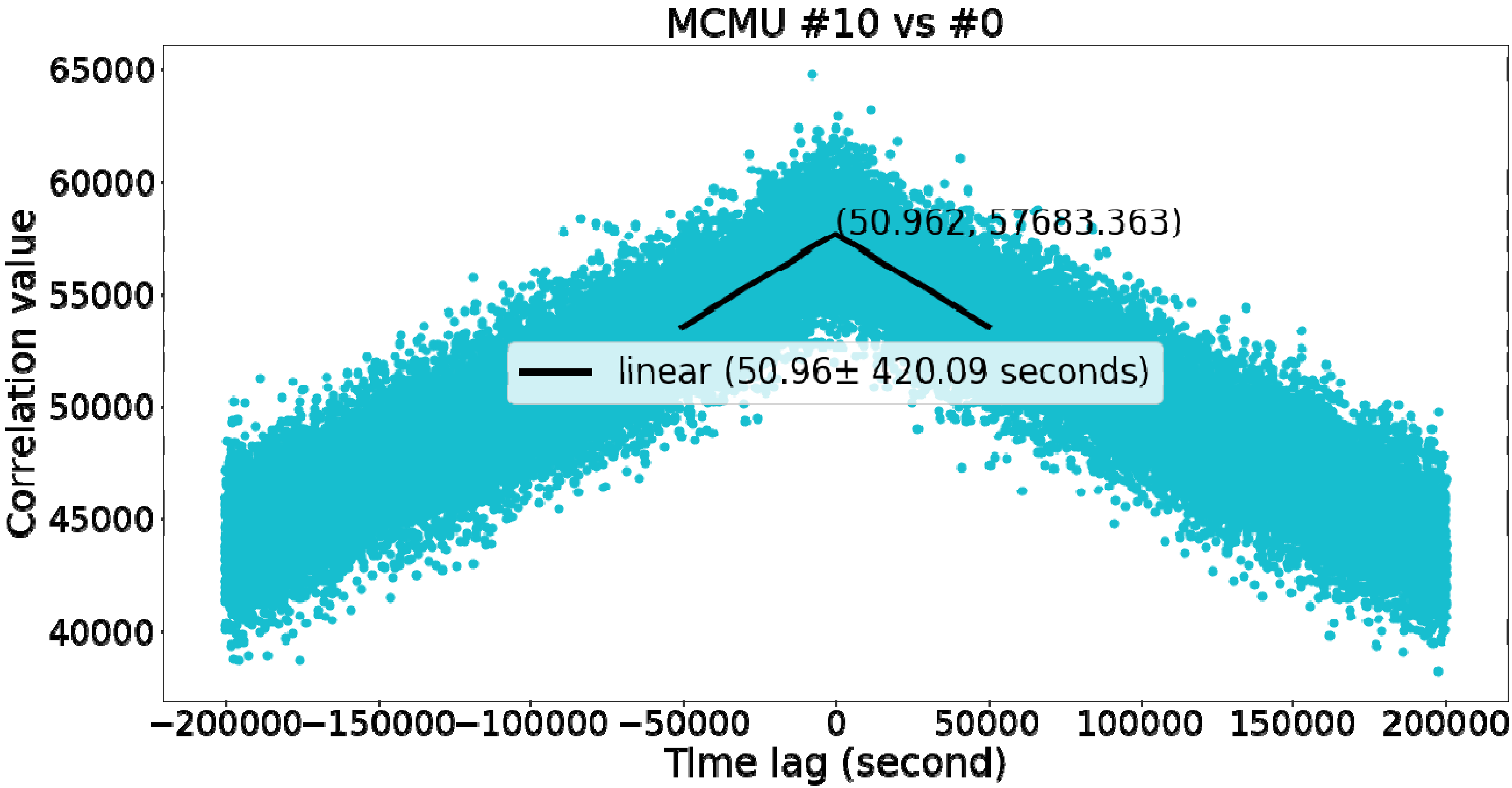
MCMU #10 vs #0
(50.962, 57683.363)
linear (50.96± 420.09 seconds)
Correlation value
65000
60000
55000
50000
45000
40000
−200000
−150000
−100000
−50000
0
50000
100000
150000
200000
TIme lag (second)

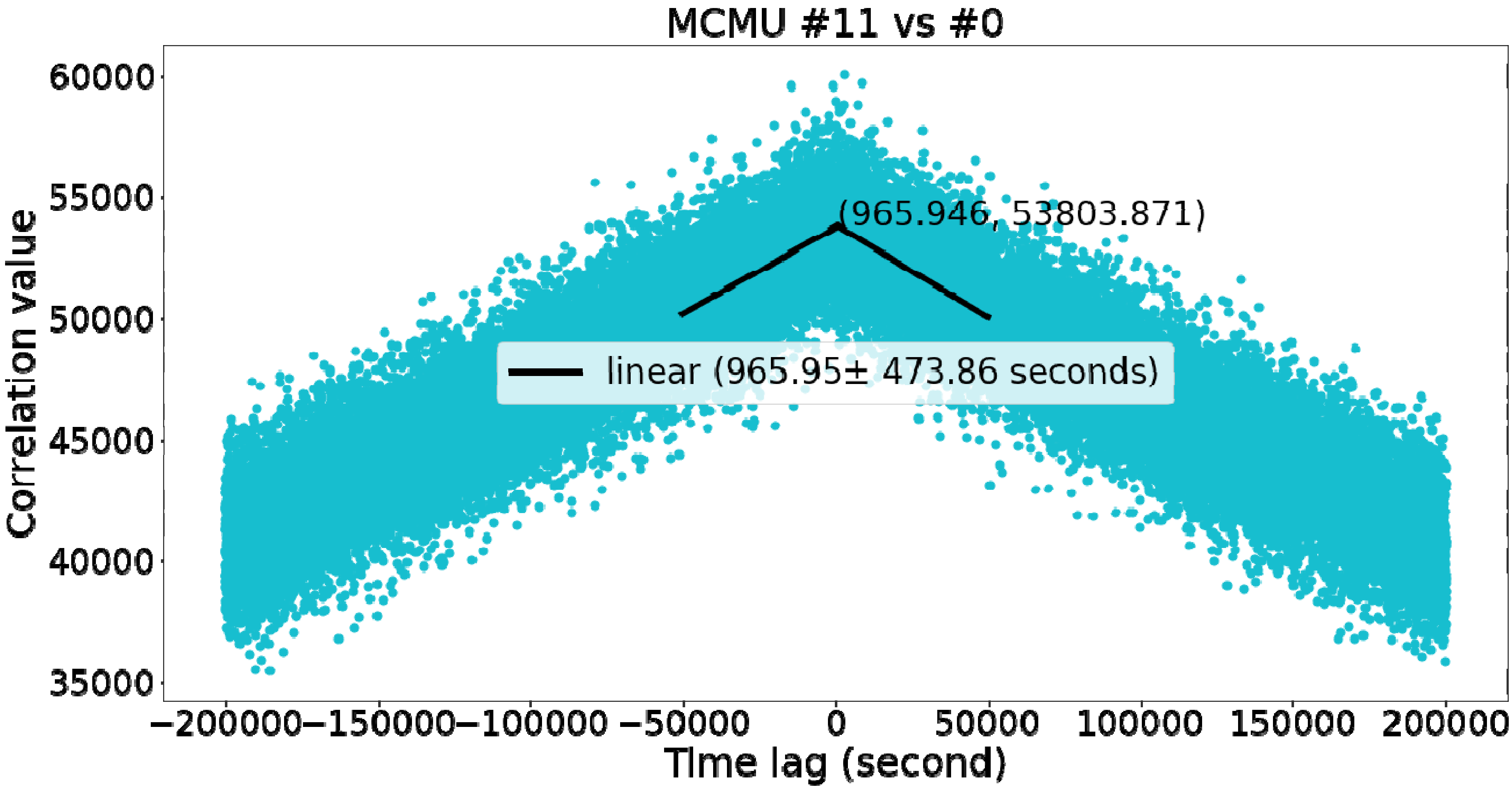

MCMU #11 vs #0
(965.946, 53803.871)
linear (965.95± 473.86 seconds)
Correlation value
60000
55000
50000
45000
40000
35000
−200000
−150000
−100000
−50000
0
50000
100000
150000
200000
TIme lag (second)

Autocorrelation

JBGO-JBGO

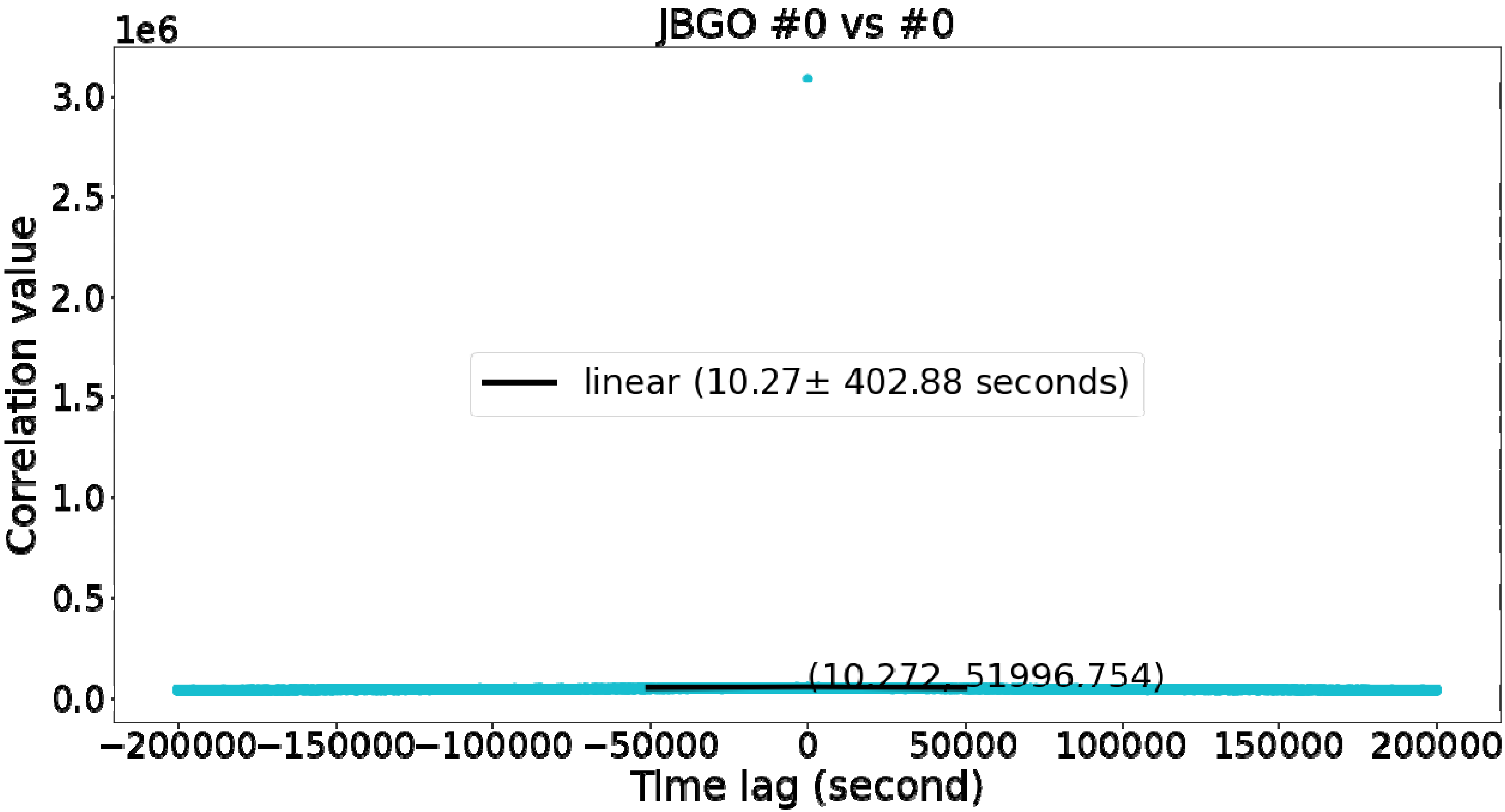
JBGO #0 vs #0
1e6
3.0
2.5
2.0
1.5
1.0
0.5
0.0
Correlation value
linear (10.27± 402.88 seconds)
(10.272, 51996.754)
−200000
−150000
−100000
−50000
0
50000
100000
150000
200000
TIme lag (second)

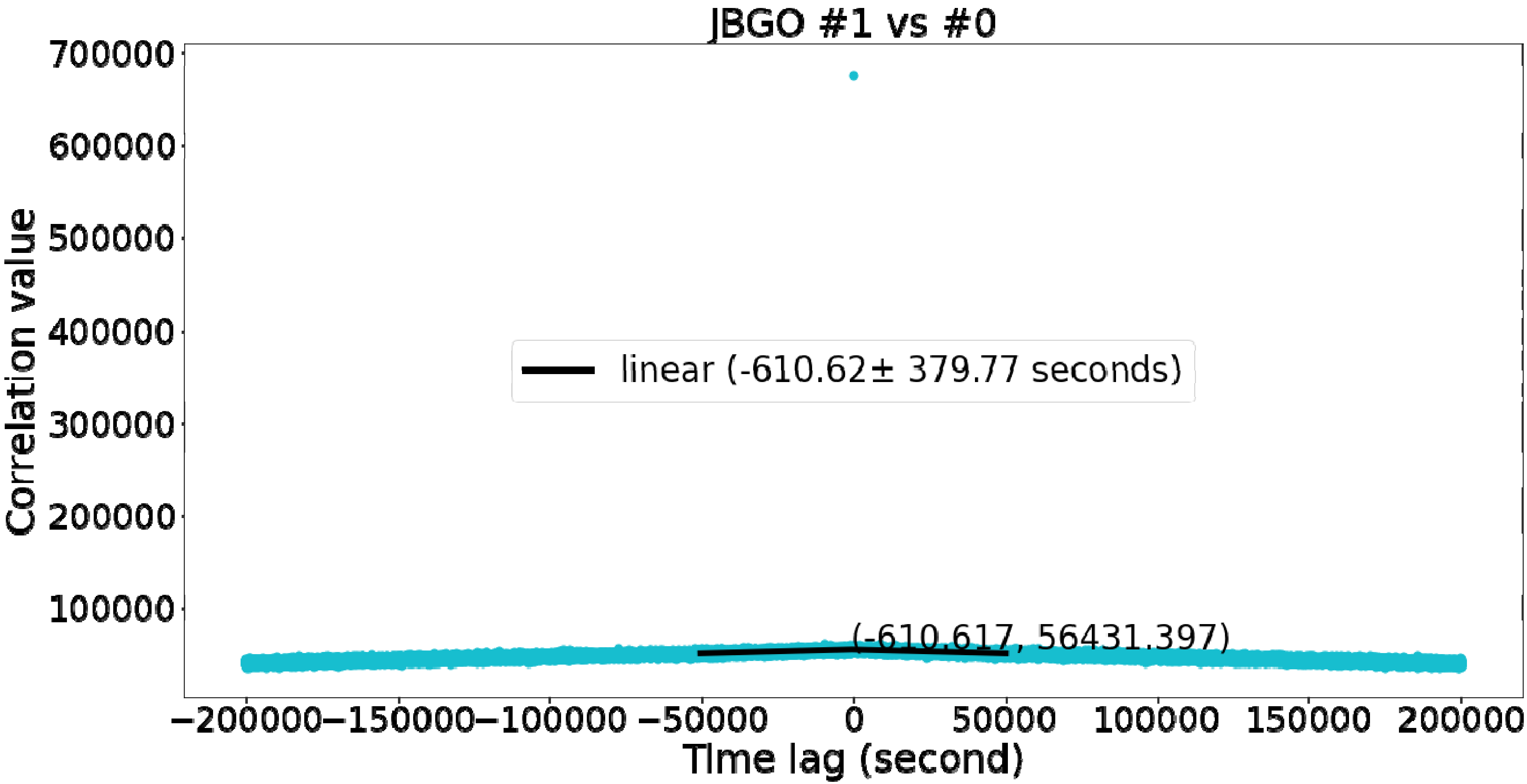

JBGO #1 vs #0
700000
600000
500000
400000
300000
200000
100000
Correlation value
linear (-610.62± 379.77 seconds)
(-610.617, 56431.397)
−200000
−150000
−100000
−50000
0
50000
100000
150000
200000
TIme lag (second)

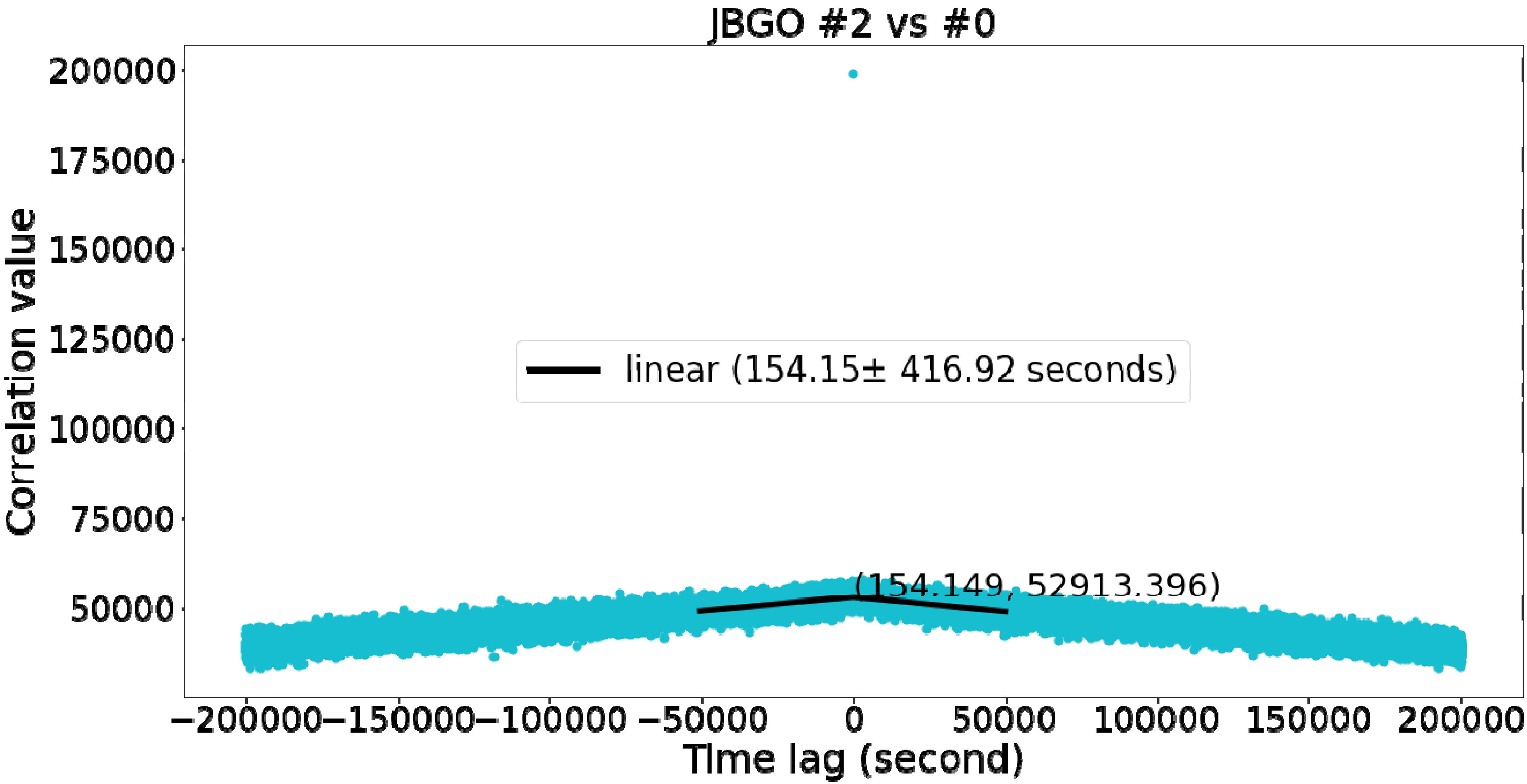

JBGO #2 vs #0
200000
175000
150000
125000
100000
75000
50000
Correlation value
linear (154.15± 416.92 seconds)
(154.149, 52913.396)
−200000
−150000
−100000
−50000
0
50000
100000
150000
200000
Time lag (second)

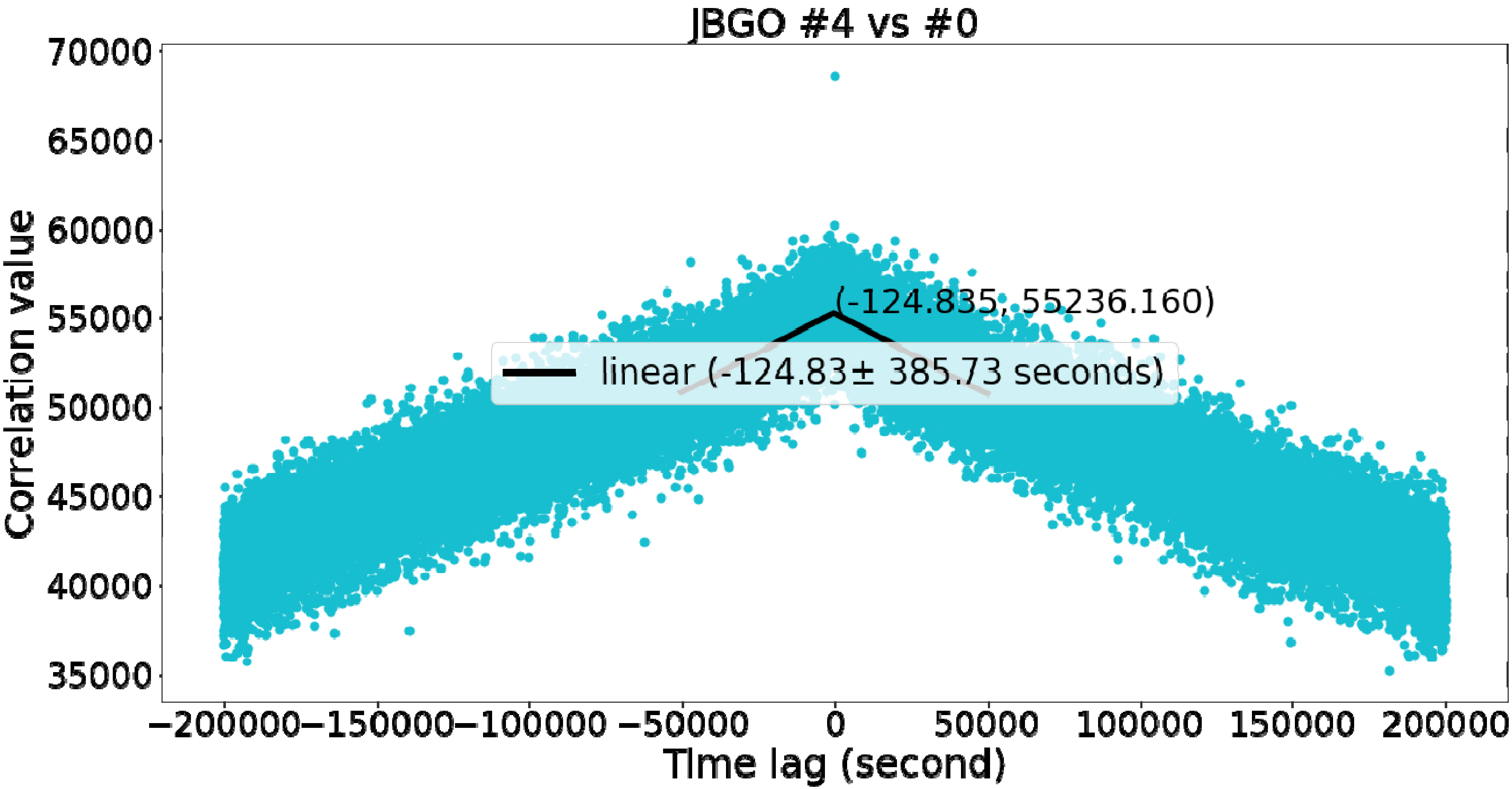
JBGO #4 vs #0
Correlation value
70000
65000
60000
55000
50000
45000
40000
35000
−200000
−150000
−100000
−50000
0
50000
100000
150000
200000
Time lag (second)
(-124.835, 55236.160)
linear (-124.83± 385.73 seconds)

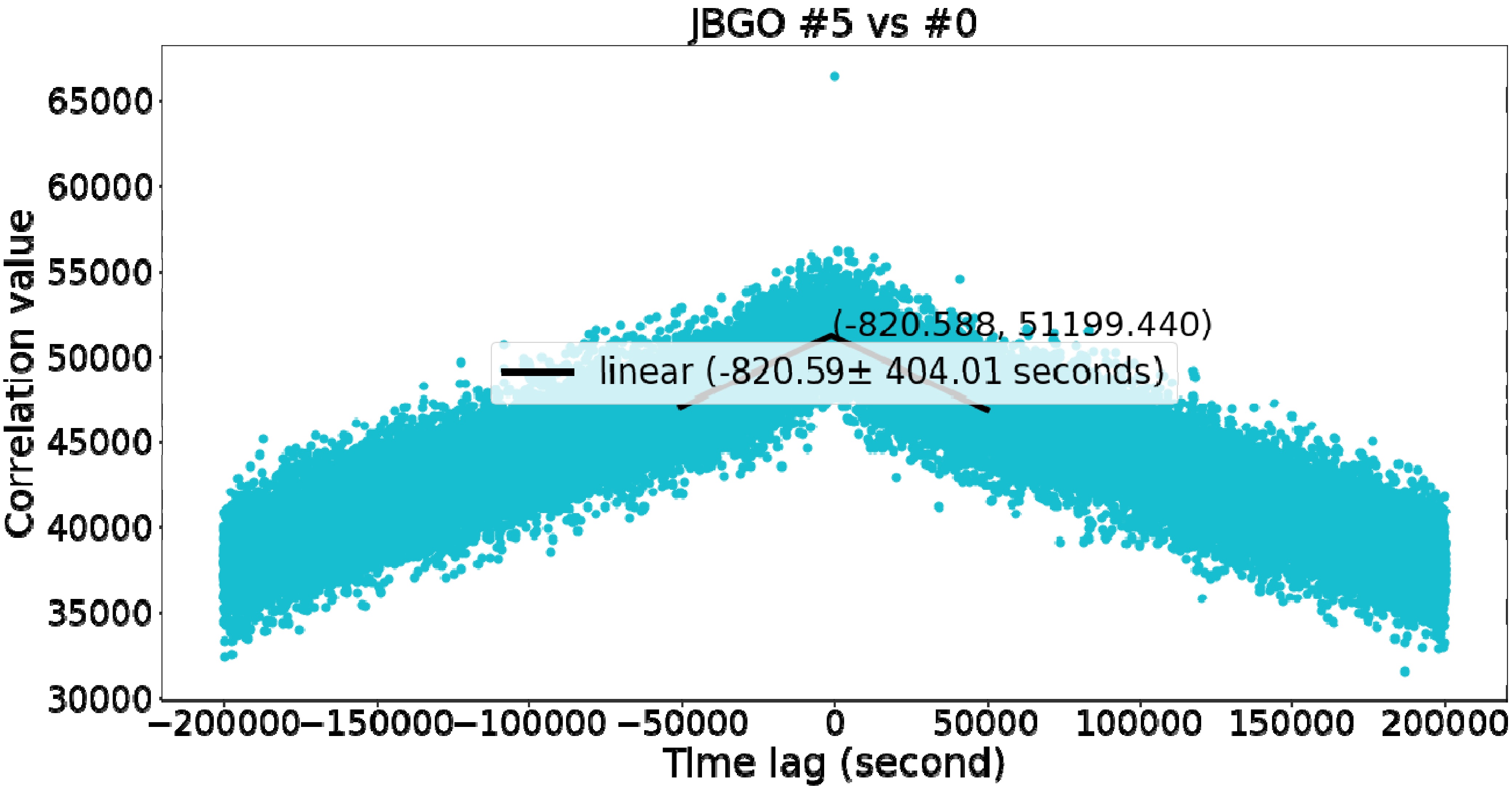

JBGO #5 vs #0
Correlation value
Time lag (second)
(-820.588, 51199.440)
linear (-820.59± 404.01 seconds)
65000
60000
55000
50000
45000
40000
35000
30000
−200000
−150000
−100000
−50000
0
50000
100000
150000
200000

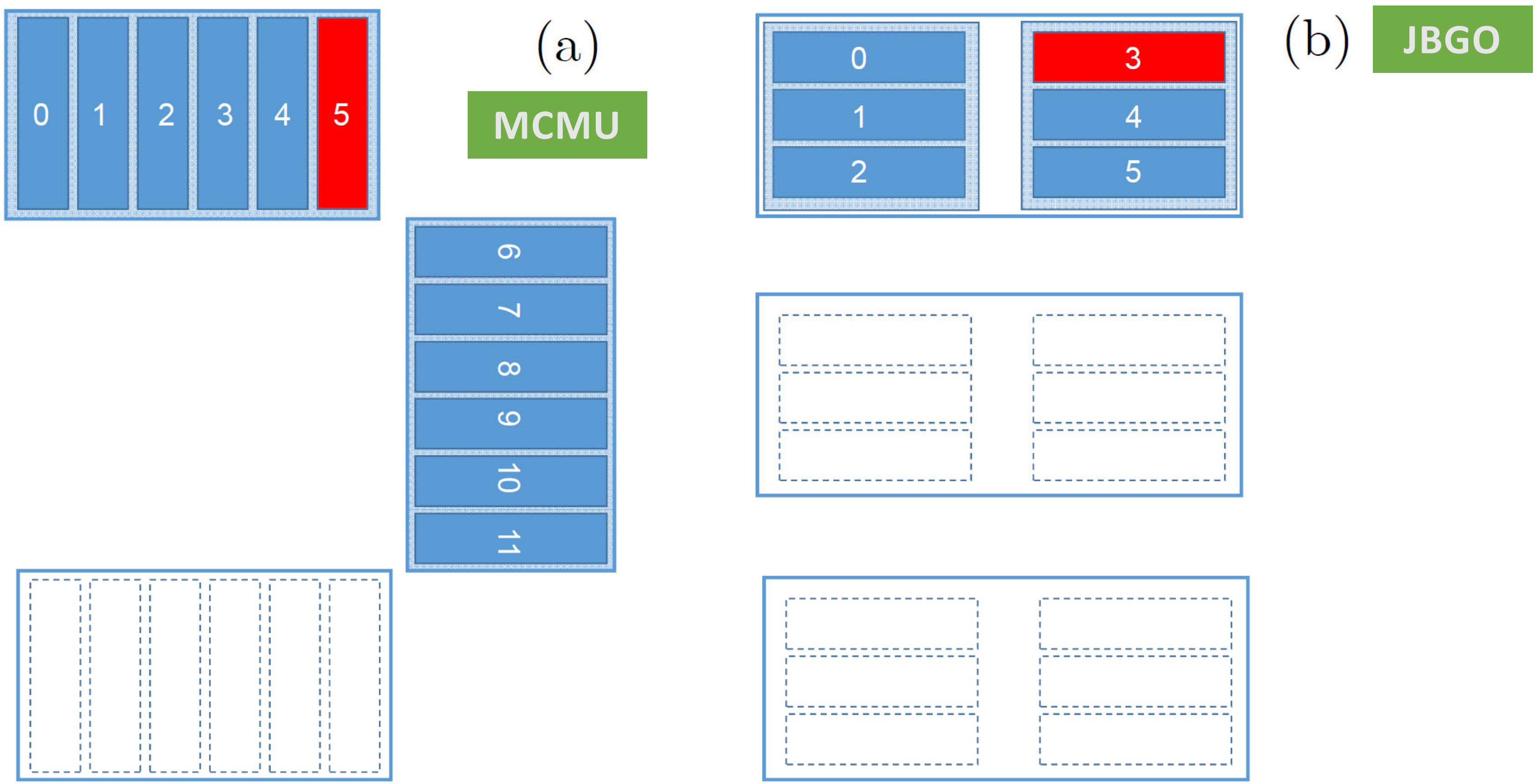

FIGURE 13 A schematic diagram of the placement of (a) McMurdo and (b) Jang Bogo neutron counters.

Courtesy: Kittiya et al. 2022

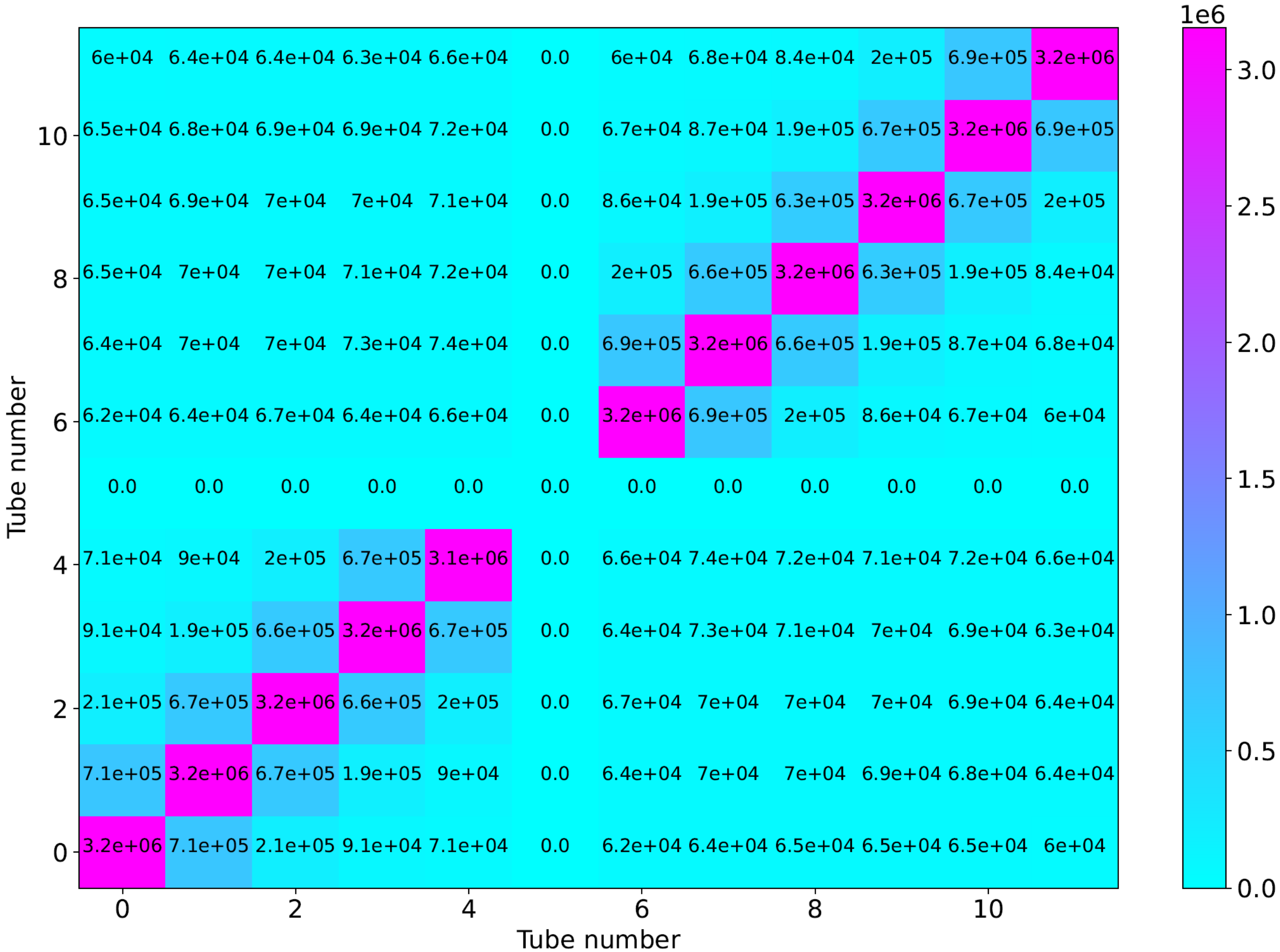

Courtesy: Kittiya et al. 2022

Figure 14 Rectangular grid of correlation values in the 12 × 12 dimensional array of McMurdo neutron counters. Color bar indicates correlation values of highest data points at around zero time lag. All values displayed in the bottom portion of this mesh grid can be seen in Figure 4 as described in the text. As unit 5 is damaged, we can see all the ingredients associated with this tube are all zeros.

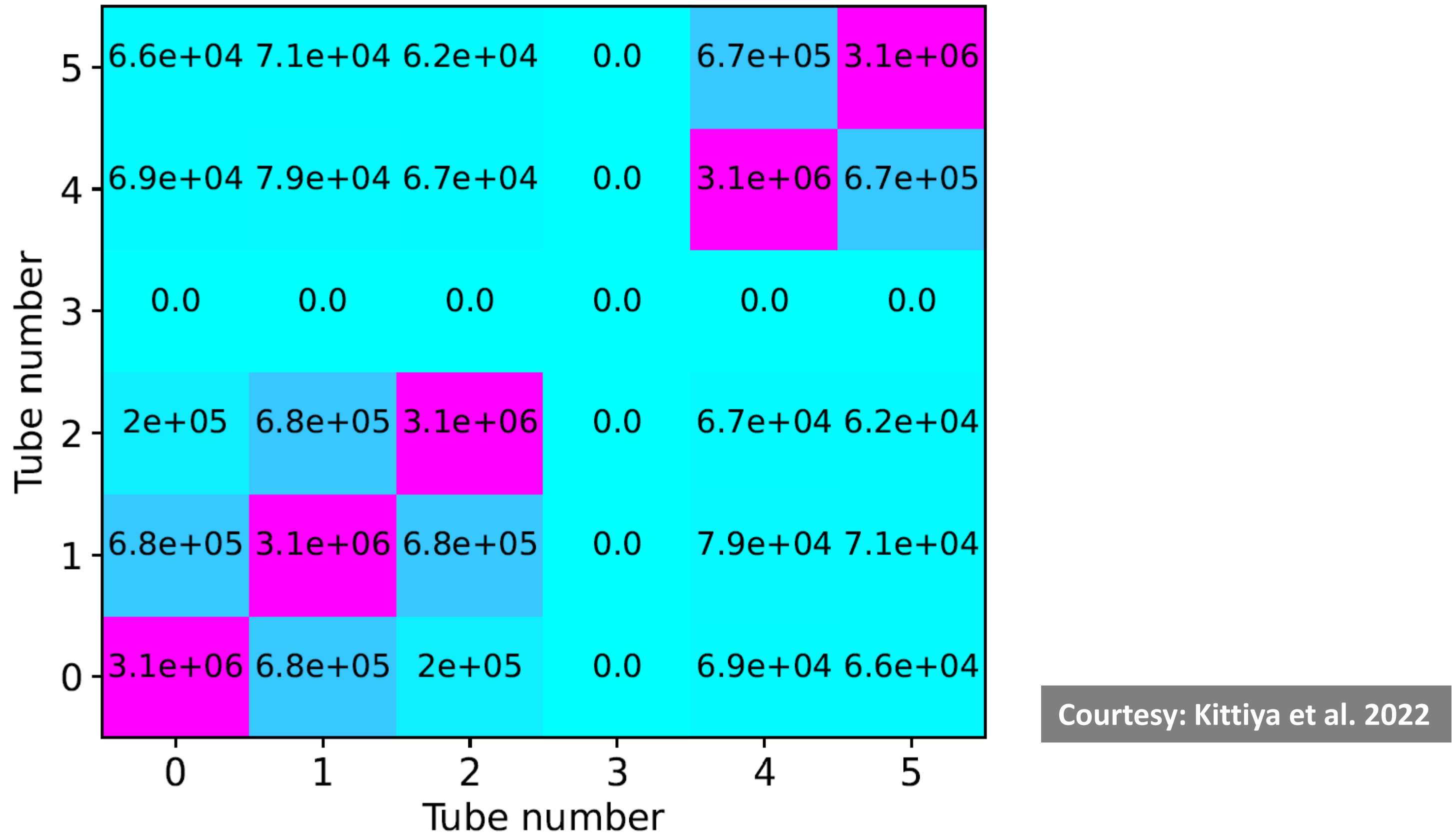

Figure 15 Rectangular grid of correlation values in the 6 × 6 dimensional array of Jang Bogo neutron counters. Color bar indicates correlation values of highest data points at around zero time lag. As unit 3 is damaged, we can see all the ingredients associated with this tube are all zeros.

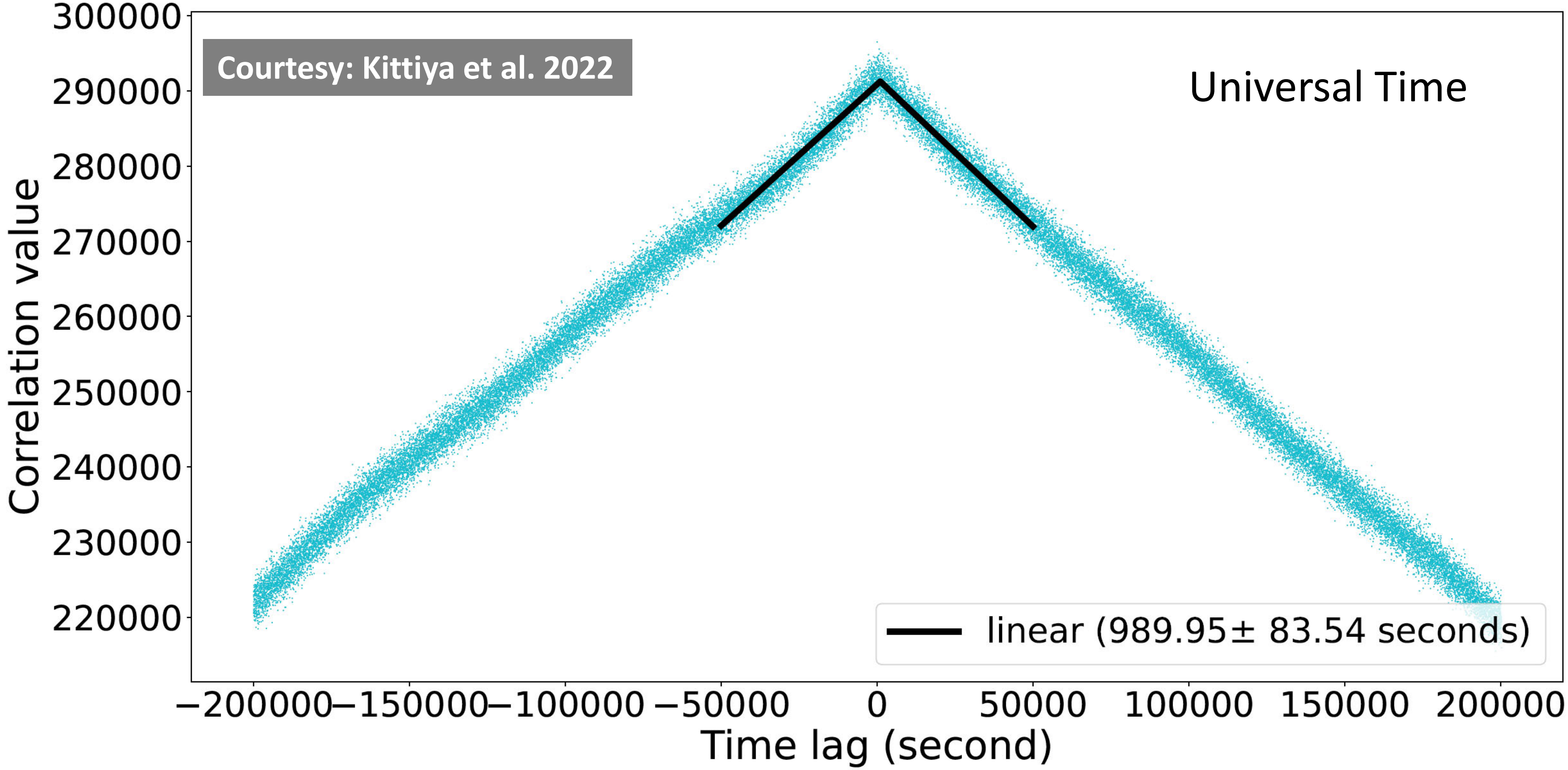
Courtesy: Kittiya et al. 2022
Universal Time
linear (989.95± 83.54 seconds)
300000
290000
280000
270000
260000
250000
240000
230000
220000
Correlation value
−200000
−150000
−100000
−50000
0
50000
100000
150000
200000
Time lag (second)

FIGURE 16

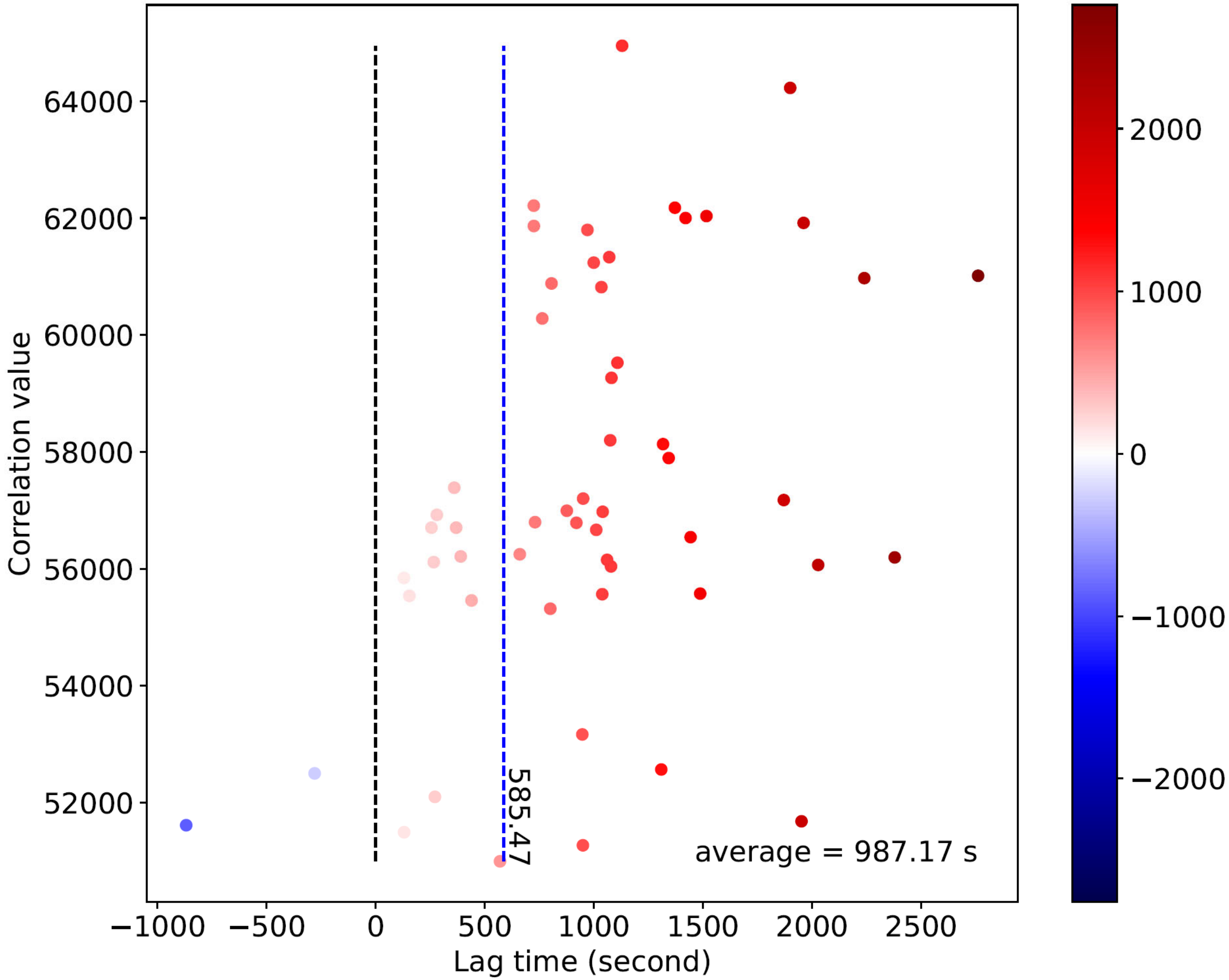

Courtesy: Kittiya et al. 2022

FIGURE 17

PLANS TO REPORT IN THE BOOTCAMP 2021 ARE:

- Update about correlation work that I've mentioned before
- In addition to the correlation work, Jumbo also has progress reports on the pulse selection!

LATITUDE SURVEYS

Chinese Icebreaker Xue Long

survey years:

- 2018-2019
- 2019-2020

GCR spectrum — heliospheric Modulation — Yield function — geomagnetic Transmission

Count Rate

$$N(\Theta,\Phi,h,t)=\int_0^{\infty}\left[\sum_i G_i(P)M_i(P,t)Y_i(P,h)\right]T(P,\Theta,\Phi,t)\mathrm{d}P$$ ----------(1)

$$N(P_c,h,t)=\int_{P_c}^{P_L}\sum_i G_i(P)M_i(P,t)Y_i(P,h)\mathrm{d}P$$ ----------(2)

Differential Response function

$$DRF(P)=-\left[\frac{dN}{dP_c}\right]_p=\sum_i G_i(P)M_i(P,t)Y_i(P,h)$$

FERN

25 Dec 14:00 – 15:30 Hrs

MISS. SIDARAT KHAMPHAKDEE

Analysis of the Changvan Neutron Monitor Operation in Latitude Surveys during 2019-2020

FIGURE 18 The placement of the 2NM64 and semi-leaded neutron detectors inside the Changvan.

Courtesy Khampakdee et al., 2020

LATITUDE SURVEY: VOYAGE IN 2018-2020 SURVEY YEARS

Chinare35-XueLong
Chinare35-Changvan
Chinare36

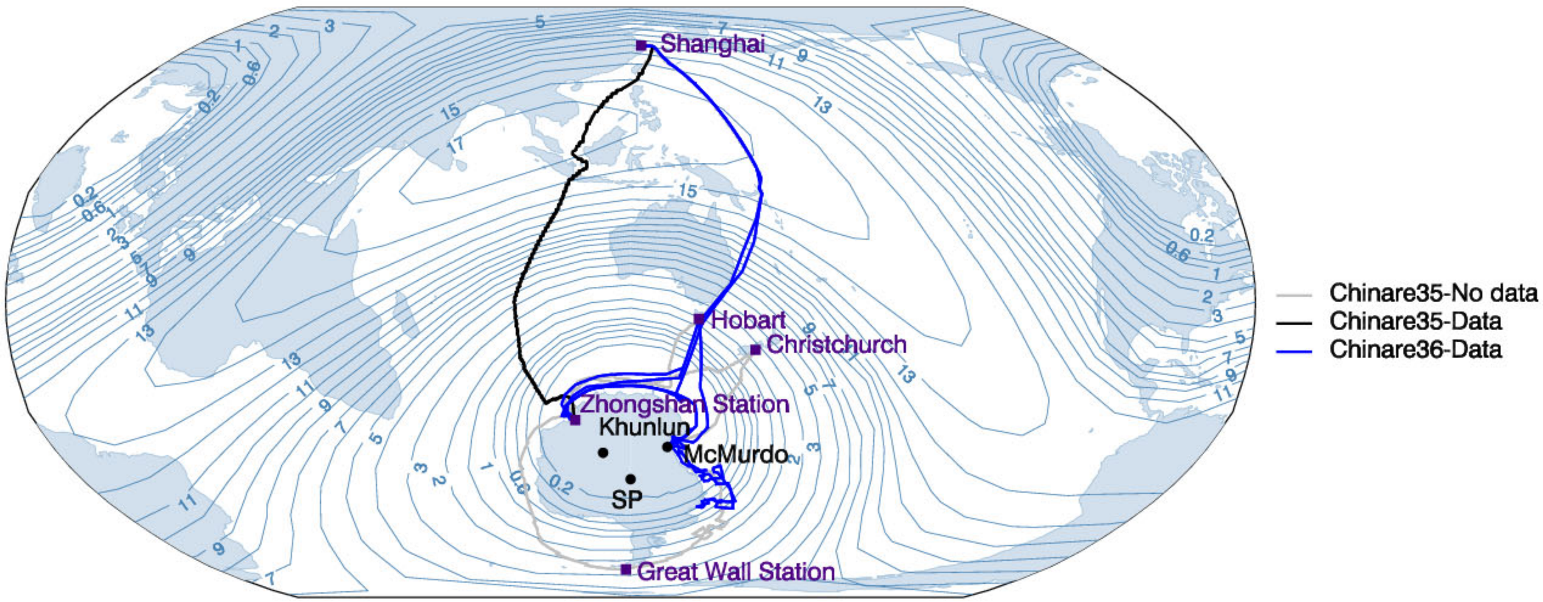

FIGURE 19 Route of the Oden for the 2019-2020 latitude survey, superimposed on contours of the 2018 effective vertical cutoff rigidity, calculated for May 01, 2018 at 12:00 UT. Numbers at each contour indicate the effective vertical cutoff rigidity in GV.

Courtesy Khampakdee et al., 2021

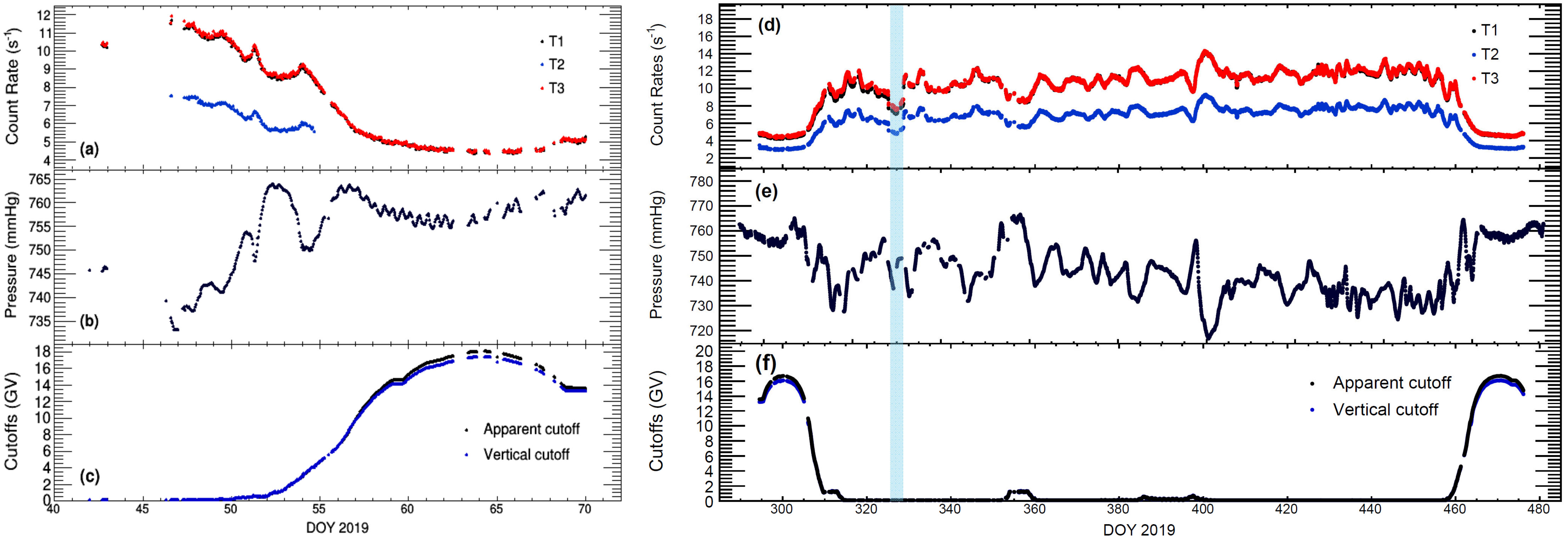

FIGURE 20 (a)-(c) Data set of the survey year 2019 and (d)-(f) of the survey year 2020, as a function of time. (a) and (d) Hourly averaged count rates for T1 (black), T2 (blue), and T3 (red). The vertical grey lines show the time period that causes the count rate to fluctuate by having other containers intervene. (b) and (e) The barometric pressure. (c) and (f) The geomagnetic cutoff rigidity, where the black line shows the apparent geomagnetic cutoff rigidity and the blue line shows the vertical effective cutoff rigidity. We will clearly see the difference between the two geomagnetic cutoffs at high cutoffs (low latitudes). Courtesy Khampakdee et al., 2020

PLANS TO REPORT IN THE BOOTCAMP 2021 ARE:

- Response functions and Dorman parameters
- Short-term modulation effect
- Temperature effect

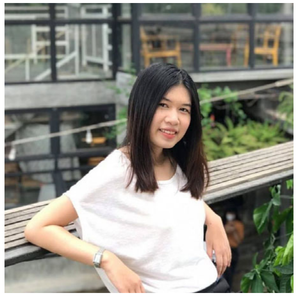

NAN

25 Dec 16:00 – 17:30 Hrs

MISS. PANUTDA YAKUM

Analysis of Neutron Time-Delay Histograms from Changvan Latitude Surveys

The leader fraction $(L) \equiv$ neutron counts that do not follow a previous neutron count in the same counter from the same atmospheric secondary particle

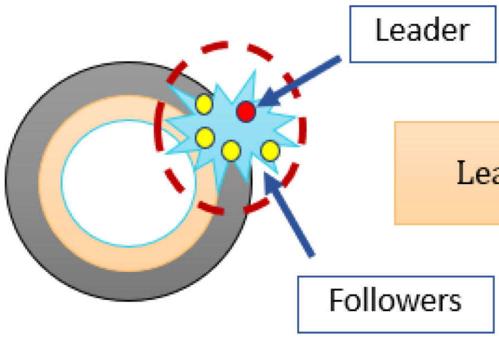

$$\text{Leader Fraction} = \frac{\text{First count (Leader)}}{\text{All pulse (Leader + Followers)}}$$

Courtesy Banglieang et al., 2020

$$L = \frac{\int_{t_d}^{\infty} A_0 e^{-\alpha t} dt}{\int_{t_d}^{t_0} N(t)dt + \int_{t_0}^{\infty} A_0 e^{-\alpha t} dt}$$

or for the discrete histogram,

$$L = \frac{\frac{A_0}{\alpha} e^{-\alpha t_d}}{\int_{t=t_d}^{t_0} N_t + \frac{A_0}{\alpha} e^{-\alpha t_d}}$$

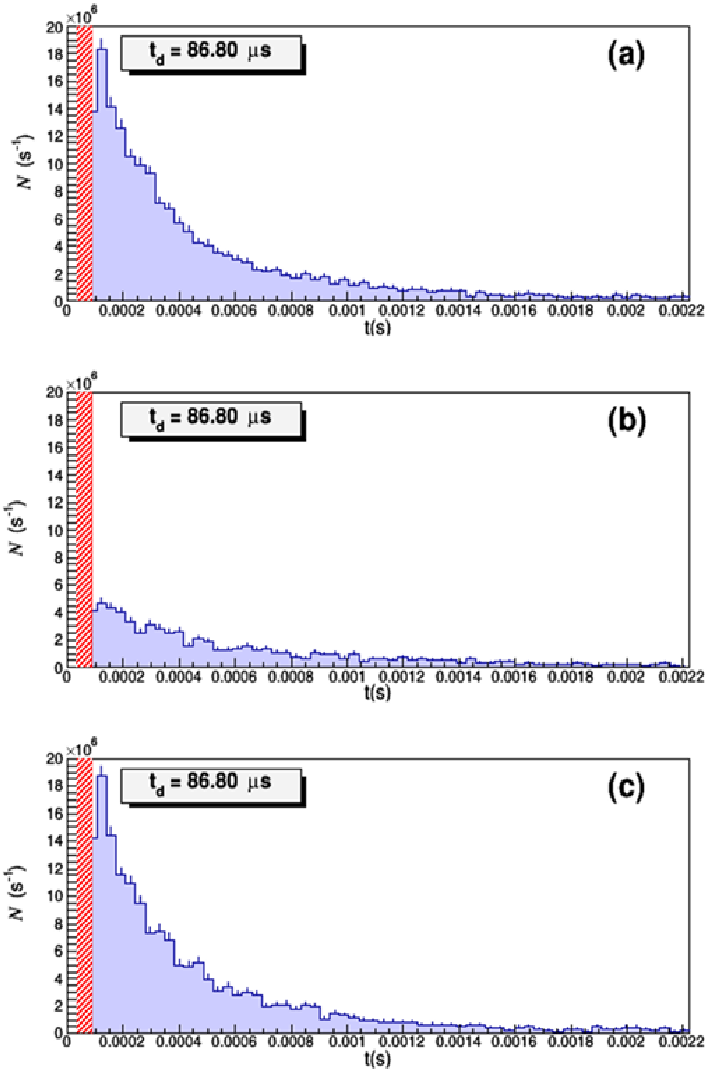

FIGURE 21 Frequency histograms of short time delays collected for each neutron counter tube during one hour (2nd hour of universal time (UT) on the 20 December 2019 of the survey year 2020): (a) tube 1, (b) tube 2, and (c) tube 3. The red vertical band shows the electronics dead time for each tube, about 87 μs. Statistical error bars are shown.

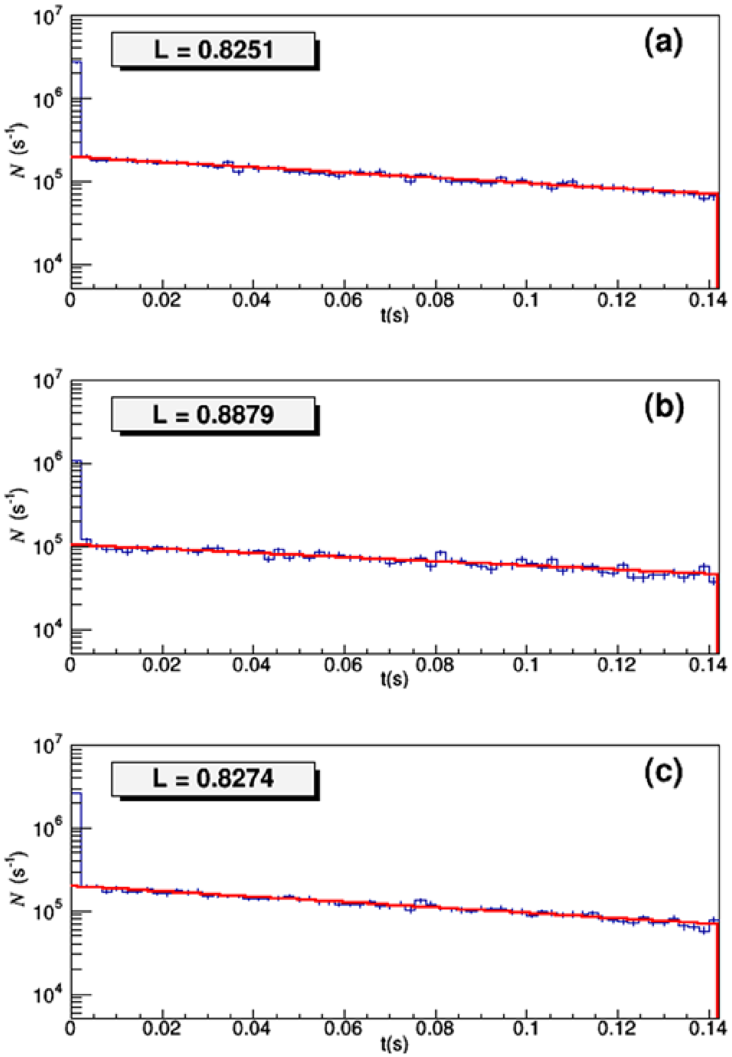

FIGURE 22 Example of analysis of long time delay histograms collected for each neutron counter tube during one hour (2nd hour UT on the 20th December 2019 of the survey year 2020) of (a) tube 1, (b) tube 2, and (c) tube 3. Error bars are shown.

Courtesy Yakum et al., 2020

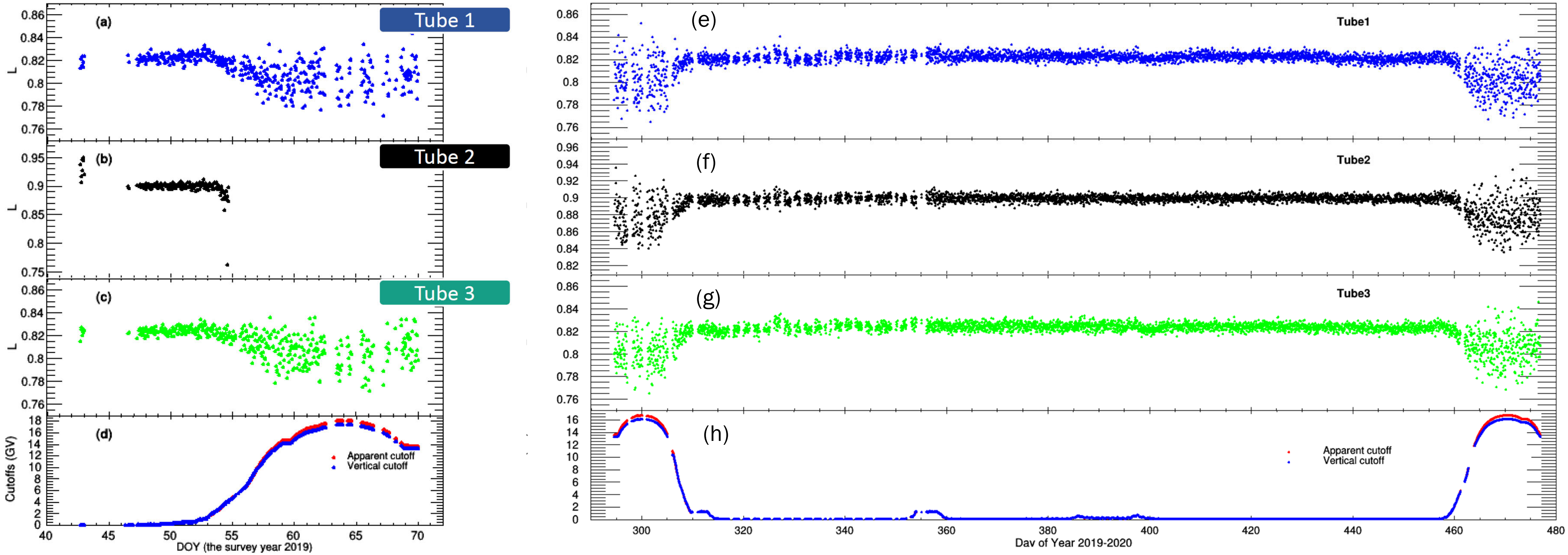

[FIGURE 23](#) Hourly leader fraction (*L*) of tube 1 (blue), tube 2 (black), and tube 3 (green), and geomagnetic cutoff rigidities as a function of time. (a)–(d) Data for the survey year 2019. (e)–(h) Data for the survey year 2020.

Courtesy Yakum et al., 2020

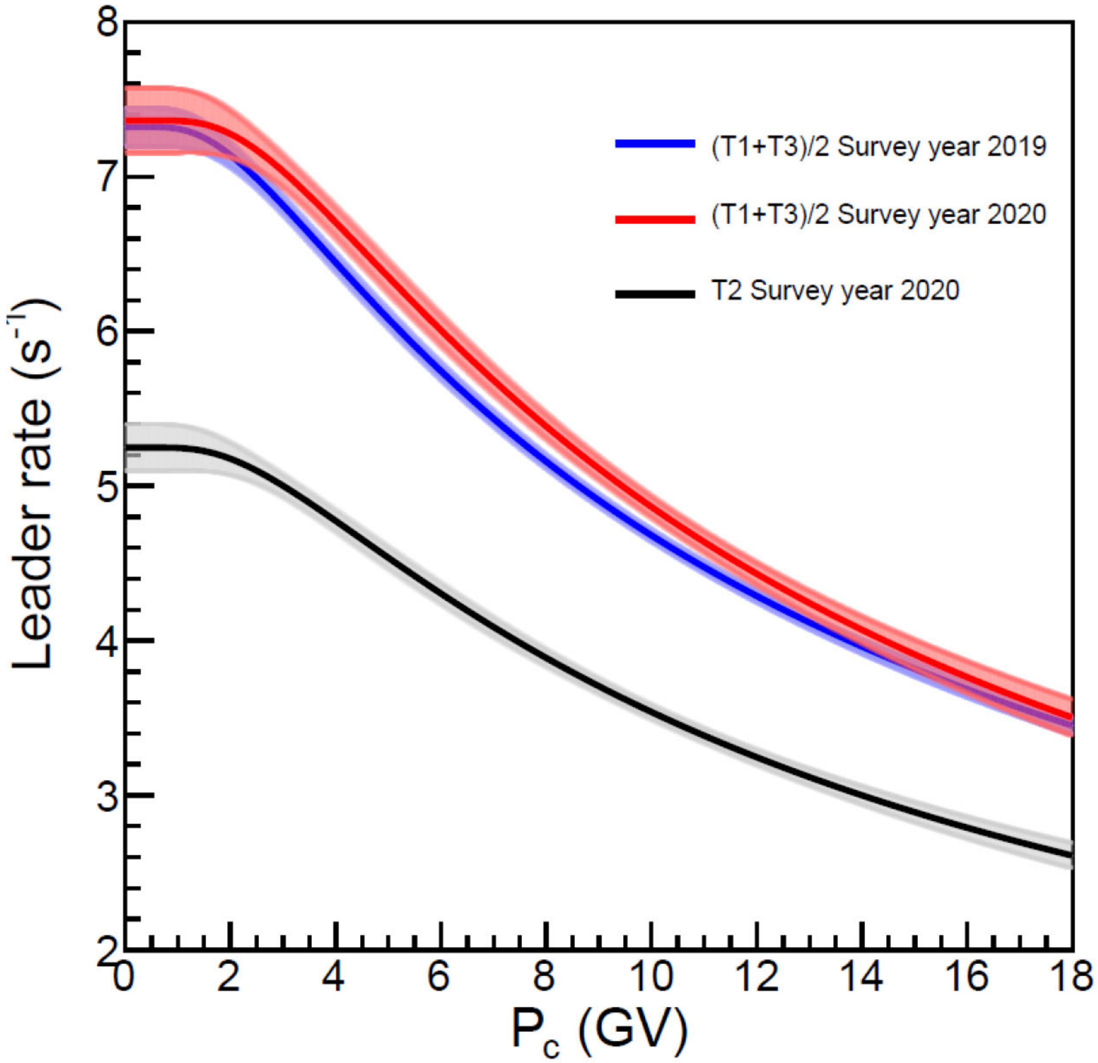

Figure 24 Leader rate function for the survey year 2019 (CN35)(blue line) and the survey year 2020 (CN36)(red line) are the averages from $(T_1 + T_3)/2$. (black line) is the Leader rate function for the unleaded (T2) of the survey year 2020 (CN36). Fitted line with .95 confidence-level band.

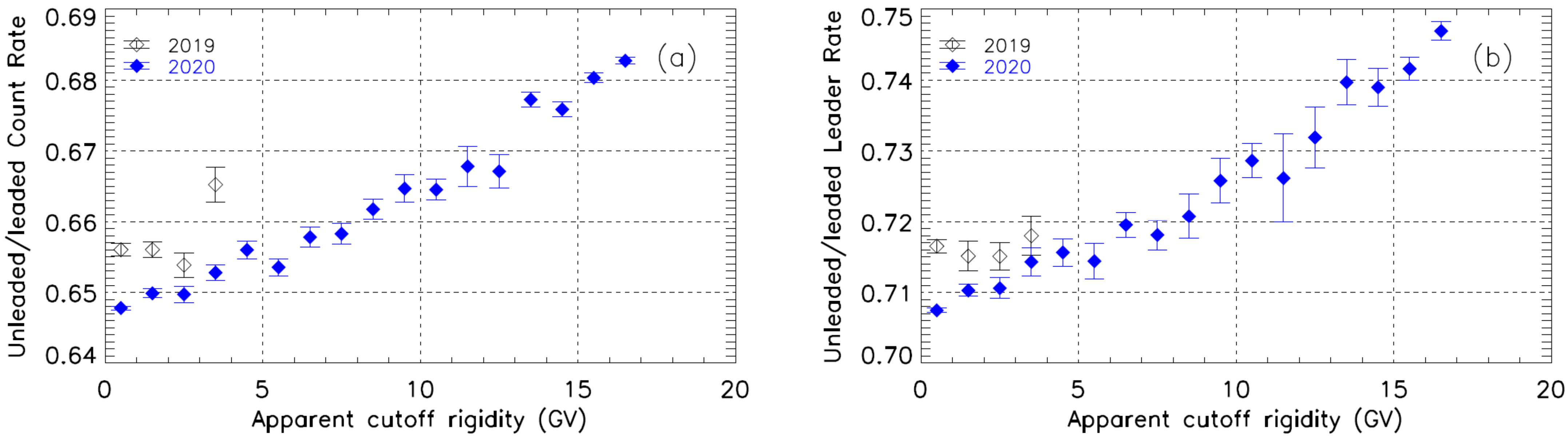

Figure 25 The count rate (left) and leader rate (right) ratio of unleaded vs. leaded counters as a function of apparent cutoff rigidity for the 2019 and 2020 survey years. Here, "unleaded" means T2, and "leaded" means the averaged T1 and T3. Error bars indicate the standard error.

PLANS TO REPORT IN THE BOOTCAMP 2021 ARE:

- Cross-counter leader fraction for latitude surveys during 2018-2020
- PHA at the South Pole

KIFT

26 Dec 09:00 – 10:30 Hrs

MISS. YANEE TANGJAI

Determining the Yield Function of Ice Cherenkov Detector Operation during a Latitude Survey

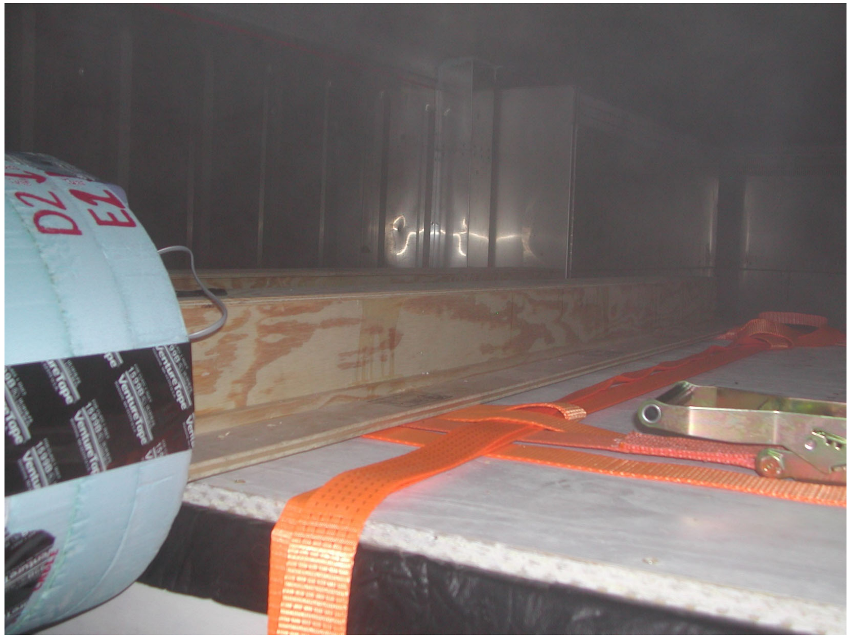

Digital Optical Module (DOM) frozen in to the surface of an IceTop "Tank" Cherenkov detector at the South Pole.

ICETOP TANKS AND THE COSMIC RAY SPECTRUM

- For a typical PeV primary, many tanks record large signals and the shower can be "reconstructed" to give an energy event by event.
- At a few GeV, typically the primary will produce a signal in one or two isolated tanks.
- The average signal in a tank is still proportional to the primary energy.
- Since the flux of GeV particles is high, the counting rate above a given discriminator setting is proportional to the particle flux in a (rather broad) range of energy.
- This proportionality is described by the Yield Function, which is essentially an energy dependent effective area.

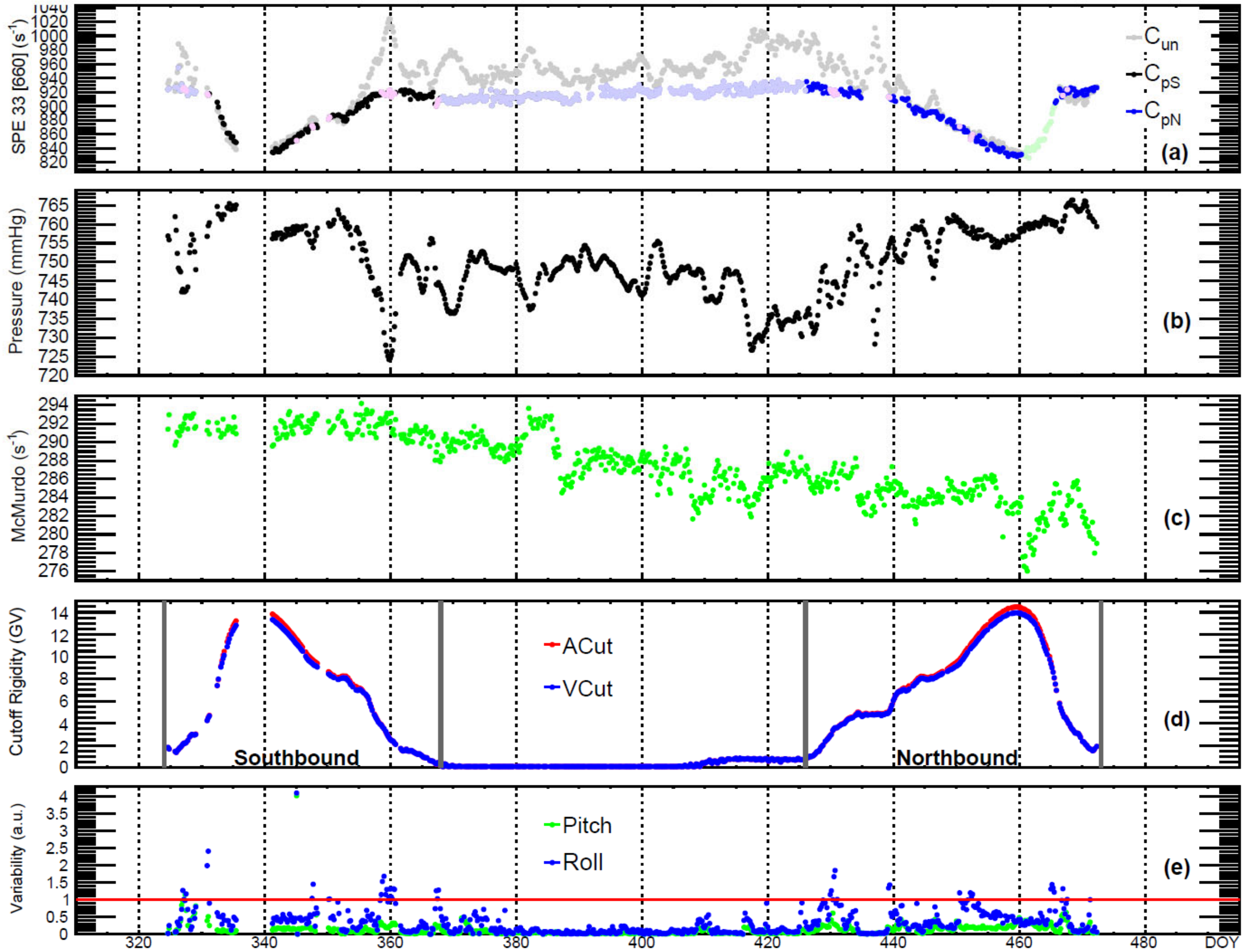

FIGURE 26 Example data from the Oden Ice Cherenkov detector as a function of time. A signal at SPE discriminator setting 660 (Condition Code 33).

Courtesy Tangjai et al., 2021

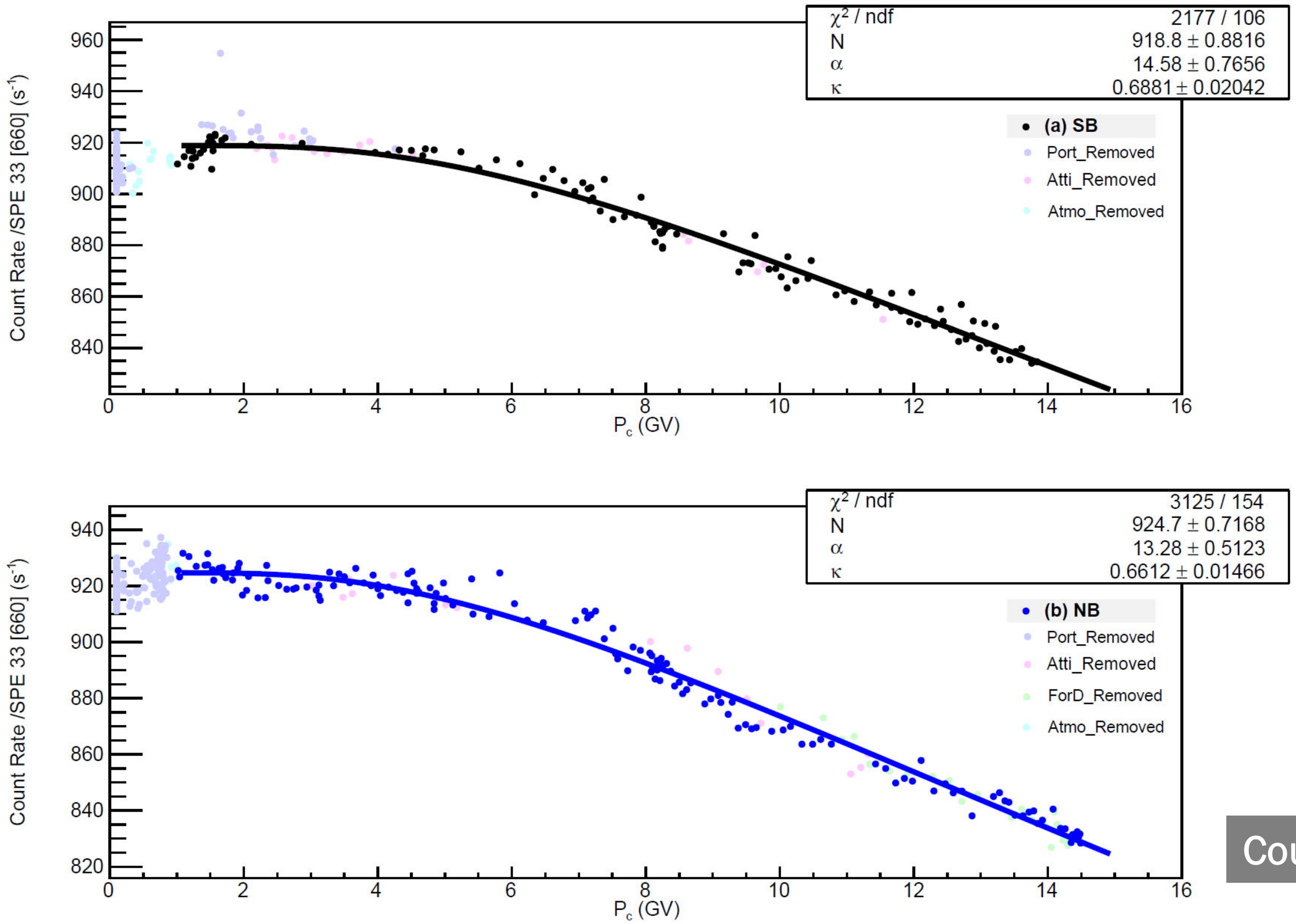

$$N(P_c) = N_0\left(1 - e^{-\alpha P_c^{-\kappa}}\right),$$

$$N(P_c) = \int_{P_c}^{\infty} DRF(P)dP,$$

$$DRF(P) = N_0 \alpha P^{-\kappa-1} \kappa e^{-\alpha P^{-\kappa}}.$$

$$DRF(P) = -\left[\frac{dN}{dP_c}\right]_p = \sum_i J_i(P,t)Y_i(P,h)$$

Courtesy Tangjai et al., 2021

FIGURE 27 The relation of the count rate (pressure correction) and apparent cutoff rigidity (GV). We use the Dorman function to fitting separately for the (a) southbound and (b) northbound intervals. Here is an example of SPE discriminator setting 660 (Condition Code 33).

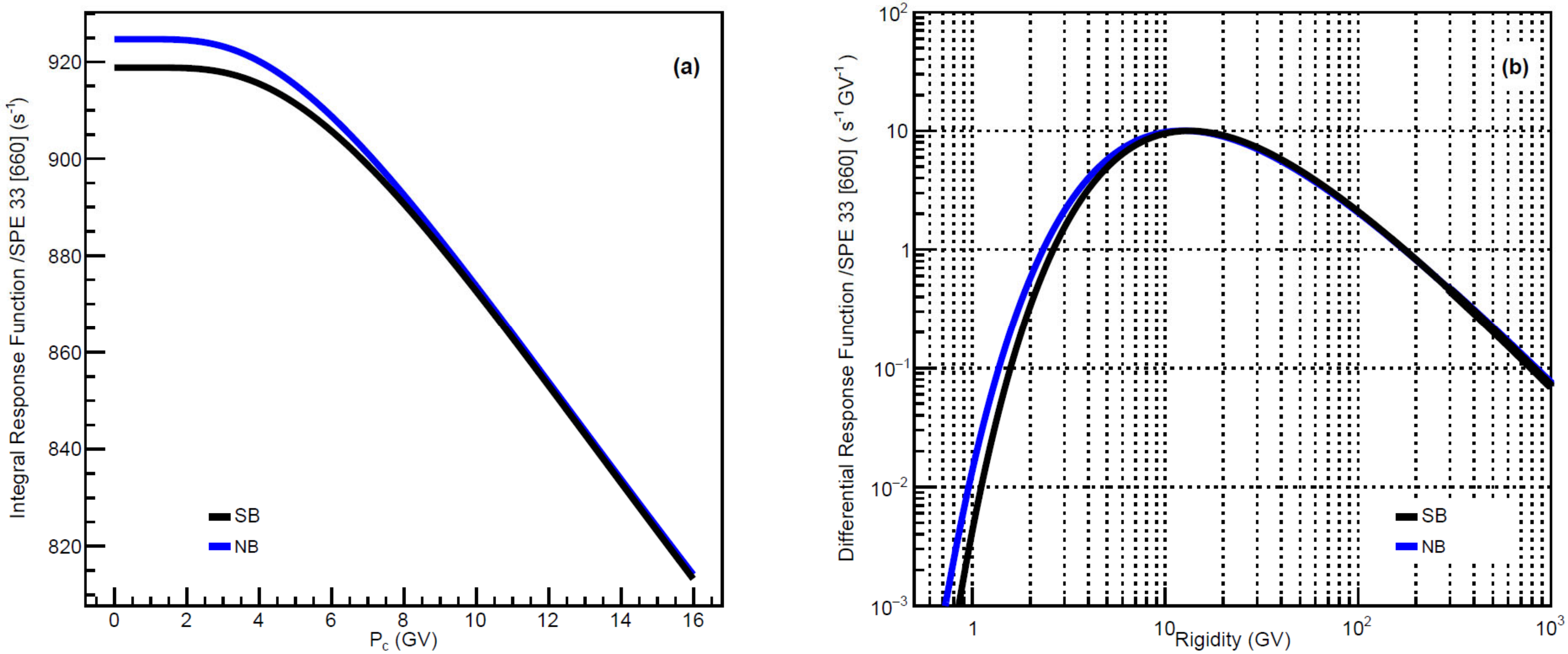

Figure 28 Comparisons of (a) Integral Response Function (*IRF*) and (b) Differential Response Function (*DRF*). Here is an example of signals at SPE discriminator setting 660 (Condition Code 33). The black line is data indicated the southbound (SB). The blue line is data showed the northbound (NB).

Courtesy Tangjai et al., 202x

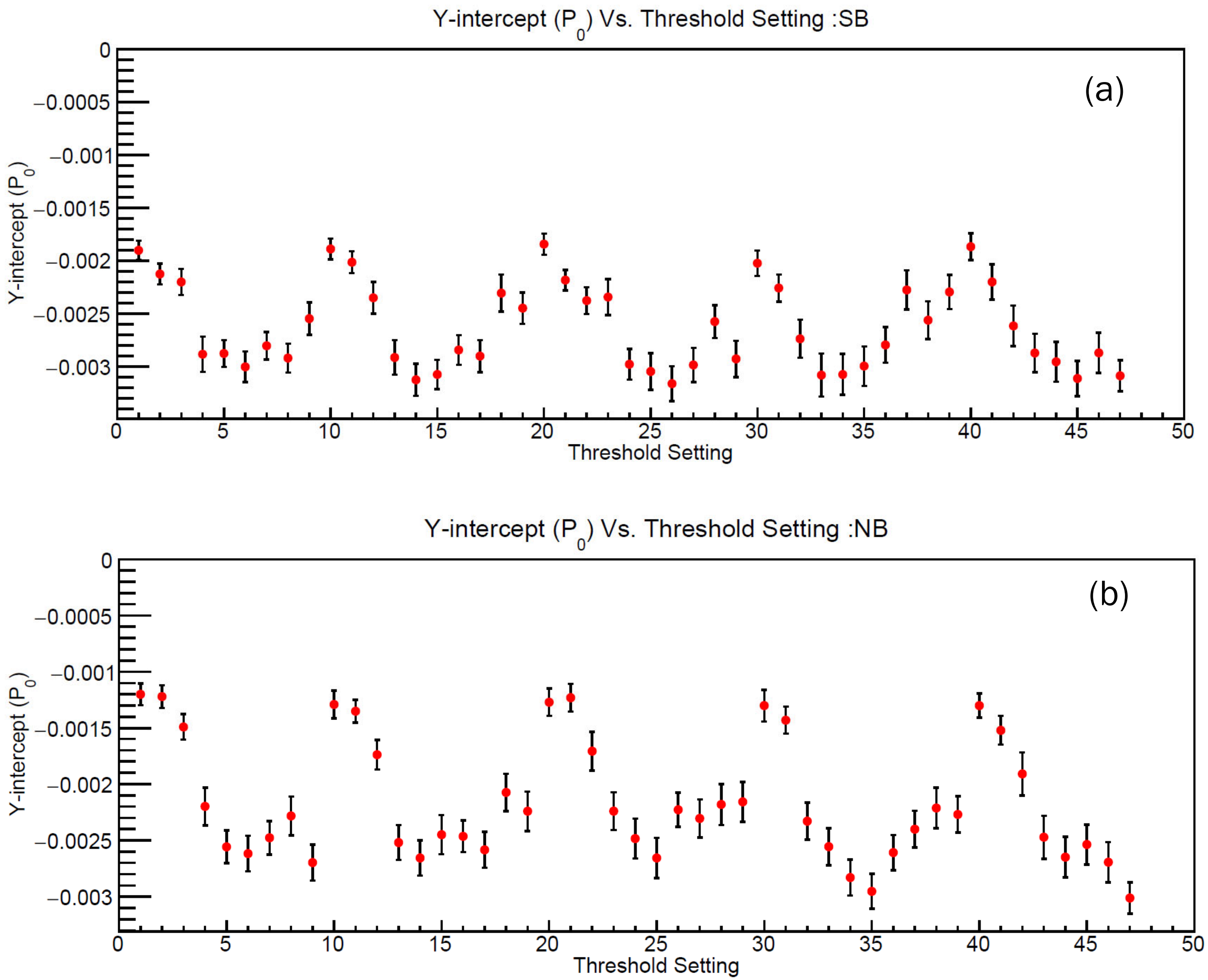

Figure 29 The relation of Y-intercept (P_0) of threshold settings discriminator settings of the (a) southbound and (b) northbound intervals.

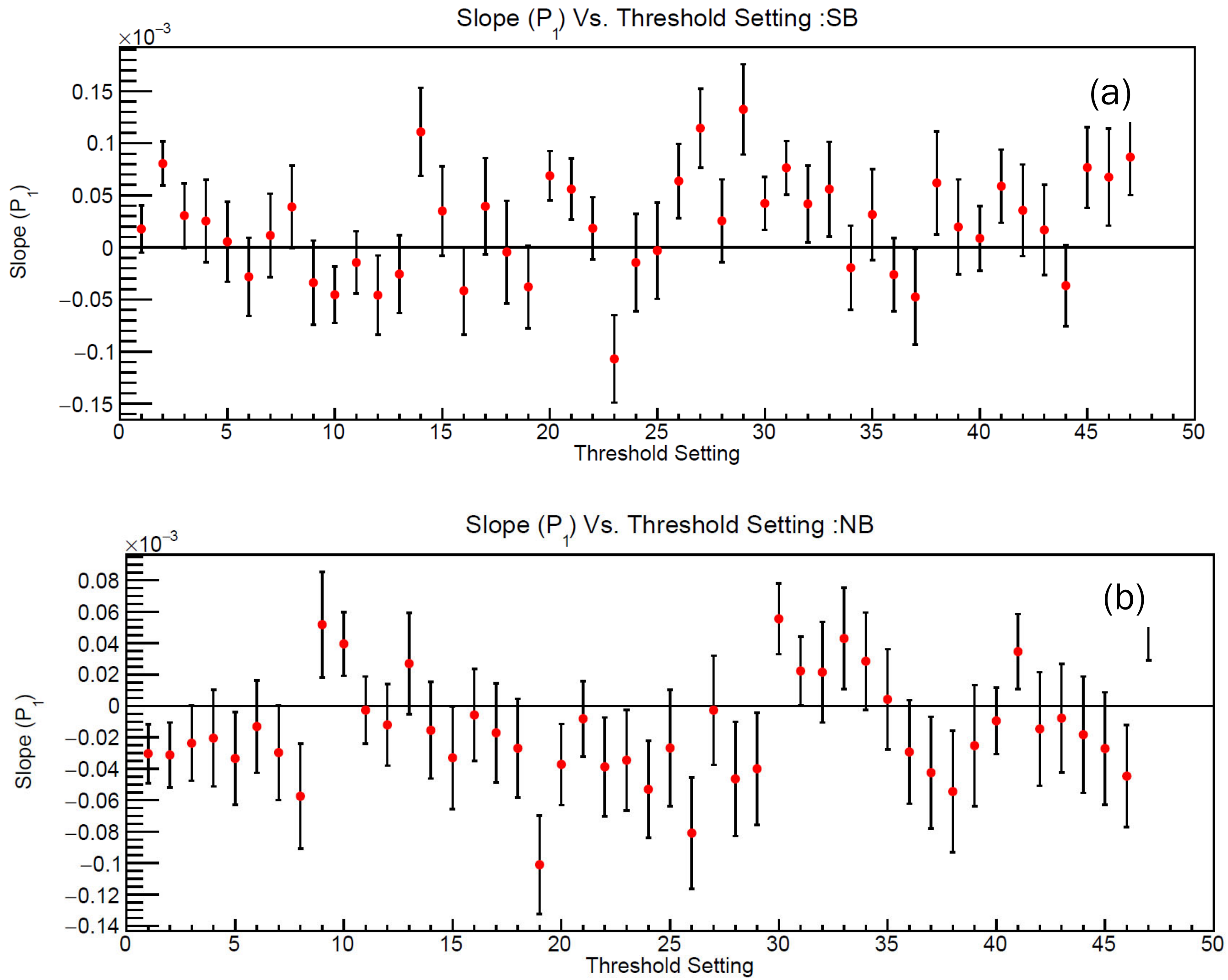

Courtesy Tangjai et al., 202x

Figure 30 The relation of Slope (P_1) of threshold settings discriminator settings of the (a) southbound and (b) northbound intervals.

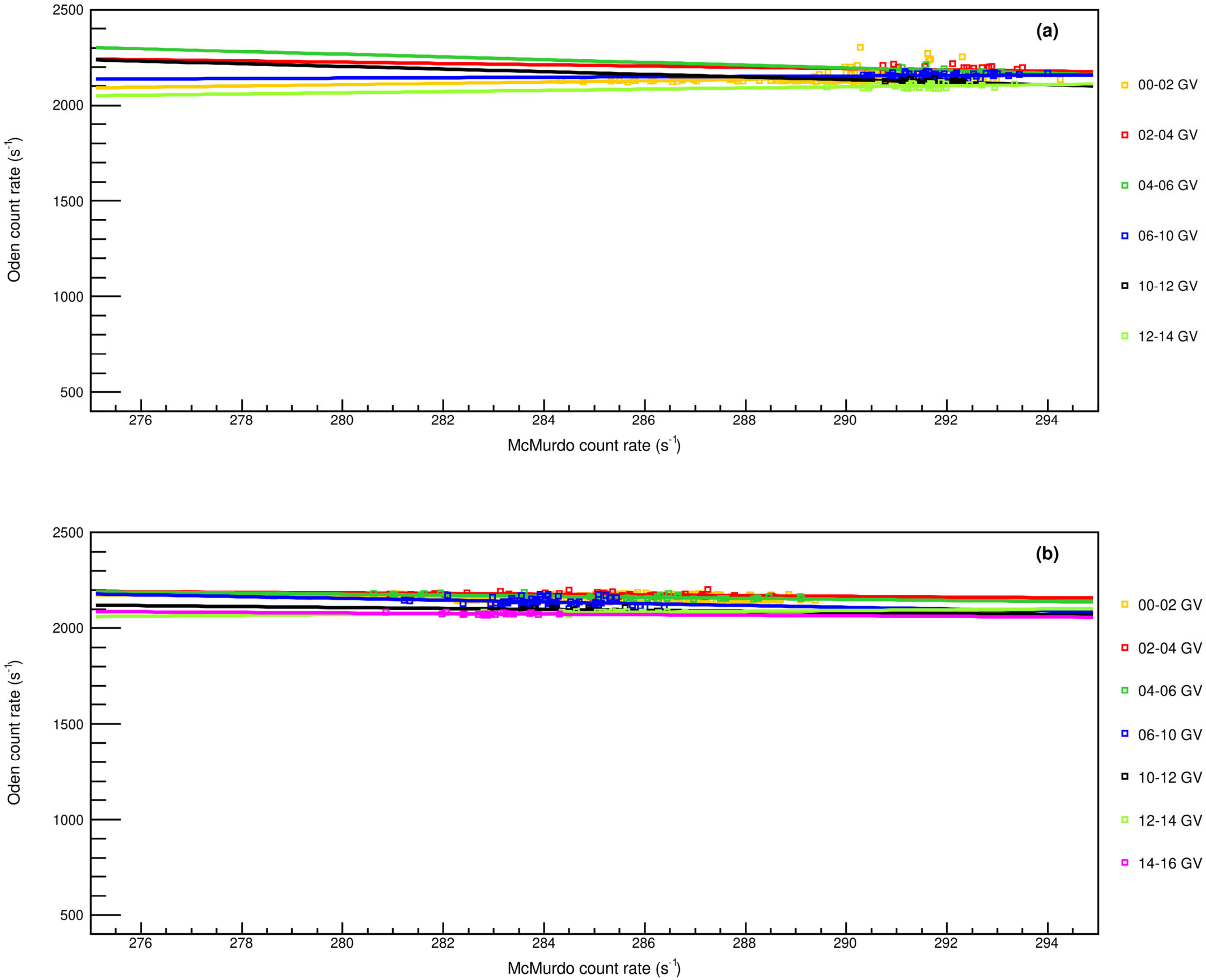

Courtesy Tangjai et al., 202x

Figure 31 The relation of Ice Cherenkov detector count rate for all 47 SPE threshold setting and McMurdo count rate at the South Pole station, both data are corrected for pressure.

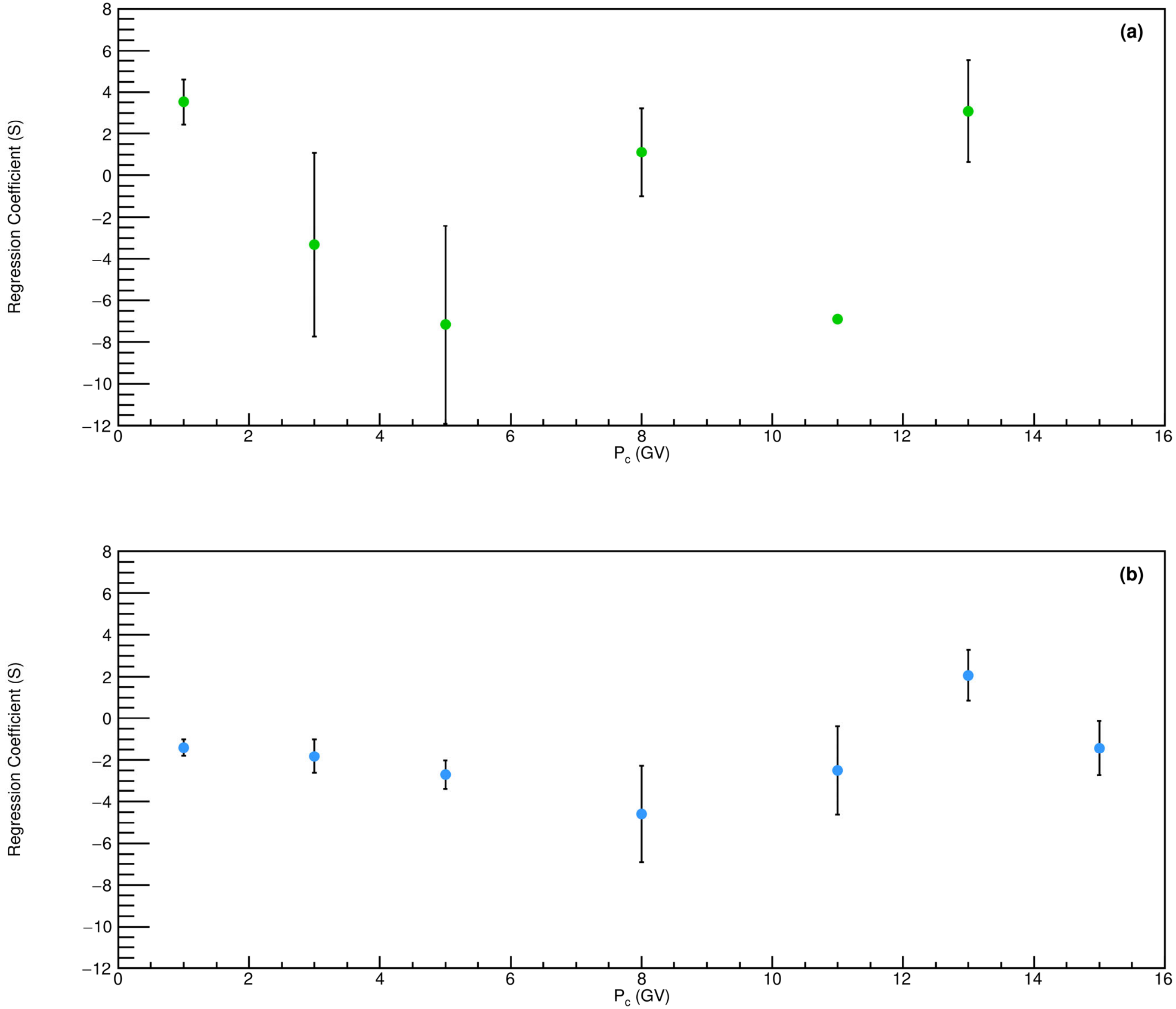

Courtesy Tangjai et al., 202x

Figure 32 The relation of regression coefficients (*S*) and cutoff rigidity (P_c) for all 47 SEP threshold setting.

DETERMINING THE YIELD FUNCTION

- The yield function can be calculated using FLUKA, but you need an accurate model of the IceTop Tank.
- We had already done with the Ice Cherenkov Detector geometry that can run in the latest version of FLUKA (shown in the next slide).
- The yield functions can also be measured, as I will describe, but only at sea level. A good model calculation is therefore also important to relate the measurement to the actual configuration at the South Pole.

Cosmic Detectors (Geometry made by FLUKA)

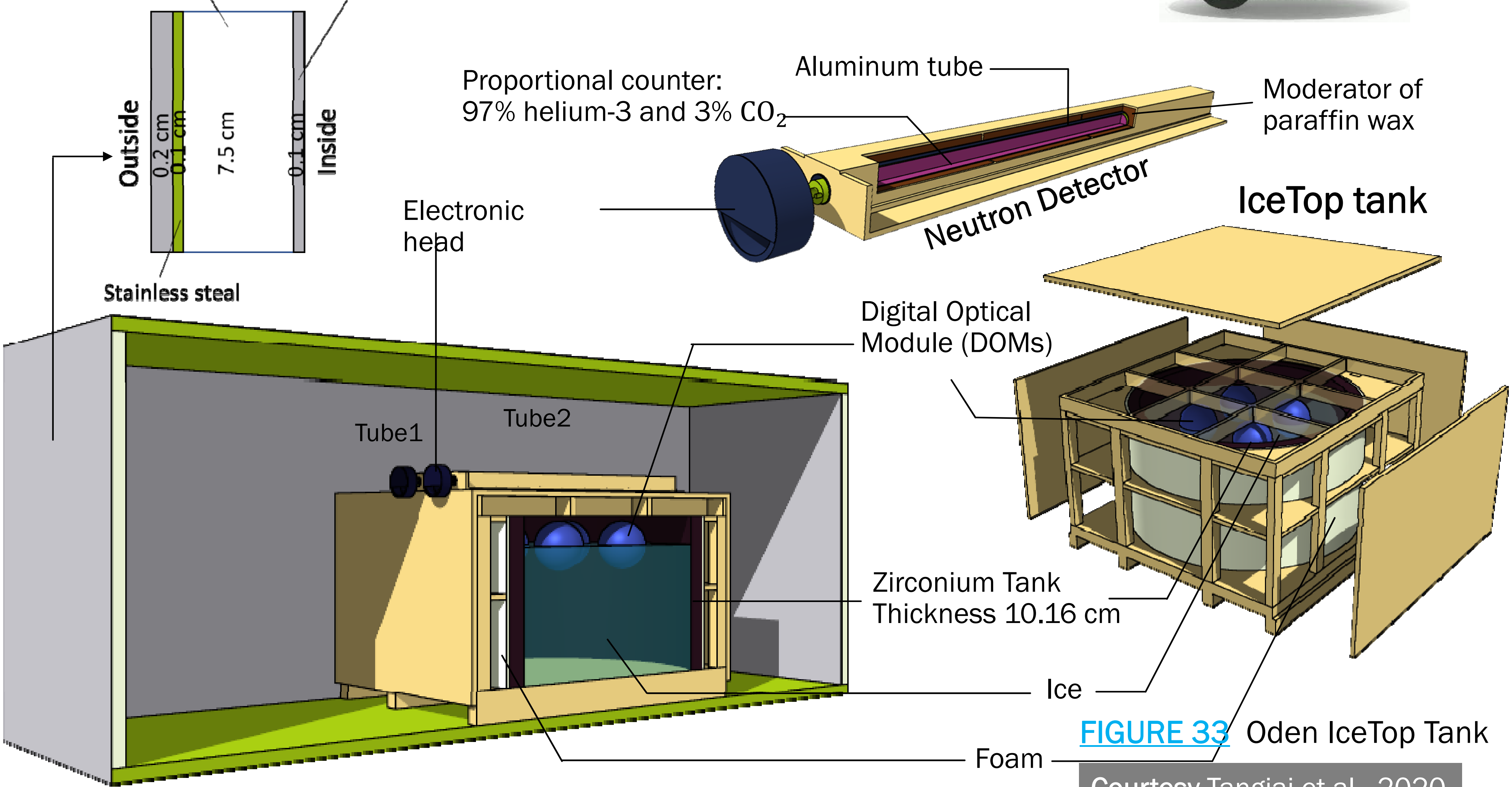

FIGURE 33 Oden IceTop Tank

Courtesy Tangjai et al., 2020

INK

26 Dec 11:00 – 12:30 Hrs

MISS. AUDCHARAPORN PAGWHAN

Determination of Yield Functions of Neutron Counters at the South Pole from Monte-Carlo Simulation

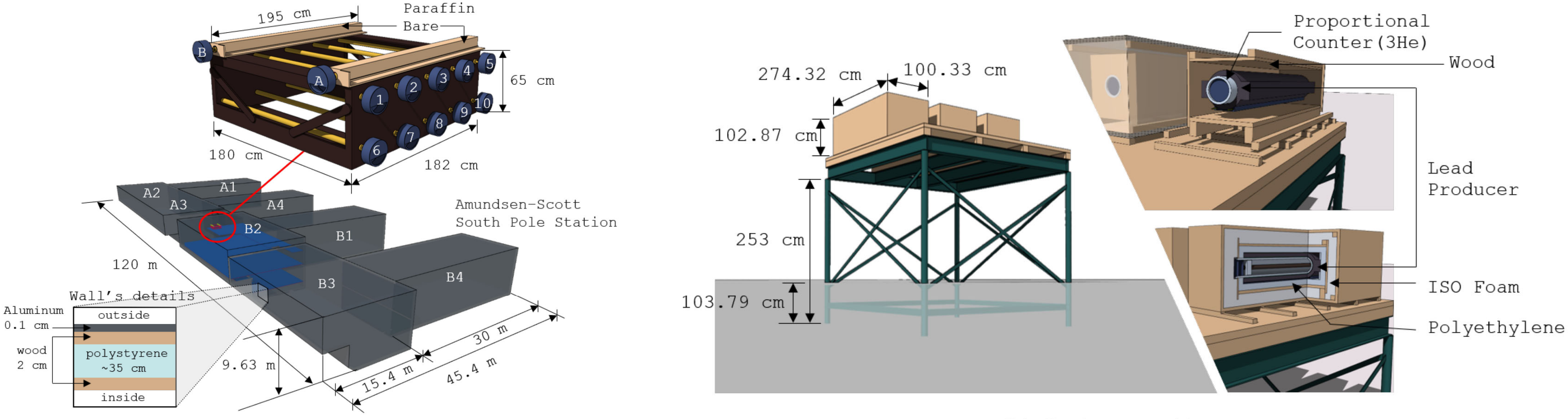

(a) Bare neutron detector

(b) Neutron monitor

Courtesy Pagwhan et al., 2021

Location	Moderator	Rate	Date
South Pole, Antarctica			
B2	None	13.492(4)	2012
B2	Paraffin	14.862(5)	2012
B2	Donut	13.82(2)	2010-01-23
Snow	Donut	12.88(9)	2010-01-26
University of Delaware, USA			
Patio	None	1.487(4)	2010-08-26
Patio	Paraffin	1.727(5)	2010-08-27
Patio	Donut	1.448(4)	2010-08-27
Patio	Standard	2.585(5)	2010-08-30
Shop	None	0.844(1)	2010-08-31
Shop	Paraffin	0.889(1)	2010-08-27
Shop	Donut	1.111(1)	2010-08-27
Shop	Standard	1.257(1)	2010-08-31

FIGURE 34 Bare ^{3}He Neutron Detector Tests

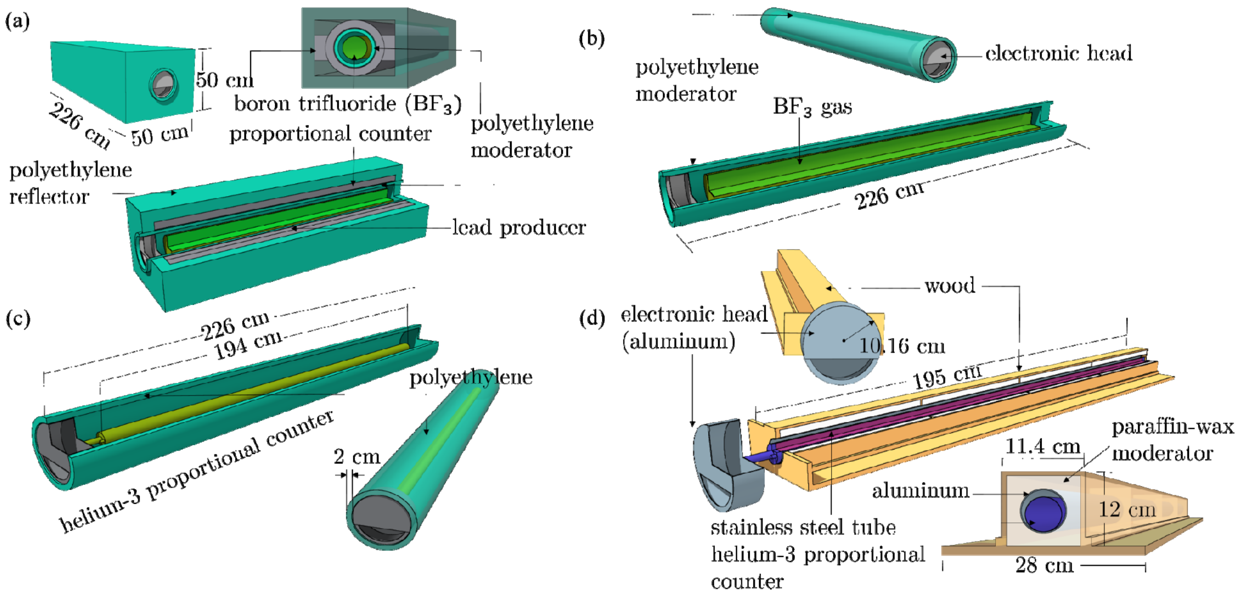

FIGURE 35 Neutron detectors

Courtesy Pagwhan et al., 2021

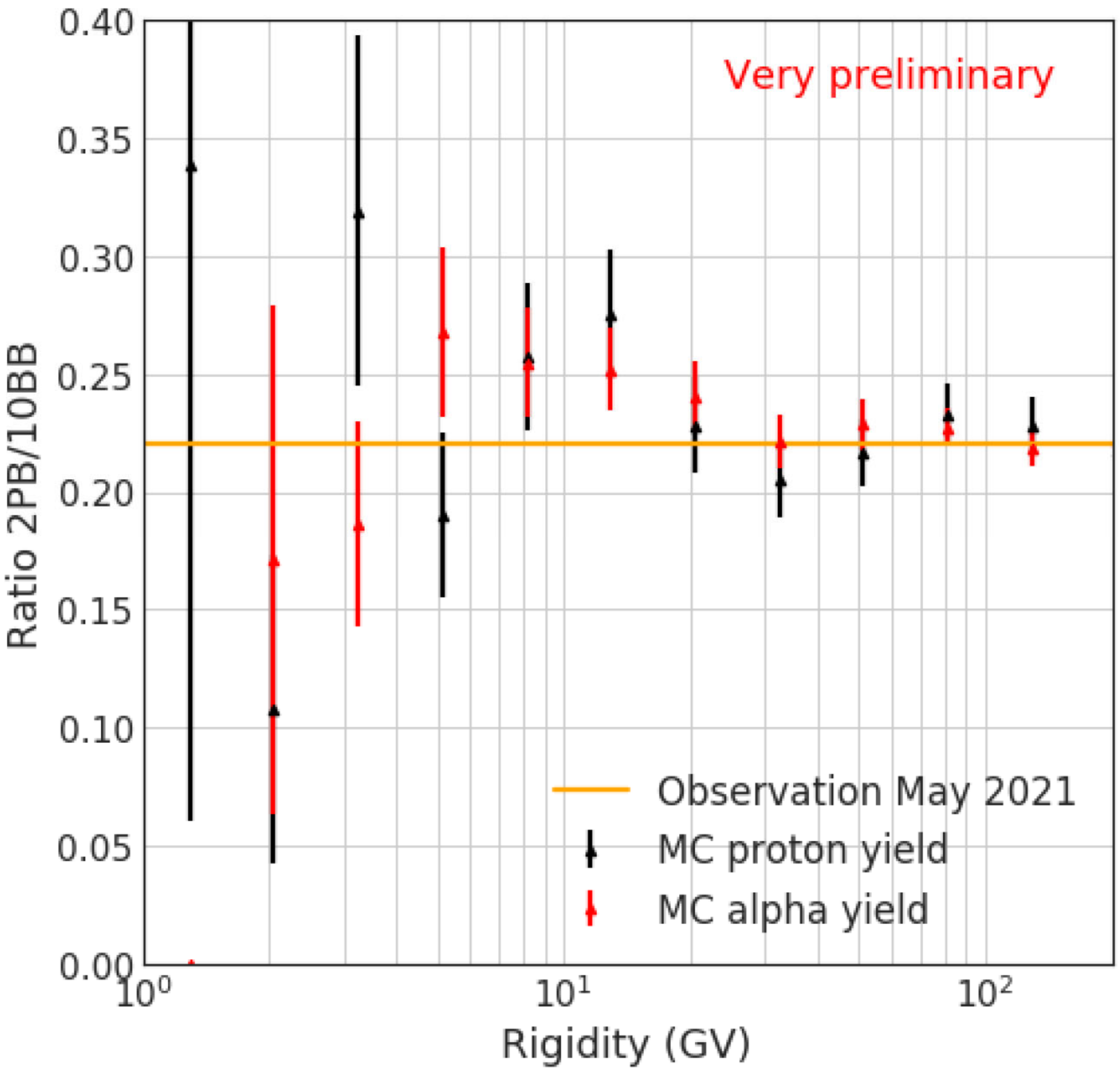

Figure 36 The ratio of the observed count rates at the South Pole for the two types of configuration (orange horizontal line) and the ratios of the simulated yield functions (red and black markers).

Courtesy Pagwhan et al., 2021

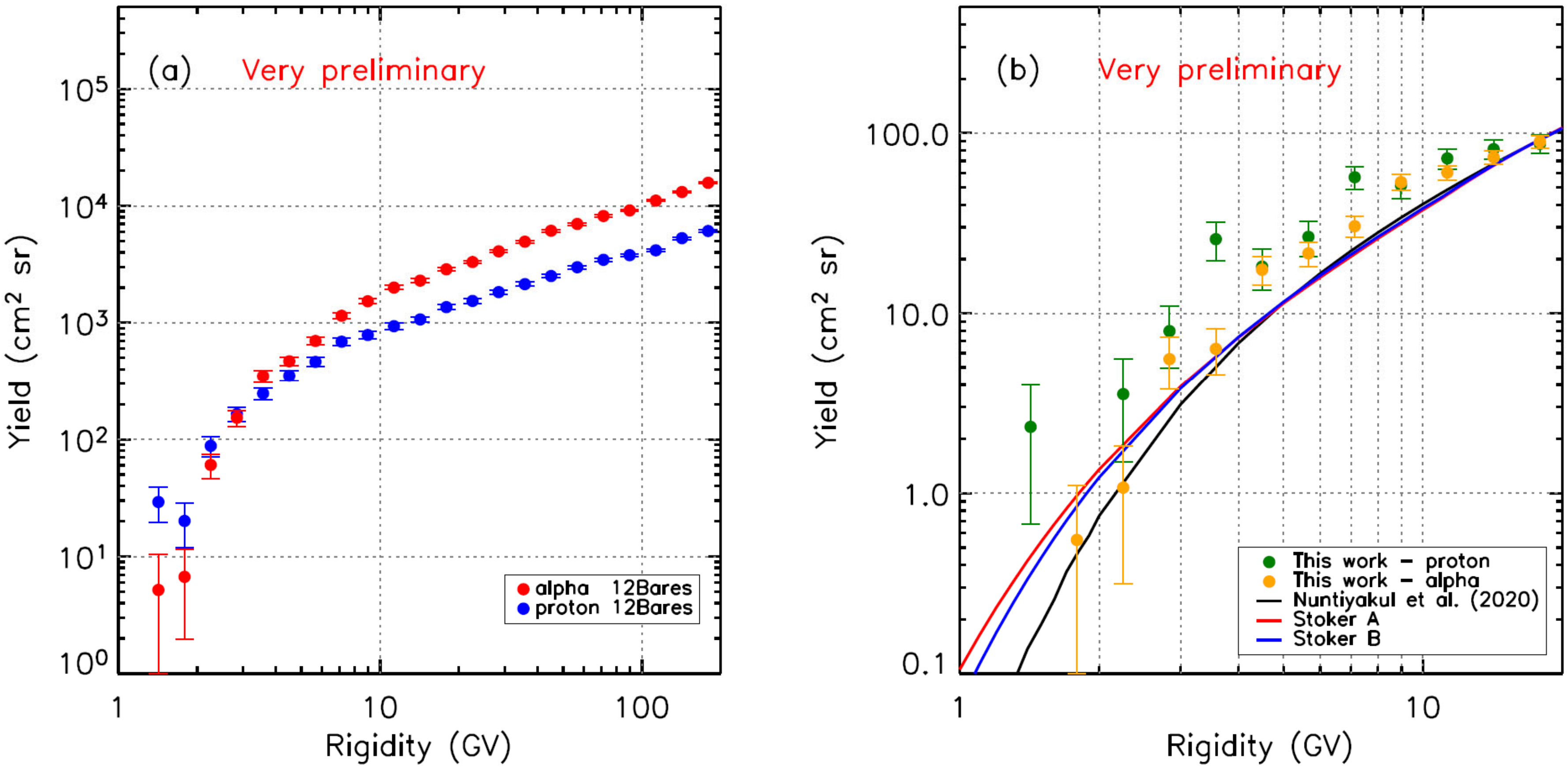

Figure 37 (a) Simulated YF for protons and alphas of 12 bare counters at the South Pole. (b) YF of the two Paraffin bares from this work compared to the determination of [6] and [17].

Courtesy Pagwhan et al., 2021

PLANS TO REPORT IN THE BOOTCAMP 2021 ARE:

- Expand beam size for bare neutron counter simulations
- Brainstorm how to improve FLUKA simulations for SP 3-1NM64

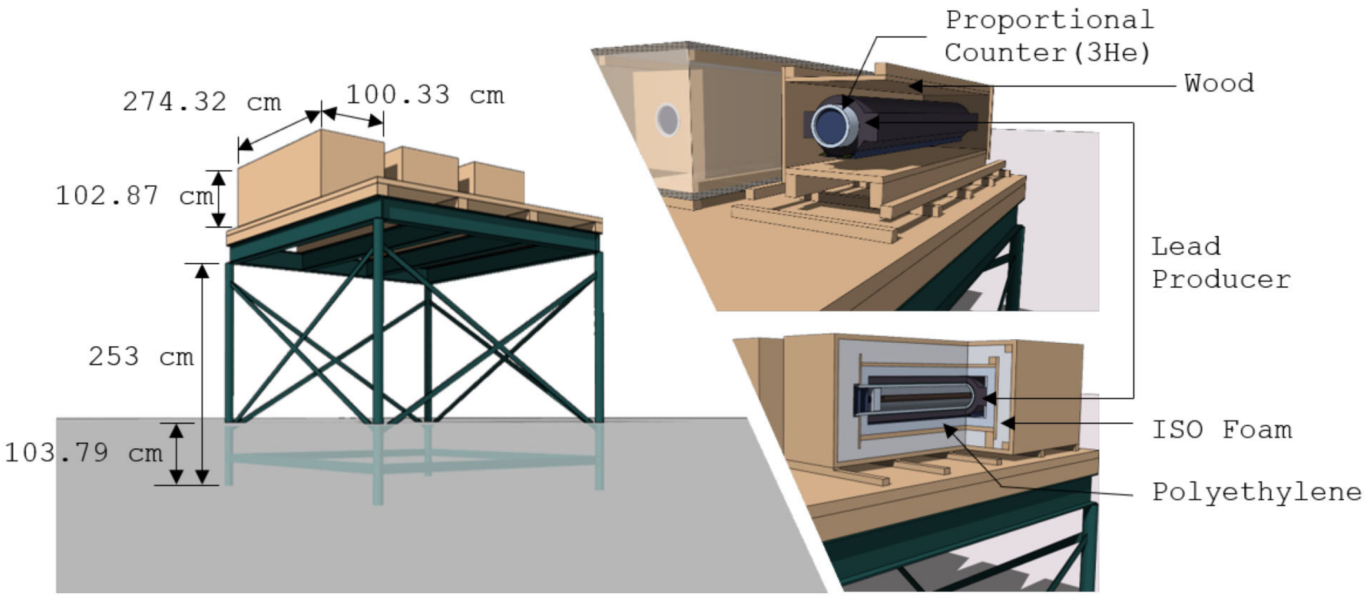

KIM

26 Dec 14:00 – 15:30 Hrs

DR.ACHARA SERIPIENLERT

Validation of Monte Carlo Yield Function of a Semi-Leaded Neutron Monitor using Latitude Survey Data in 2019 and 2020

Courtesy *Fongsamut et al., 2020*

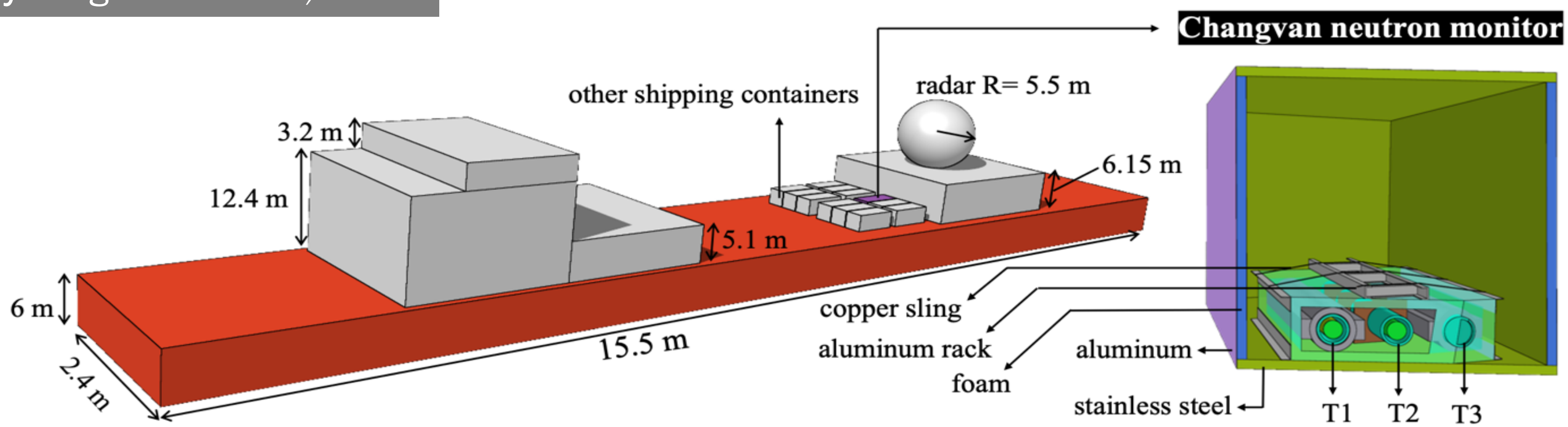

FIGURE 38 The geometry of the Changvan neutron monitor implemented in the FLUKA program. The dimensions and materials of some the main components are provided.

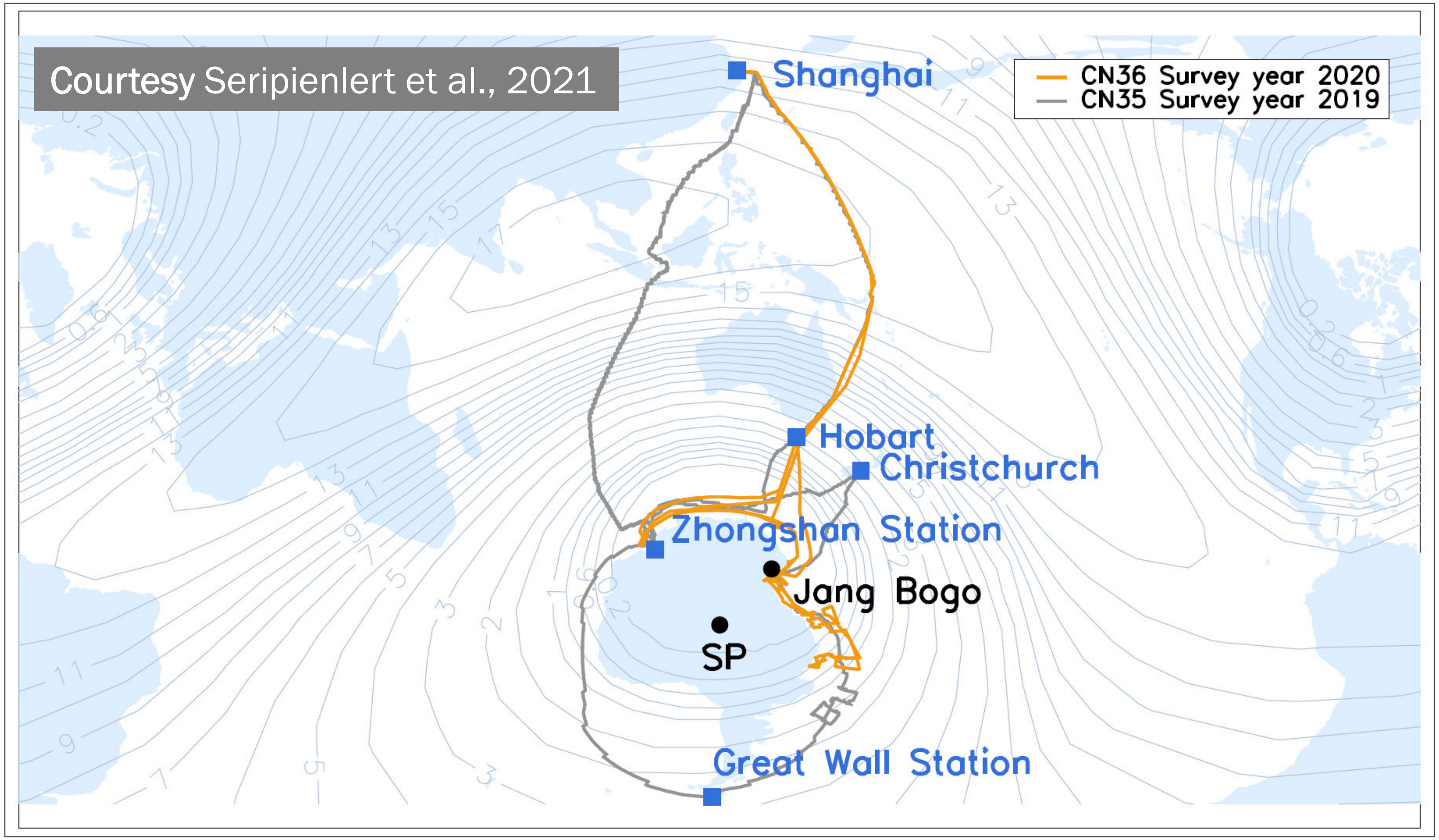

FIGURE 39 Path of Changvan neutron monitor in the 2019 (CN35: grey line) and 2020 (CN36: orange line) survey years. The contours with numbers indicate vertical cutoff rigidity (in the units of GV), calculated for February 11, 2019, at 12:00 UT.

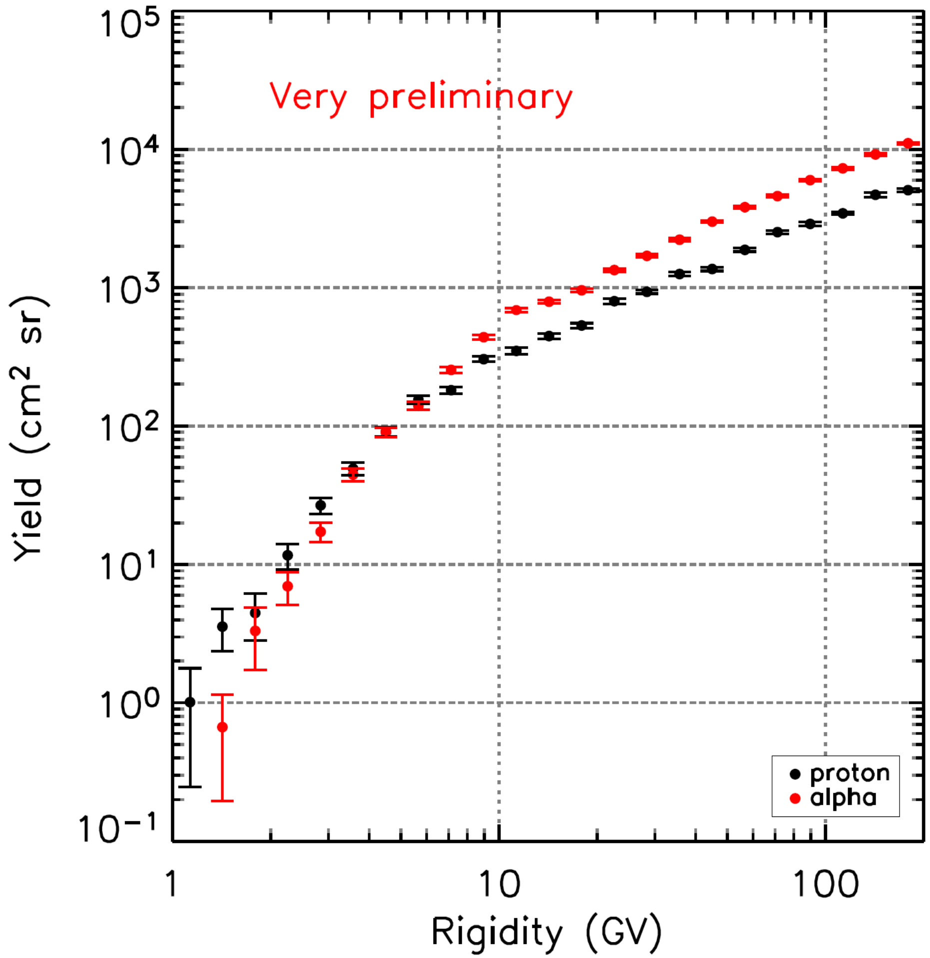

FIGURE 40 Yield functions for protons and alphas of Changvan neutron monitor

Courtesy Seripienlert et al., 2021

Courtesy Seripienlert et al., 2021

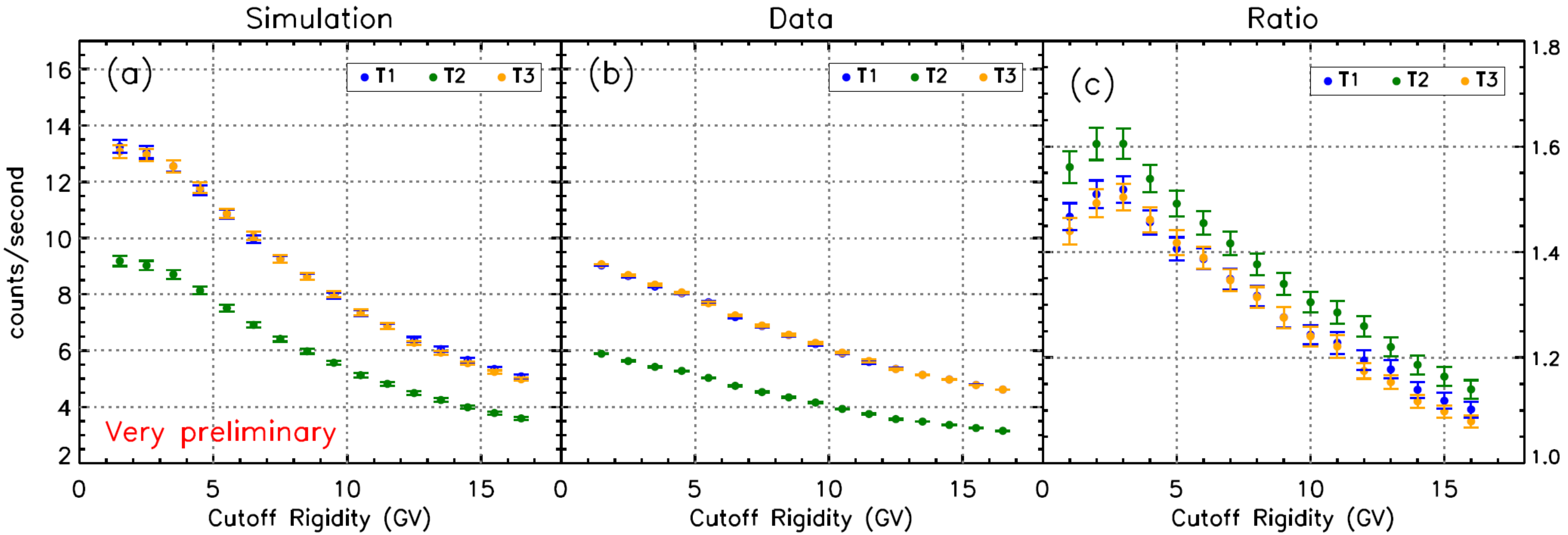

[Figure 41](#) Comparison between (a) Simulation count rate and (b) Data count rate. The simulation count rate is higher than the Data count rate. The ratio of Simulation/Data count rate is provided in (c). The vertical error bar in (a)–(b) represents the standard error, and (c) the error propagation of the ratio; in many cases, the error bar is smaller than the plot symbol.

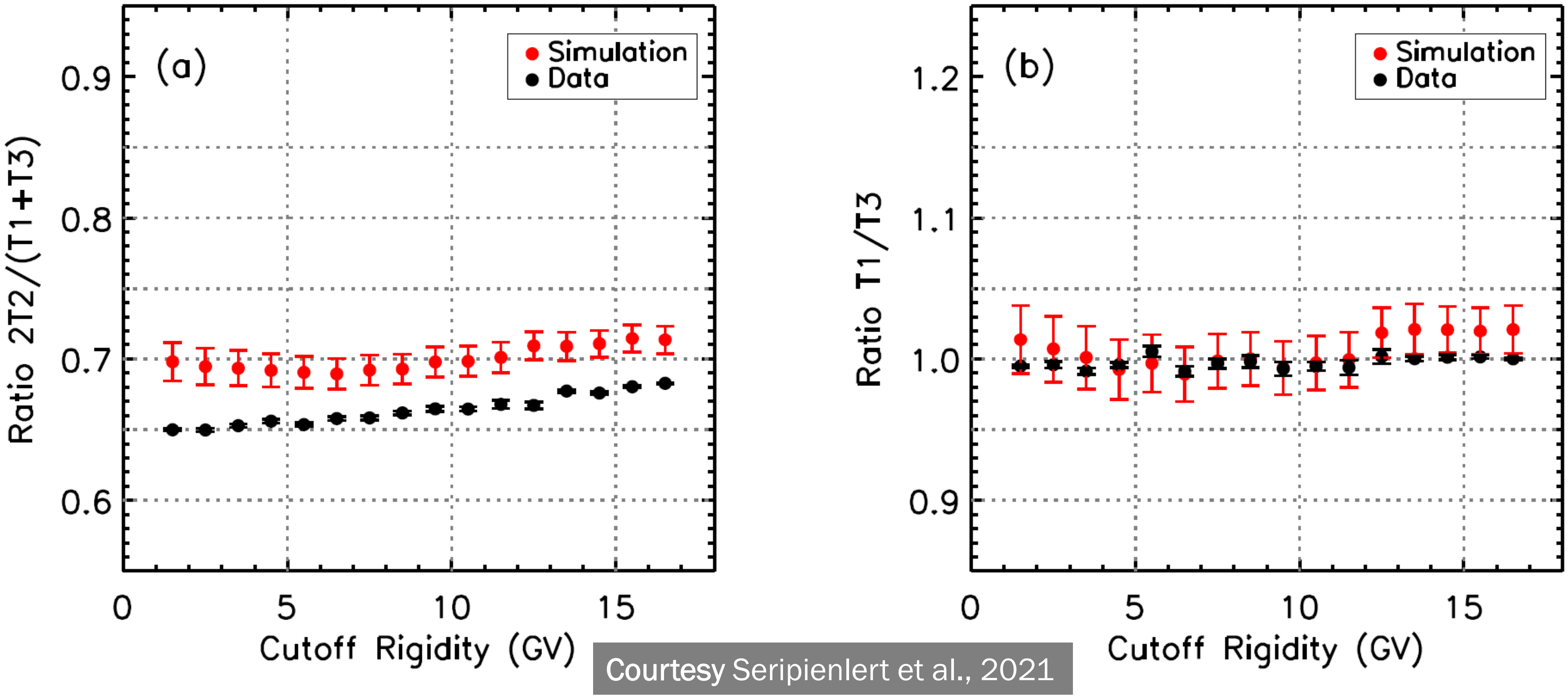

Figure 42 (a) The ratios of unleaded/leaded NM count rates. (b) The ratio of leaded/leaded NM rates. The vertical error bar represent the error propagation of the ratio, which still large for the simulated results.

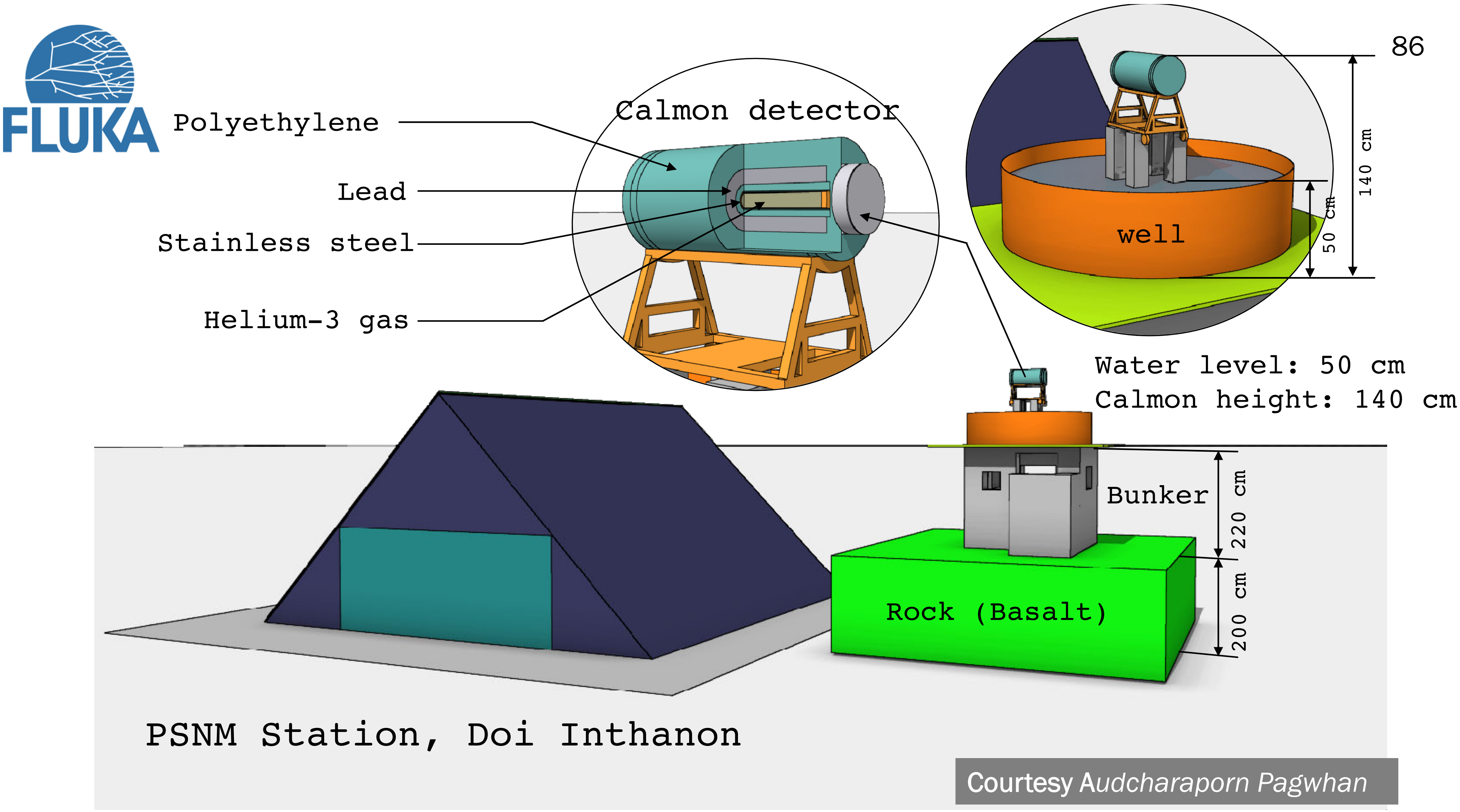
FLUKA
Polyethylene
Lead
Stainless steel
Helium-3 gas
Calmon detector
well
140 cm
50 cm
Water level: 50 cm
Calmon height: 140 cm
Bunker
220 cm
200 cm
Rock (Basalt)
PSNM Station, Doi Inthanon
Courtesy Audcharaporn Pagwhan

FIGURE 43

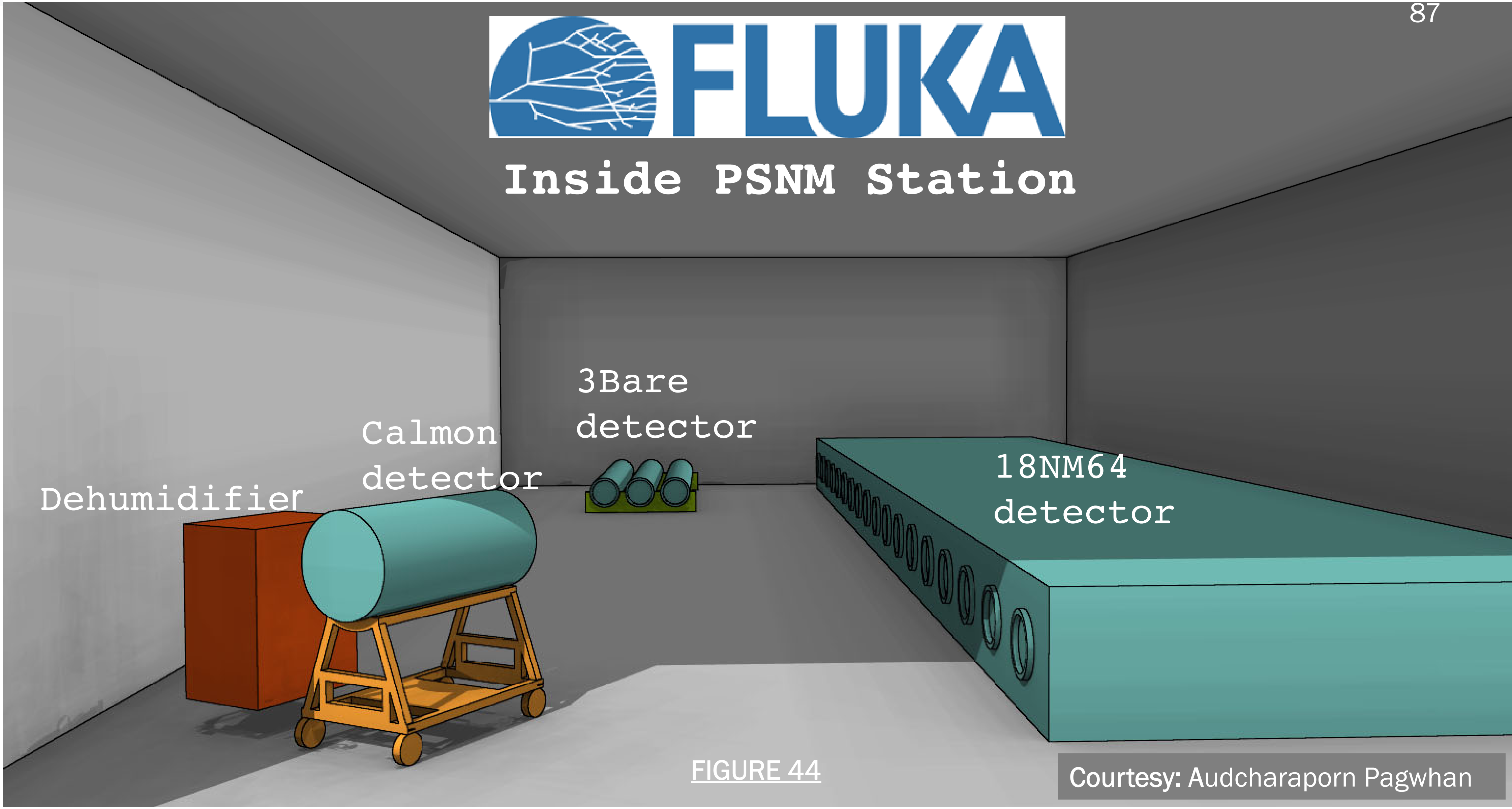
FLUKA
Inside PSNM Station
3Bare detector
Calmon detector
18NM64 detector
Dehumidifier
Courtesy: Audcharaporn Pagwhan

FIGURE 44

Table 1. Observations With the Calibrator at Doi Inthanon[a]

Courtesy Aiemsa-ad et al., 2015

Configuration	Calibrator Height (cm)	Water Height (cm)	Start Time[b]	Stop Time[b]	Electronics	Cal/NM[c]	N^d
1	140	0	2009/327/11	2009/341/03	NWU1	0.005710(6)	2.97×10^6
2	140	50	2009/342/01	2009/349/03	NWU1	0.005635(6)	1.98×10^6
3	140	68	2009/349/08	2009/357/06	NWU1	0.005622(6)	2.11×10^6
4	140	25	2009/357/07	2009/362/02	NWU1	0.005659(7)	1.27×10^6
5	70	0	2009/362/08	2010/005/01	NWU1	0.005744(7)	2.17×10^6
6	70	60	2010/008/11	2010/017/04	NWU1	0.005505(5)	2.28×10^6
8	70	65	2010/042/07	2010/096/23	BRI	0.004860(2)	9.12×10^6
9	70	65	2010/098/08	2010/110/08	NWU1	0.005506(4)	2.68×10^6
10	70	65	2010/112/05	2010/127/05	NWU2	0.005637(6)	2.76×10^6
11	70	50	2010/127/06	2010/132/01	NWU2	0.005771(12)	8.99×10^5
12	70	25	2010/132/02	2010/155/02	NWU2	0.005695(6)	4.54×10^6
13	70	0	2010/155/04	2010/158/04	NWU2	0.005756(15)	6.45×10^5
15	55	0	2010/162/07	2010/179/02	BRI	0.005007(2)	4.48×10^6

[a]For Configurations 1–13, the calibrator was outside the PSNM building as in Figure 3. For Configuration 15, the calibrator was inside the PSNM building as in Figure 2.

[b]Year/day of year/hour (UT).

[c]Calibrator to PSNM count rate ratio. Parentheses indicate statistical standard error in the final digits.

[d]Counts detected by the calibrator during usable times.

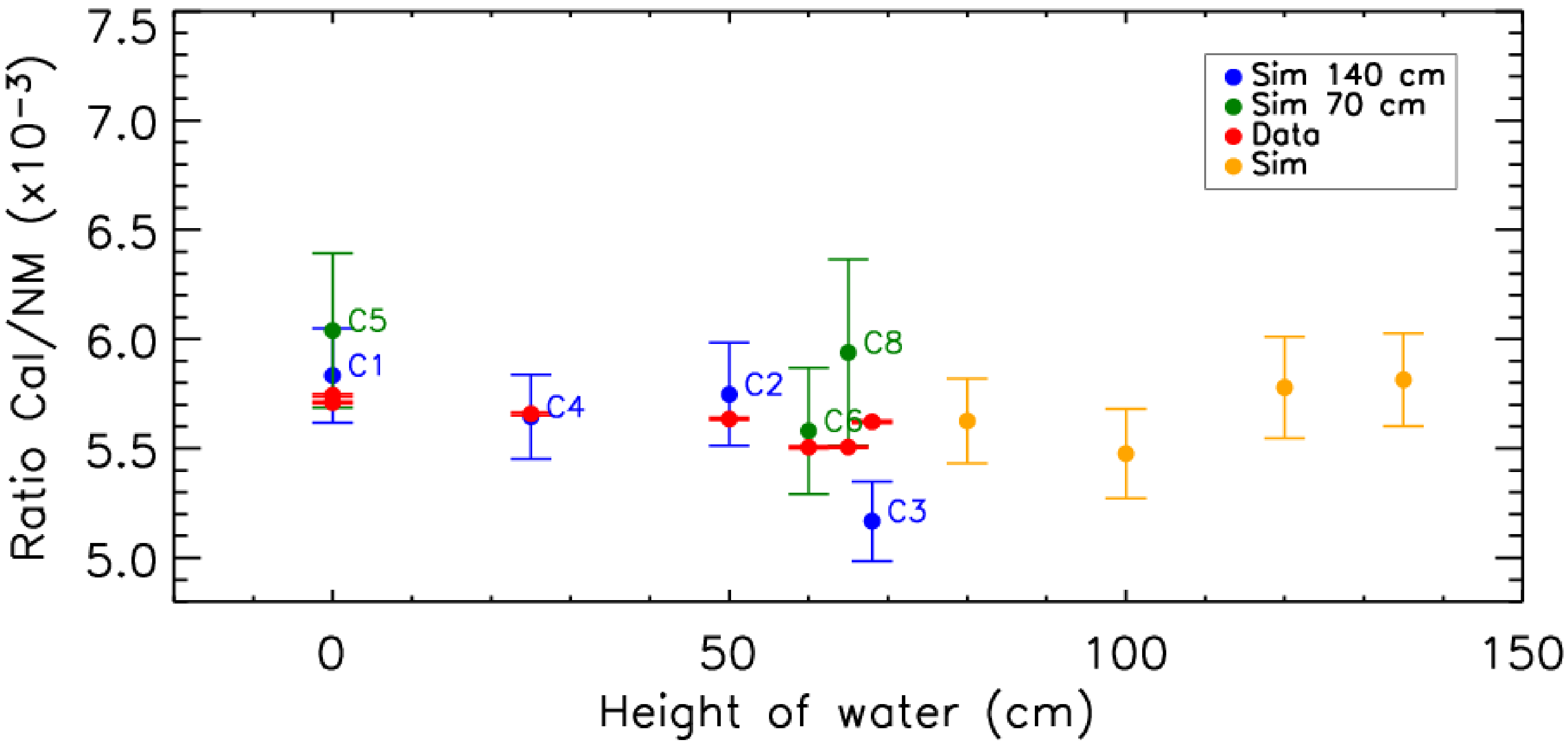

FIGURE 45 Ratio Cal/NM Vs. height of water (cm)

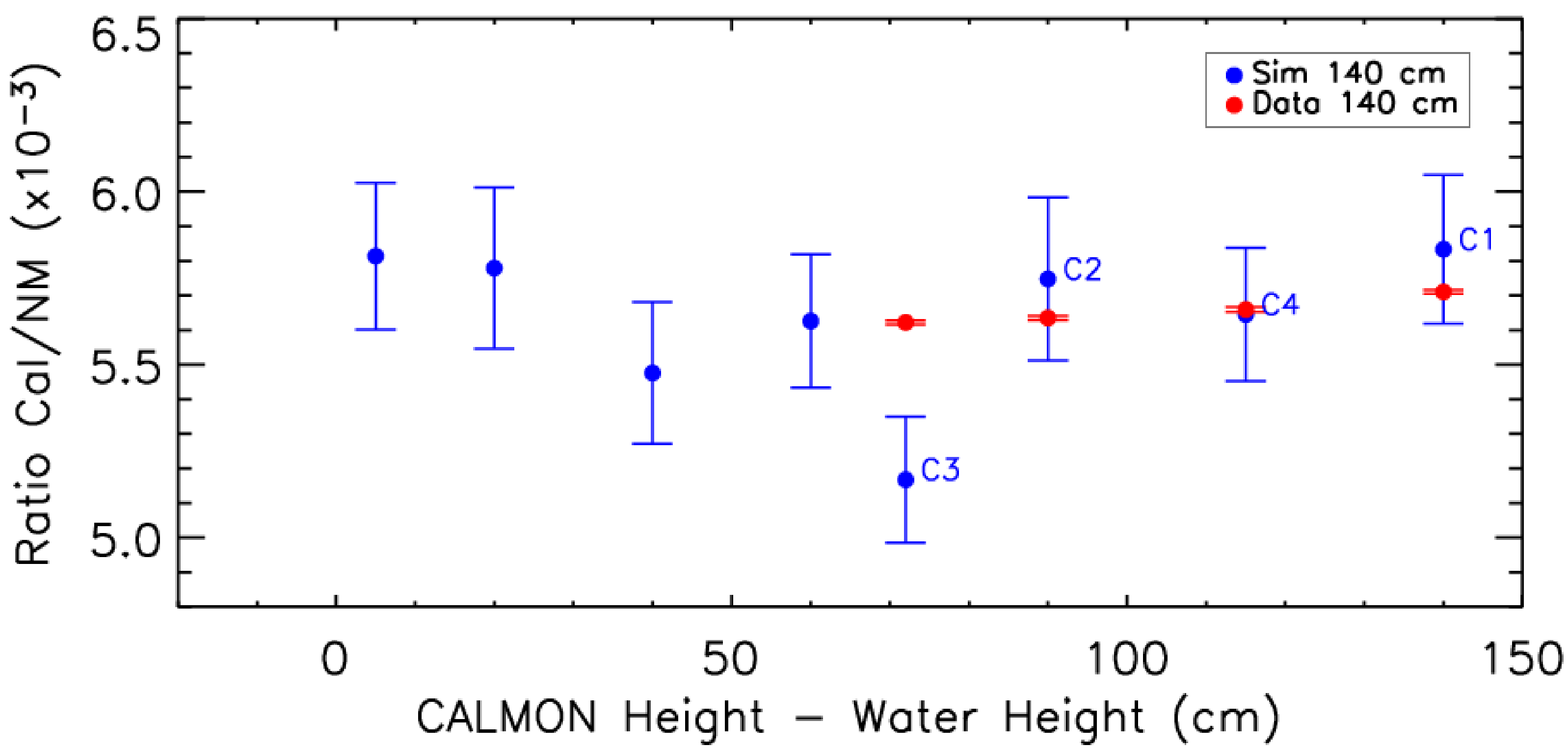

FIGURE 46 Ratio Cal/NM Vs. Calmon height – water height (cm)

JOE

26 Dec 16:00 – 17:30 Hrs

MR. MONTREE PHETA

Maser polarization in 3D with numerical implementation

A **maser** (/ˈmeɪzər/, an acronym for **microwave amplification by stimulated emission of radiation**) is a device that produces coherent electromagnetic waves through amplification by stimulated emission.

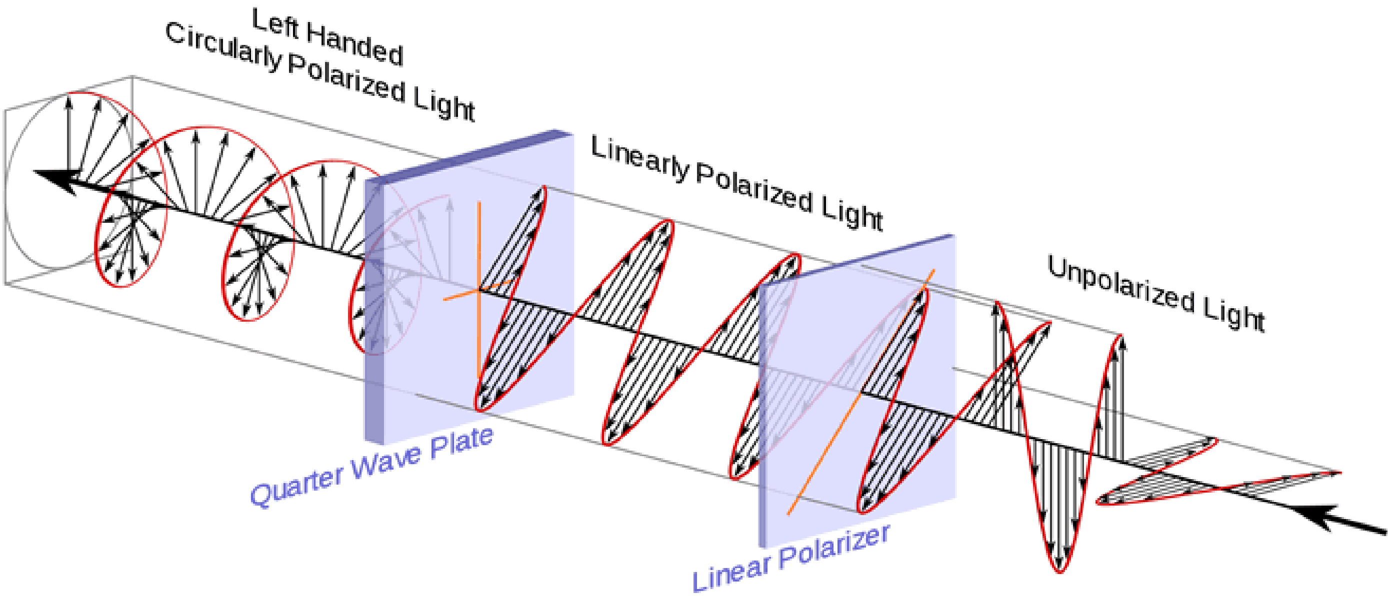

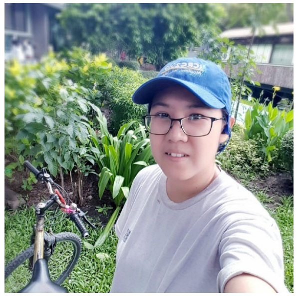

Nok

27 Dec 18:00 – 19:00 Hrs

DR. CHANOKNAN BANGLIENG

GPS – (Water Vapour Pressure) WVP Workshop and GDAS

National Centers for Environmental Information
NATIONAL OCEANIC AND ATMOSPHERIC ADMINISTRATION

Search NCEI

Home Products Services Resources News About Contact

Home / *Products* / *Weather and Climate Models* / Global Data Assimilation System

Global Data Assimilation System

The National Center for Environmental Prediction (NCEP) uses the Global Data Assimilation System (GDAS) to interpolate data from a variety of observing systems and instruments onto a three-dimensional grid. NCEI provides access to this gridded output data, which is used to initialize the NCEP Global Forecasting System (GFS) model.

Alex

27 Dec 18:00 – 19:00 Hrs

DR. ALEJANDRO SAIZ

Antarctica adventure

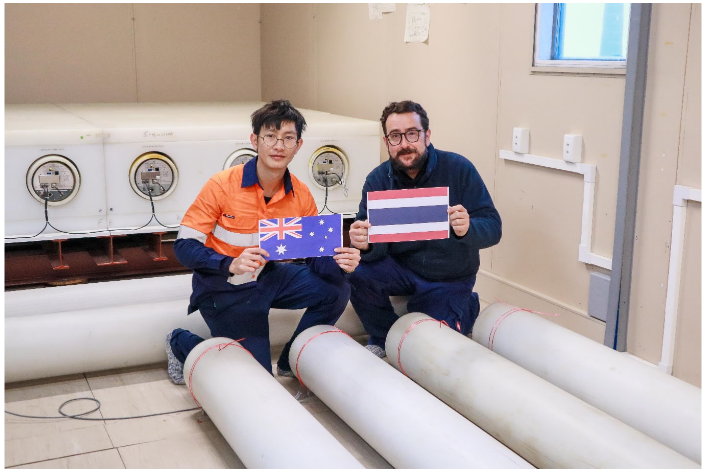

FLUKA

28 Dec 09:00 – 22:00 Hrs

Instructors

DR.ACHARA SERIPIENLERT
MISS Audcharaporn pagwhan

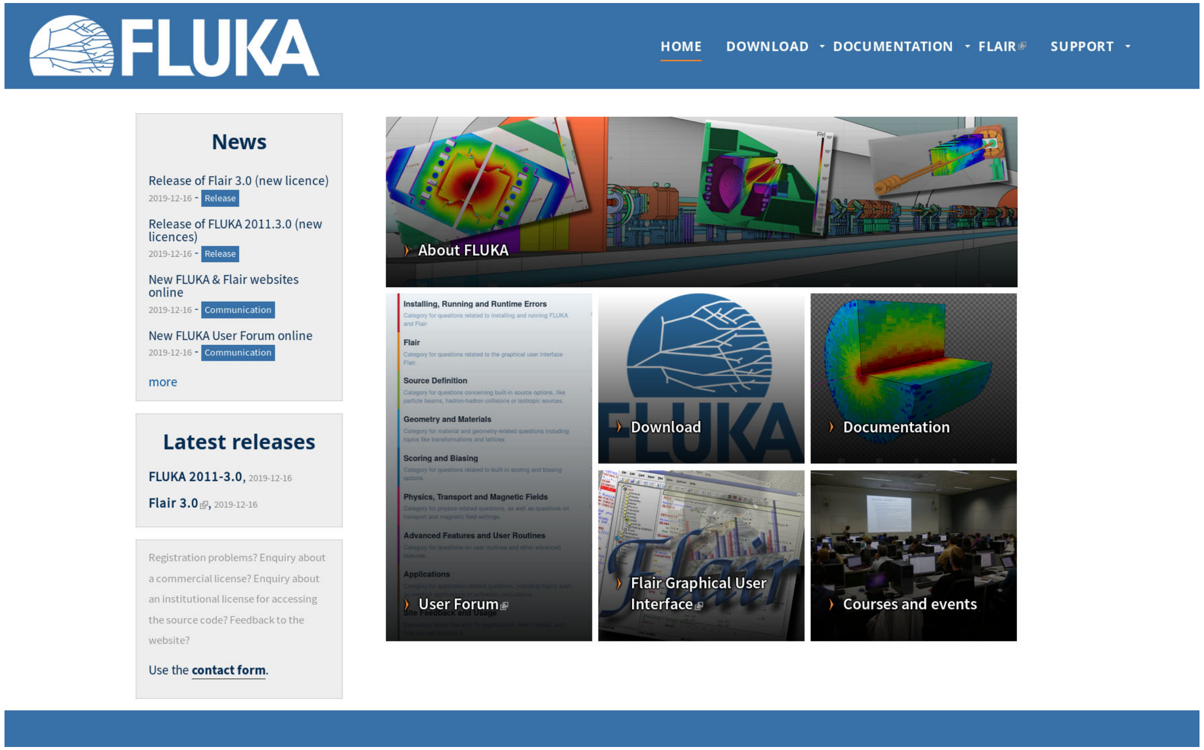

M

MR. EKKARACH SOOMBOON

Analysis of Neutron Time-Delay Histograms from Mawson NM Station

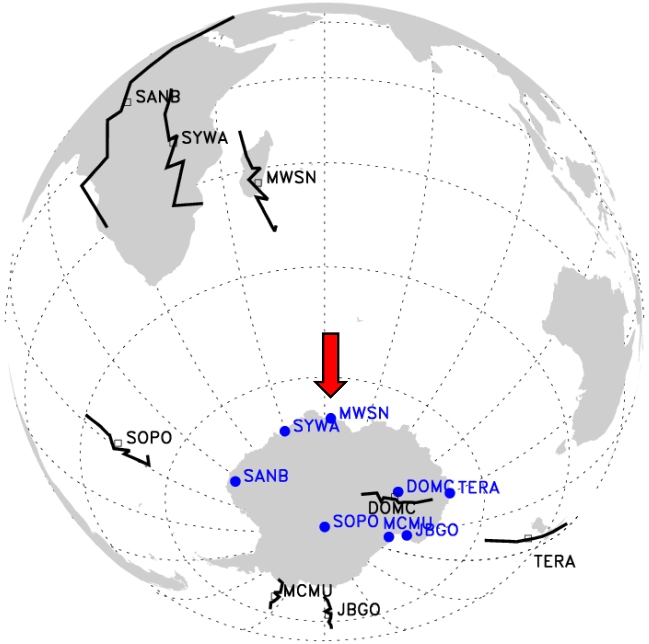

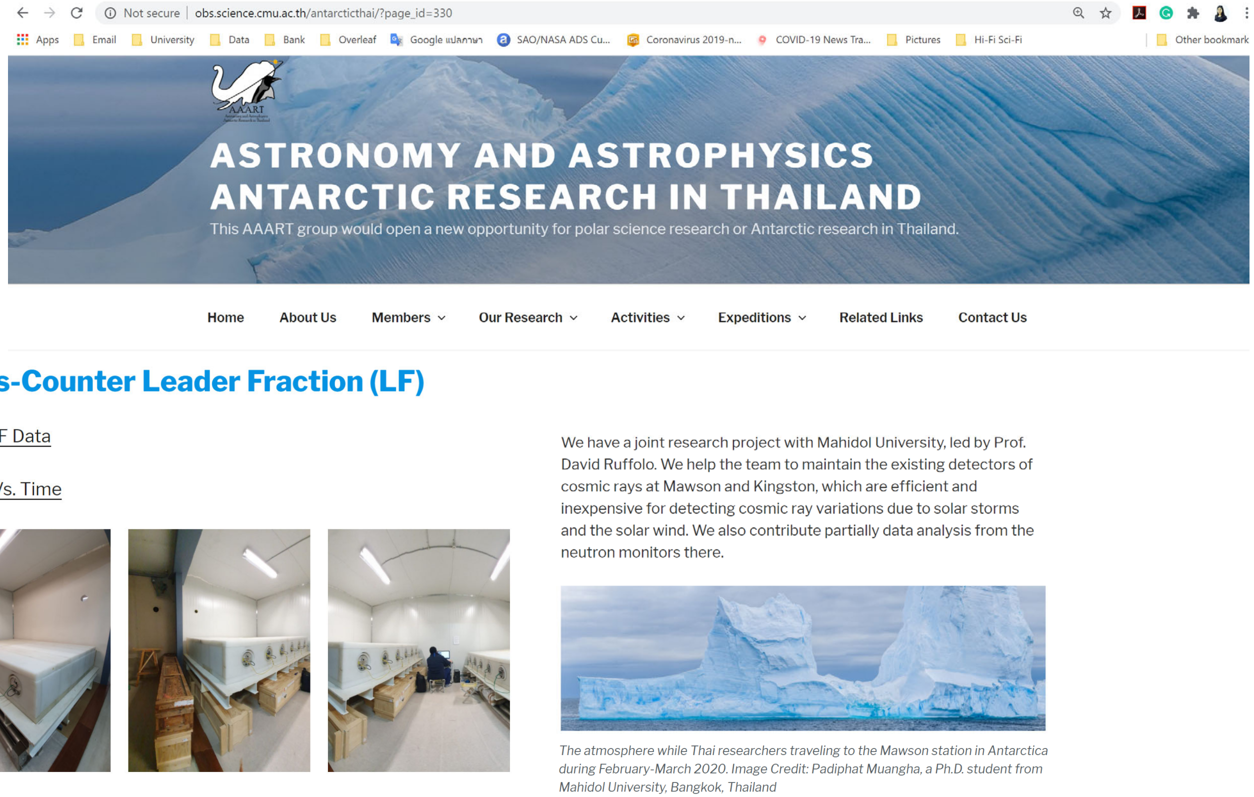

Courtesy Nuntiyakul et al.

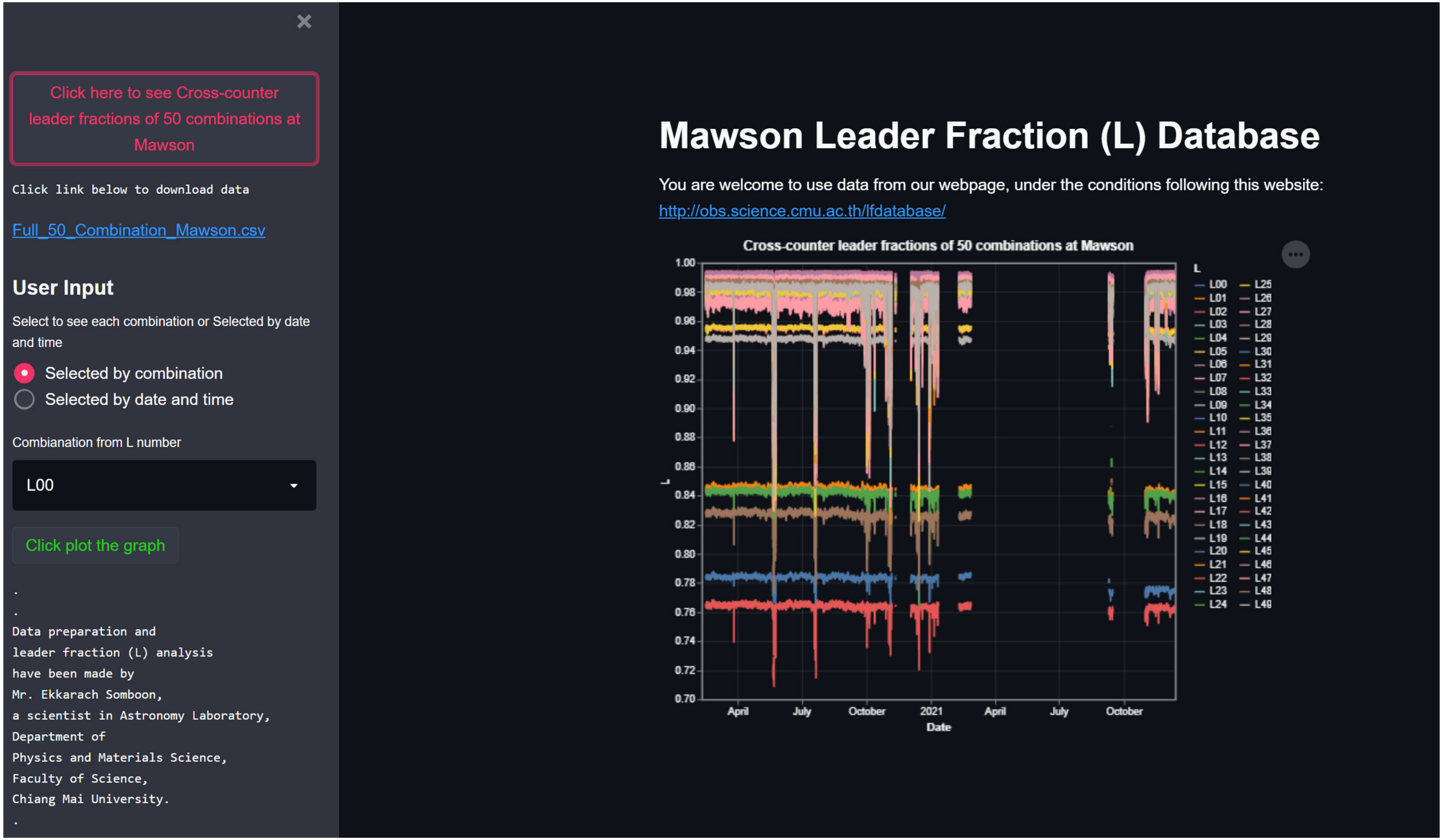
Click here to see Cross-counter leader fractions of 50 combinations at Mawson
Click link below to download data
Full_50_Combination_Mawson.csv
User Input
Select to see each combination or Selected by date and time
Selected by combination
Selected by date and time
Combianation from L number
L00
Click plot the graph
Data preparation and leader fraction (L) analysis have been made by Mr. Ekkarach Somboon, a scientist in Astronomy Laboratory, Department of Physics and Materials Science, Faculty of Science, Chiang Mai University.
Mawson Leader Fraction (L) Database
You are welcome to use data from our webpage, under the conditions following this website:
http://obs.science.cmu.ac.th/lfdatabase/
Cross-counter leader fractions of 50 combinations at Mawson
1.00
0.98
0.96
0.94
0.92
0.90
0.88
0.86
0.84
0.82
0.80
0.78
0.76
0.74
0.72
0.70
L
April
July
October
2021
April
July
October
Date

FIGURE 47

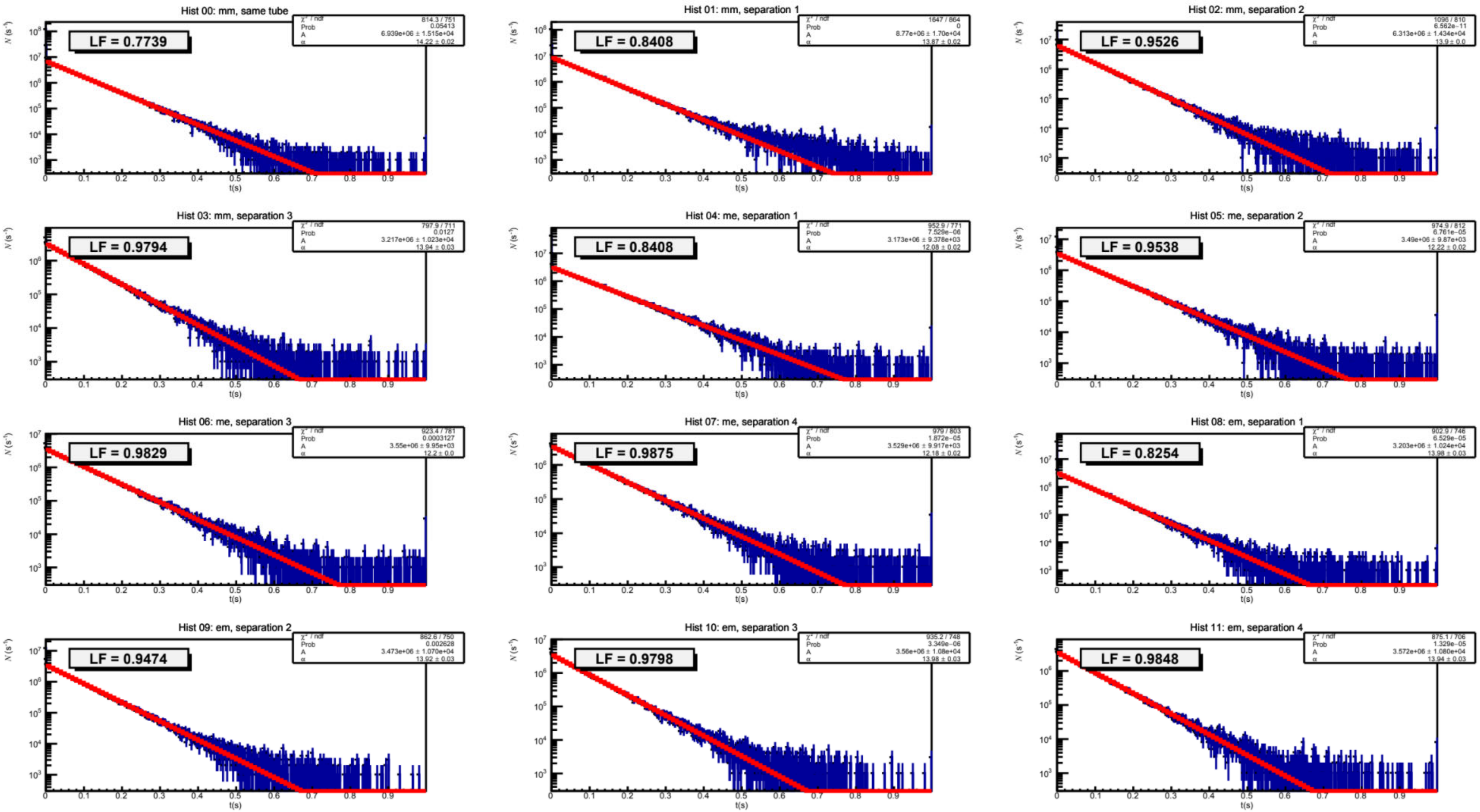
Hist 00: mm, same tube
LF = 0.7739
Hist 01: mm, separation 1
LF = 0.8408
Hist 02: mm, separation 2
LF = 0.9526
Hist 03: mm, separation 3
LF = 0.9794
Hist 04: me, separation 1
LF = 0.8408
Hist 05: me, separation 2
LF = 0.9538
Hist 06: me, separation 3
LF = 0.9829
Hist 07: me, separation 4
LF = 0.9875
Hist 08: em, separation 1
LF = 0.8254
Hist 09: em, separation 2
LF = 0.9474
Hist 10: em, separation 3
LF = 0.9798
Hist 11: em, separation 4
LF = 0.9848
t(s)

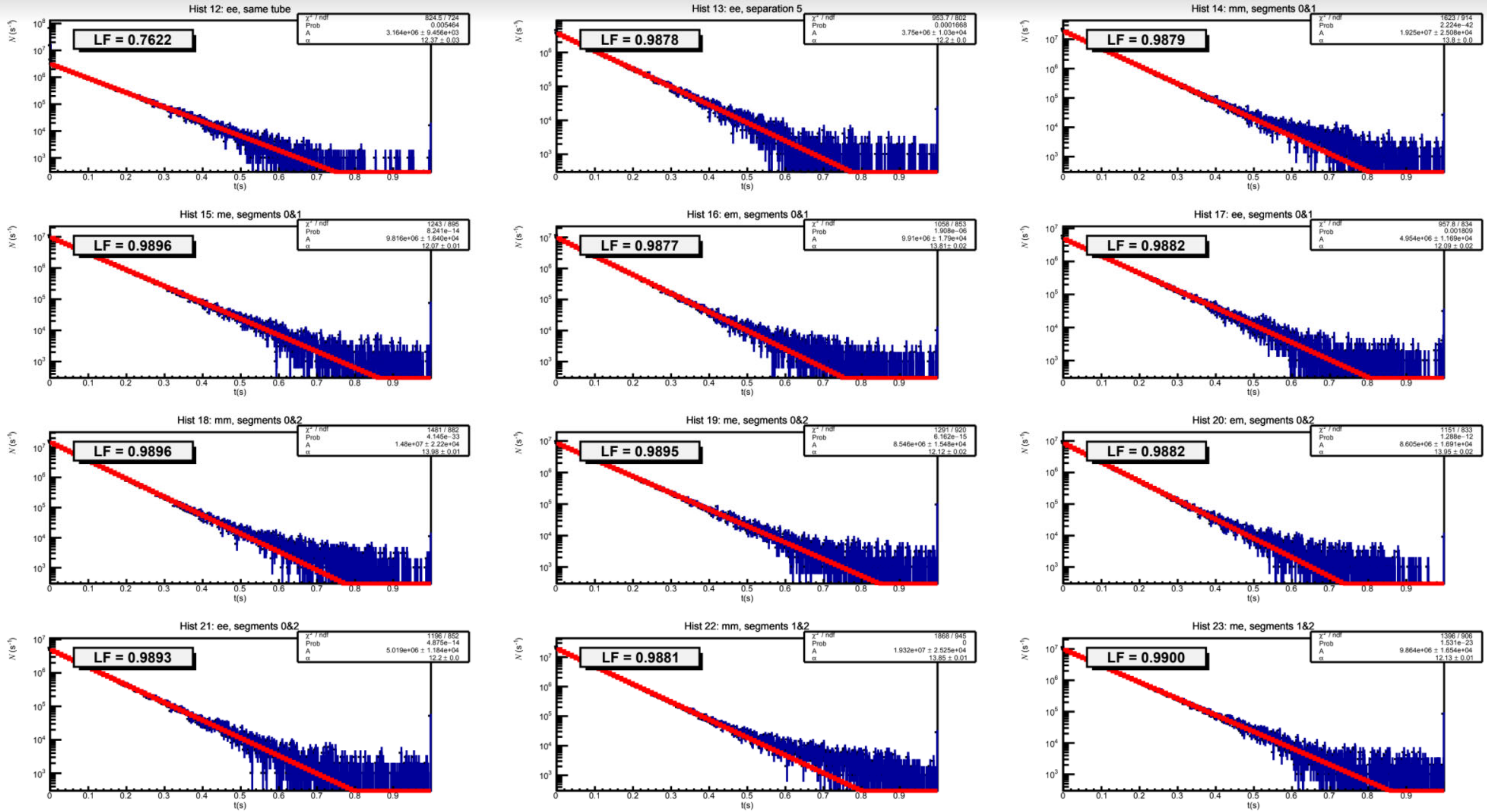
Hist 12: ee, same tube
LF = 0.7622
Hist 13: ee, separation 5
LF = 0.9878
Hist 14: mm, segments 0&1
LF = 0.9879
Hist 15: me, segments 0&1
LF = 0.9896
Hist 16: em, segments 0&1
LF = 0.9877
Hist 17: ee, segments 0&1
LF = 0.9882
Hist 18: mm, segments 0&2
LF = 0.9896
Hist 19: me, segments 0&2
LF = 0.9895
Hist 20: em, segments 0&2
LF = 0.9882
Hist 21: ee, segments 0&2
LF = 0.9893
Hist 22: mm, segments 1&2
LF = 0.9881
Hist 23: me, segments 1&2
LF = 0.9900
t(s)

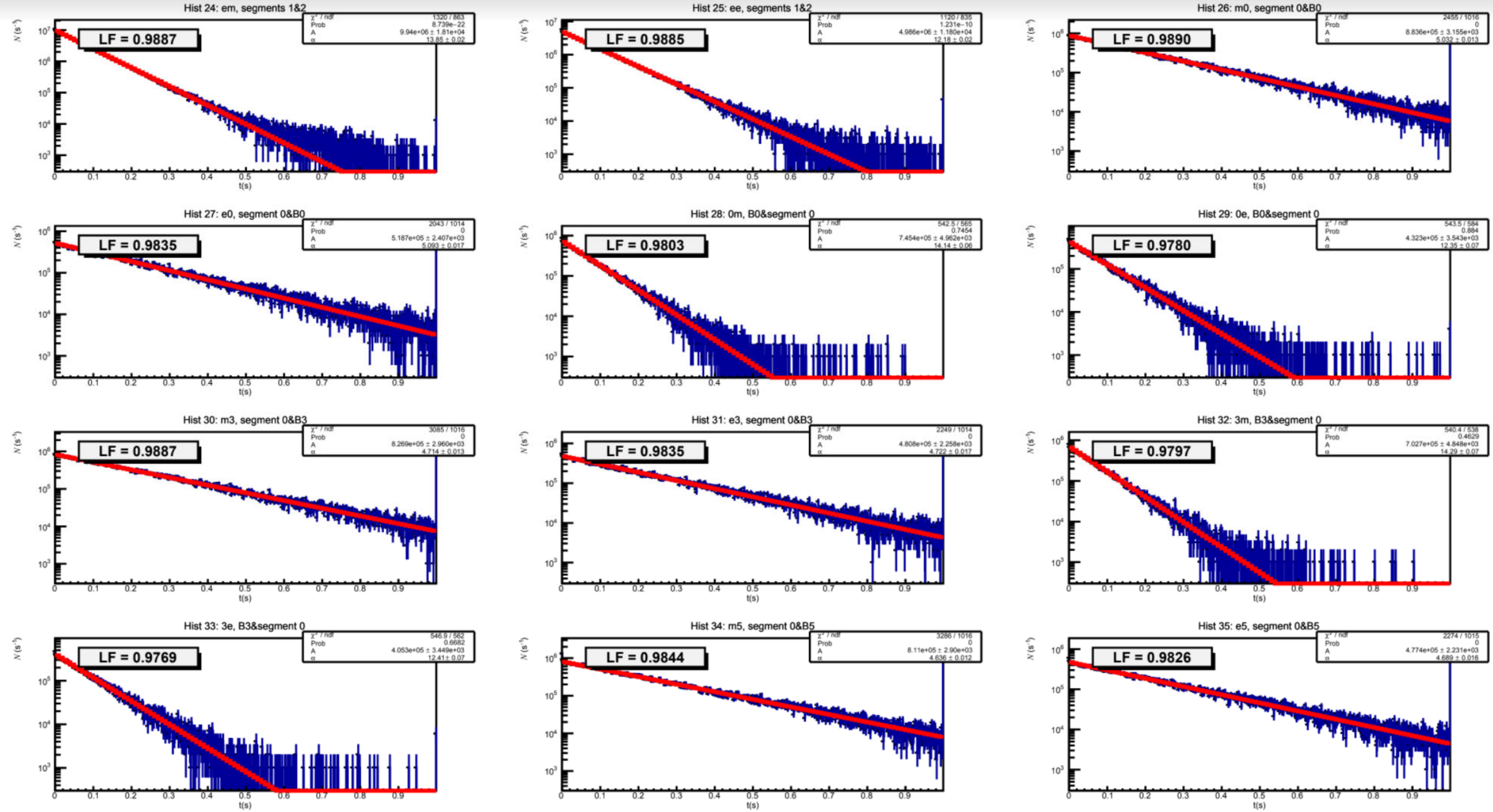
Hist 24: em, segments 1&2
LF = 0.9887
χ² / ndf 1320 / 863
Prob 8.739e−22
A 9.94e+06 ± 1.81e+04
α 13.85 ± 0.02
Hist 25: ee, segments 1&2
LF = 0.9885
χ² / ndf 1120 / 835
Prob 1.231e−10
A 4.986e+06 ± 1.180e+04
α 12.18 ± 0.02
Hist 26: m0, segment 0&B0
LF = 0.9890
χ² / ndf 2455 / 1016
Prob 0
A 8.836e+05 ± 3.155e+03
α 5.032 ± 0.013
Hist 27: e0, segment 0&B0
LF = 0.9835
χ² / ndf 2043 / 1014
Prob 0
A 5.187e+05 ± 2.407e+03
α 5.093 ± 0.017
Hist 28: 0m, B0&segment 0
LF = 0.9803
χ² / ndf 542.5 / 565
Prob 0.7454
A 7.454e+05 ± 4.962e+03
α 14.14 ± 0.06
Hist 29: 0e, B0&segment 0
LF = 0.9780
χ² / ndf 543.5 / 584
Prob 0.884
A 4.323e+05 ± 3.543e+03
α 12.35 ± 0.07
Hist 30: m3, segment 0&B3
LF = 0.9887
χ² / ndf 3085 / 1016
Prob 0
A 8.269e+05 ± 2.960e+03
α 4.714 ± 0.013
Hist 31: e3, segment 0&B3
LF = 0.9835
χ² / ndf 2249 / 1014
Prob 0
A 4.808e+05 ± 2.258e+03
α 4.722 ± 0.017
Hist 32: 3m, B3&segment 0
LF = 0.9797
χ² / ndf 540.4 / 538
Prob 0.4629
A 7.027e+05 ± 4.848e+03
α 14.29 ± 0.07
Hist 33: 3e, B3&segment 0
LF = 0.9769
χ² / ndf 546.9 / 562
Prob 0.6682
A 4.053e+05 ± 3.449e+03
α 12.41 ± 0.07
Hist 34: m5, segment 0&B5
LF = 0.9844
χ² / ndf 3286 / 1016
Prob 0
A 8.11e+05 ± 2.90e+03
α 4.636 ± 0.012
Hist 35: e5, segment 0&B5
LF = 0.9826
χ² / ndf 2274 / 1015
Prob 0
A 4.774e+05 ± 2.231e+03
α 4.689 ± 0.016
N (s⁻¹)
t(s)

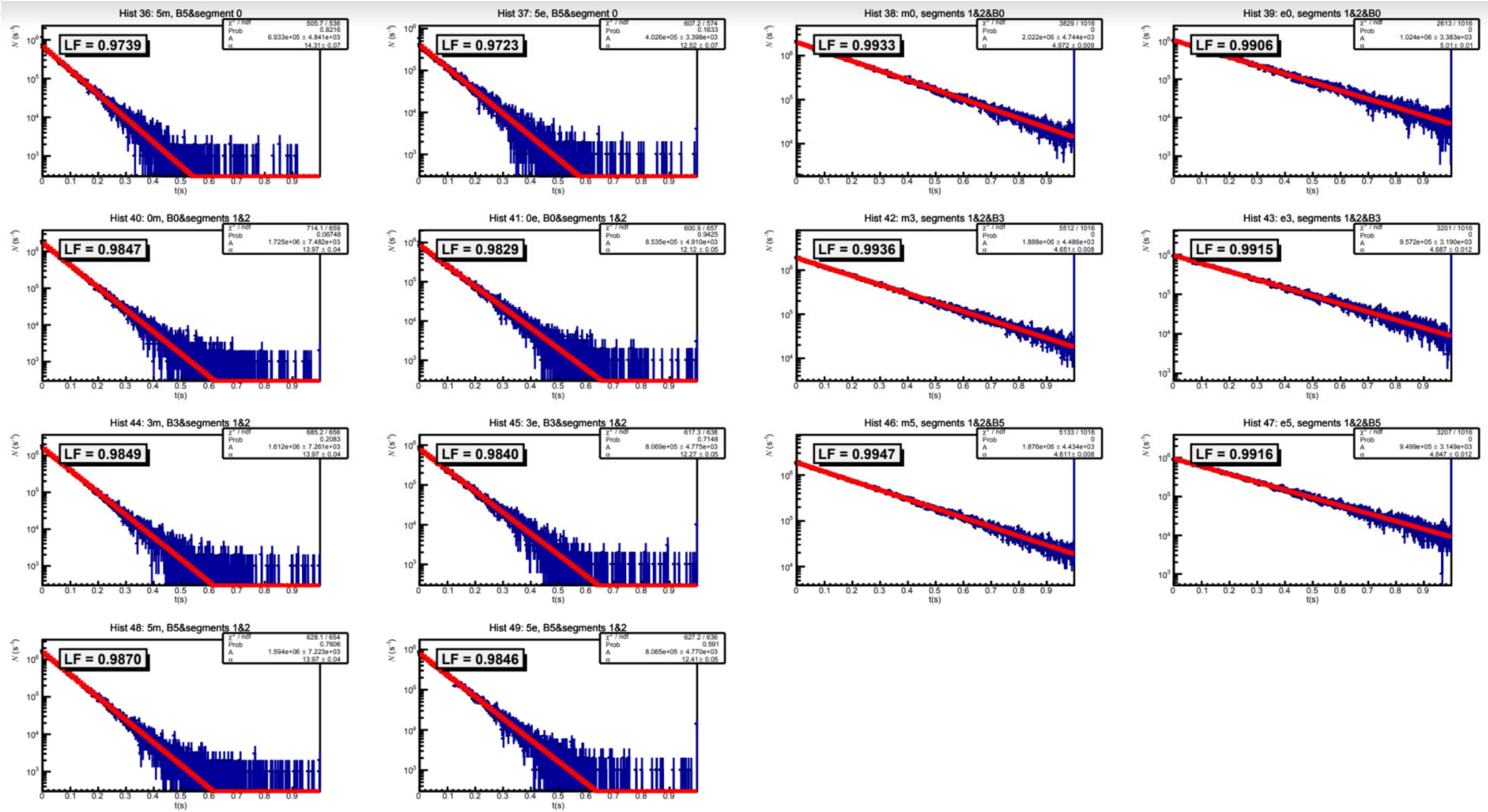
Hist 36: 5m, B5&segment 0
LF = 0.9739
Hist 37: 5e, B5&segment 0
LF = 0.9723
Hist 38: m0, segments 1&2&B0
LF = 0.9933
Hist 39: e0, segments 1&2&B0
LF = 0.9906
Hist 40: 0m, B0&segments 1&2
LF = 0.9847
Hist 41: 0e, B0&segments 1&2
LF = 0.9829
Hist 42: m3, segments 1&2&B3
LF = 0.9936
Hist 43: e3, segments 1&2&B3
LF = 0.9915
Hist 44: 3m, B3&segments 1&2
LF = 0.9849
Hist 45: 3e, B3&segments 1&2
LF = 0.9840
Hist 46: m5, segments 1&2&B5
LF = 0.9947
Hist 47: e5, segments 1&2&B5
LF = 0.9916
Hist 48: 5m, B5&segments 1&2
LF = 0.9870
Hist 49: 5e, B5&segments 1&2
LF = 0.9846
t(s)

OUTREACH

Web resources & Facebook Page

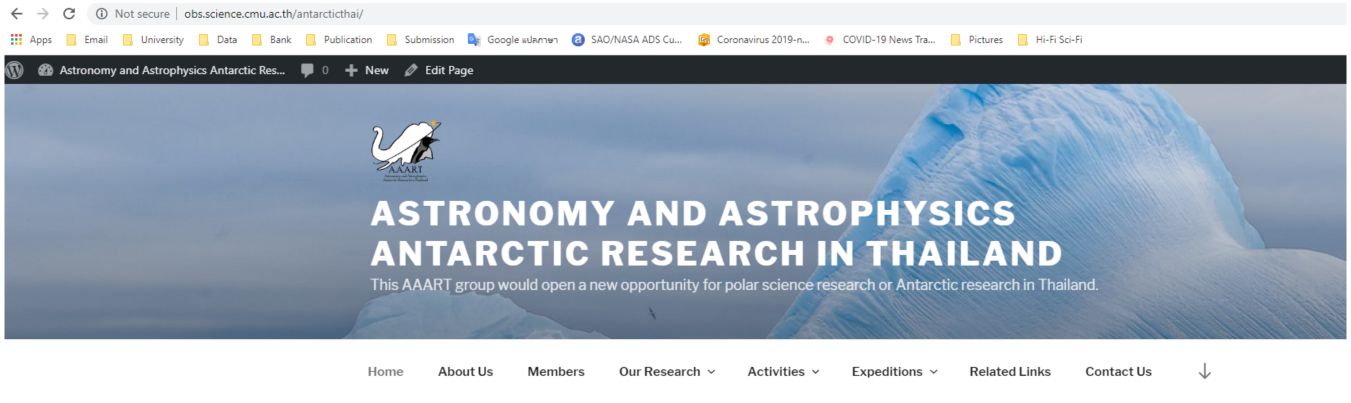

- Establish http://obs.science.cmu.ac.th/antarcticthai/ to provide information and present activities regarding our research

- Update Facebook Page that we have already been developed highlighting ongoing Astronomy and Astrophysics Research in Antarctica, especially projects with Thai involvement.

And more ....

Translation IceCube comic books

https://icecube.wisc.edu/outreach/activities/rosie-gibbs/

Adventure 1:
The Journey to the South Pole

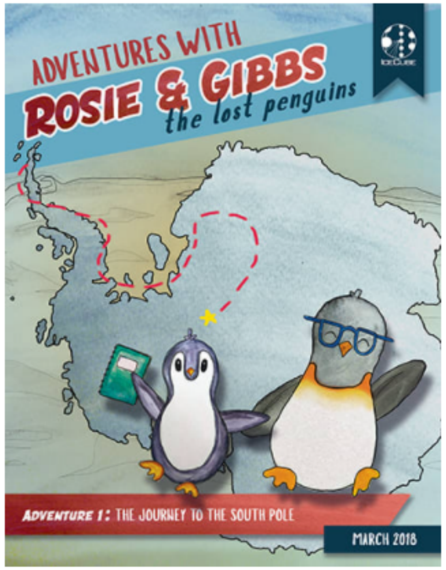

Download the comic:

English:	4 pages letter, folded tabloid
Dansk:	4 pages letter, folded tabloid
Deutsch:	4 pages letter, folded tabloid
Español:	4 pages letter, folded tabloid
Français:	4 pages letter, folded tabloid
한국어:	4 pages letter, folded tabloid
Italiano:	4 pages letter, folded tabloid
Nederlands:	4 pages letter, folded tabloid
ภาษาไทย:	4 pages letter, folded tabloid
Português:	4 pages letter, folded tabloid
中文:	4 pages letter, folded tabloid

Adventure 2:
A Detector in the Ice

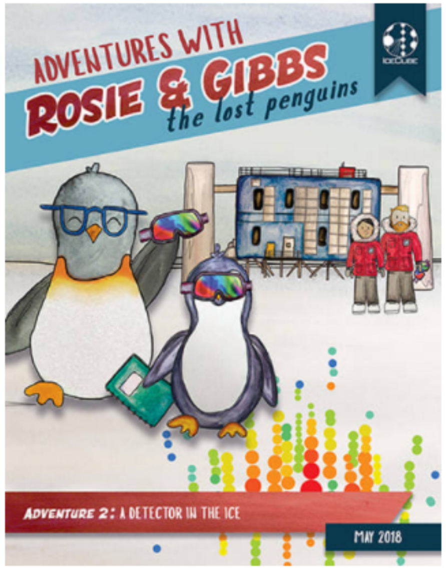

Download the comic:

English:	4 pages letter, folded tabloid
Dansk:	4 pages letter, folded tabloid
Deutsch:	4 pages letter, folded tabloid
Español:	4 pages letter, folded tabloid
Français:	4 pages letter, folded tabloid
Nederlands:	4 pages letter, folded tabloid
ภาษาไทย:	4 pages letter, folded tabloid
Português:	4 pages letter, folded tabloid
中文:	4 pages letter, folded tabloid

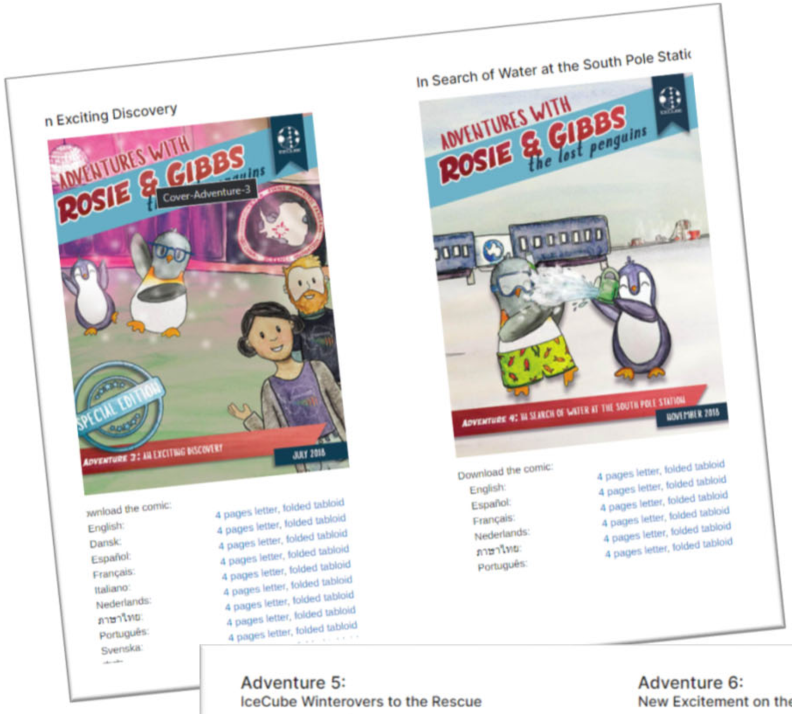

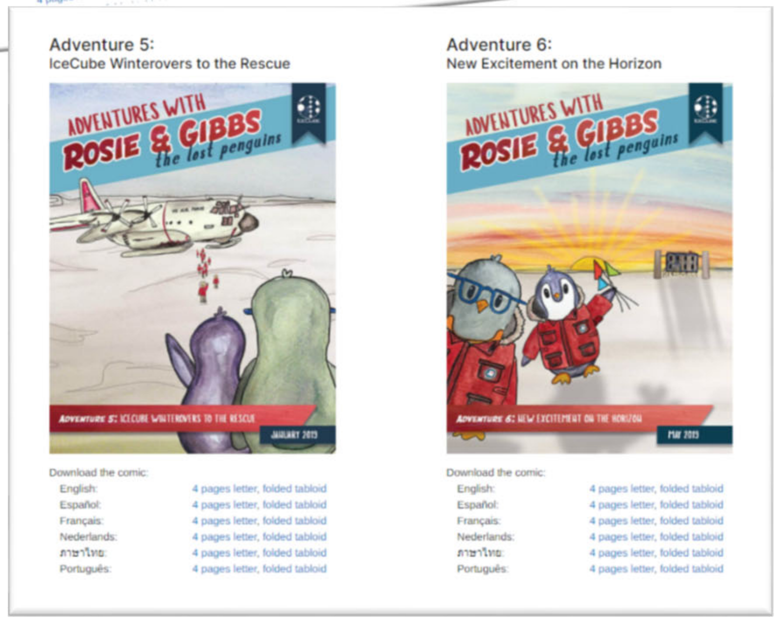

FUTURE WORK

See you again at the Discussion Panel at 3:30 PM

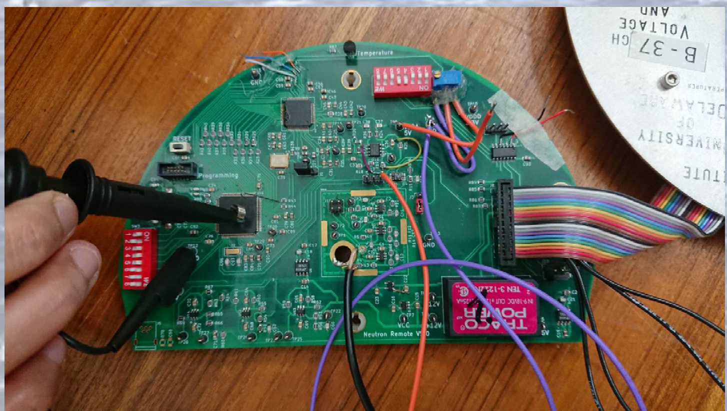

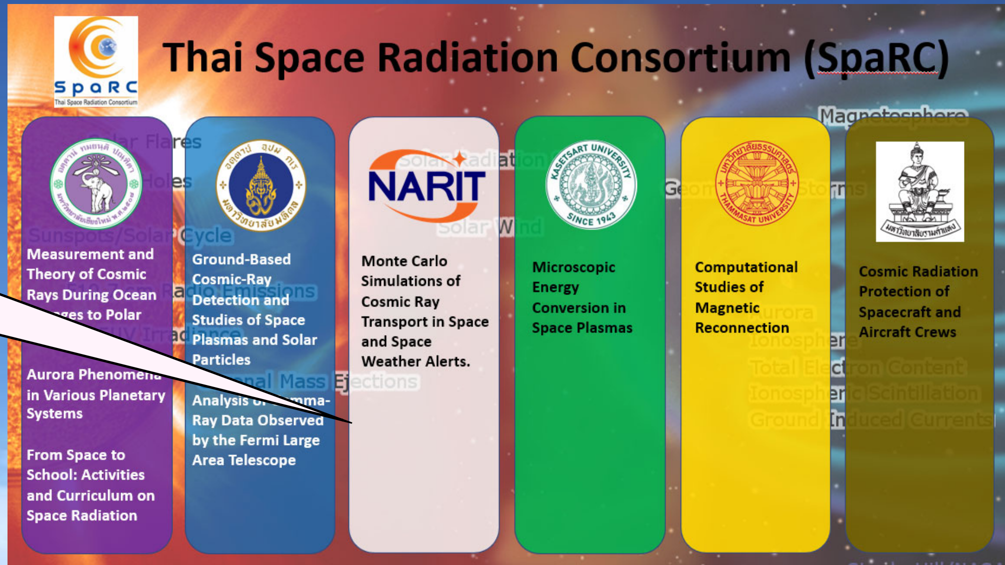

THE 3RD POST-NEUTRON MONITOR BOOTCAMP (2020)
24-27 DECEMBER 2021 @ ASTROPARK, CHIANG MAI


Changvan
CHIANG MAI UNIVERSITY
NARIT
River Falls


雪 龍
XUE LONG

Thank You